CHAPTER 6

CHEMISTRY

Forty two tholeiitic rocks have been analysed for major elements. These comprise fifteen low-Si tholeiitic andesites, thirteen volcanics from the high-Si series, ranging from tholeiitic andesite to rhyodacite, and fourteen rhyolites. Thirty of these rocks were selected for trace element analysis. Details of analytical procedures employed for major and trace elements are outlined in Appendix I.

Deuteric groundmass alteration, relatively common in most members of the low-Si series, may adversely modify original rock chemistries, especially the $Fe_2O_3/FeO+Fe_2O_3$ ratios which partly control the levels of saturation indicated by the C.I.P.W. norms. An increase in the $Fe_2O_3/FeO+Fe_2O_3$ ratio by oxidation increases mt in the norm which in turn results in increased qz or alternatively increased hy at the expense of ol. It is therefore essential that only the freshest specimens are selected for analysis, especially since the differing level of silica saturation of otherwise fairly comparable specimens is one of the principal distinguishing features between the two series. The $Fe_2O_3/FeO+Fe_2O_3$ ratios of the analysed specimens discussed below are in fact relatively low (0.13-0.37) and they therefore permit valid comparisons between the series. The low Fe_2O_3/FeO ratios are undoubtedly enhanced by the predominance of Fe^{3+}-poor ilmenite in the opaque oxide assemblage of most of the analysed rocks, to the virtual exclusion of titanomagnetite (Section 5.3).

6.1 MAJOR ELEMENT DATA

Major element data for the tholeiitic rocks are listed in Tables 6.1-6.3 together with their C.I.P.W. norms. Previous analyses of related rocks of the Tweed Shield, mostly from outside the present area of investigation, are given in Table 6.4. These analyses have been compiled from Wilkinson (1968) and D.C. Green (1970). In terms of their major element geochemistry the Tweed tholeiitic rocks as a group comprise a relatively alkali-rich (especially with respect to K_2O) suite exhibiting moderate iron enrichment. Especially notable is the andesine-normative character of even the most mafic members of the suite. As a consequence, basalts *sensu stricto* are absent or at best extremely rare in this part of the Shield; tholeiitic andesites predominate as the most mafic members of both series.

i) Comparison with Other Tholeiitic Associations

Tholeiitic suites exhibiting a continuum from mafic variants through to felsic rhyolites apparently have been only rarely described, probably the best known example being the Thingmuli volcano in eastern Iceland (Carmichael, 1964). The Ebor Volcano, some 200 km south-south-west of the Tweed Shield (McDougall and Wilkinson, 1967), would appear to be another closely similar example although chemical data on this suite are as yet virtually non-existent. Another comparable suite, the Talasea series in New Britain (Lowder and Carmichael, 1970), which exhibits moderate iron enrichment, would be regarded as essentially tholeiitic by some workers. It may in fact belong to the recently defined island arc tholeiitic suite (Jakes and Gill, 1970). The Thingmuli and Talasea occurrences notwithstanding, it

Table 6.1

ANALYSES OF ROCKS OF THE LOW-Si SERIES

	1	2	3	4	5	6	7	8	9	10	11	12	13	14	15
Specimen No.	28046	28047	28048	28049	28050	28051	28052	28053	28055	28057	28058	28059	28060	27290	27291
SiO_2	50.44	49.74	53.79	51.89	50.61	50.66	52.68	50.05	54.33	52.33	51.86	53.23	52.07	52.90	55.73
TiO_2	1.80	1.59	1.75	2.49	2.75	3.09	1.95	1.97	2.19	2.52	2.65	2.43	2.18	2.15	1.29
Al_2O_3	14.70	14.94	16.39	15.24	14.94	14.47	15.39	15.63	14.42	15.40	14.38	15.61	15.37	18.25	14.45
Fe_2O_3	1.59	3.83	1.04	1.90	2.64	2.66	1.92	3.75	2.77	1.98	2.86	2.27	1.64	2.50	2.35
FeO	8.62	6.68	7.02	9.16	9.66	10.46	7.66	7.38	9.20	8.48	9.13	6.96	8.43	5.23	9.77
MnO	0.15	0.13	0.12	0.15	0.15	0.16	0.13	0.13	0.15	0.16	0.17	0.12	0.13	0.09	0.18
MgO	7.45	5.18	5.25	4.31	3.98	3.52	4.08	5.53	2.38	4.62	3.41	3.05	4.84	3.34	2.38
CaO	8.94	9.52	8.35	7.21	7.06	7.94	8.20	8.80	6.17	7.52	6.69	8.08	8.64	7.79	4.99
Na_2O	3.45	3.60	3.70	3.73	3.38	3.73	4.00	3.78	4.17	3.73	3.49	3.74	3.80	4.29	3.49
K_2O	0.89	0.77	1.14	1.72	2.42	1.80	1.27	1.16	2.74	1.40	2.29	1.56	1.25	1.40	3.58
H_2O+	0.78	1.29	0.93	1.09	1.53	0.17	0.78	1.08	0.65					0.54	1.25
H_2O-	0.77	1.33	0.40	0.83	0.48	0.68	1.03	0.85	0.33	1.30	2.60	2.26	1.26	0.82	0.25
P_2O_5	0.57	0.82	0.29	0.76	0.76	0.82	0.53	0.49	0.78	0.38	0.71	0.34	0.33	0.41	0.60
Total	100.15	99.42	100.17	100.48	100.36	100.16	99.62	100.60	100.22	99.82	100.24	99.65	99.94	99.71	100.31
							C.I.P.W. Norms								
Qz	-	1.21	1.93	1.07	0.14	0.16	1.72	-	2.98	1.72	3.20	4.96	-	2.24	4.36
Or	5.26	4.55	6.74	10.16	14.30	10.64	7.50	6.86	16.19	8.27	13.53	9.22	7.39	8.27	21.16
Ab	29.25	30.46	31.31	31.56	28.60	31.56	33.85	31.98	34.77	31.56	29.53	31.64	32.15	36.30	29.53
An	22.00	22.35	24.75	19.77	18.46	17.43	20.30	22.26	12.81	21.15	16.82	21.21	21.20	26.41	13.20
Di	15.18	15.83	12.09	9.15	9.65	13.89	11.98	14.76	10.73	11.26	9.78	13.75	16.07	7.73	6.51
Hy	11.74	11.94	16.51	17.60	16.41	14.02	11.75	8.37	11.76	16.02	13.96	7.92	13.73	8.74	16.81
Ol	8.17	-	-	-	-	-	-	4.12	-	-	-	-	0.83	-	-
Mt	2.31	5.55	1.51	2.76	3.83	3.86	2.78	5.44	4.02	2.87	4.15	3.29	2.33	3.63	3.41
Il	3.42	3.02	3.32	4.73	5.22	5.87	3.70	3.74	4.16	4.79	5.03	4.61	4.14	4.08	2.45
Ap	1.32	1.90	0.69	1.76	1.76	1.90	1.23	1.13	1.81	0.88	1.64	0.79	0.77	0.95	1.39
Rest	1.55	2.62	1.33	1.92	2.01	0.85	1.81	1.93	0.98	1.30	2.60	2.26	1.26	1.36	1.50
Total	100.20	99.43	100.18	100.48	100.38	100.18	99.52	100.59	100.21	99.82	100.24	99.65	99.92	99.71	100.32
100 an/ab+an	42.9	42.3	44.1	38.5	39.2	35.6	37.5	41.0	26.9	40.1	36.3	40.1	39.7	42.1	31.0
Diff. Index	35.0	36.7	40.5	43.4	43.7	42.7	46.1	39.3	54.3	41.8	47.4	47.0	40.2	47.6	55.8
Mafic Index	57.8	67.0	60.6	72.0	75.2	78.8	70.1	66.8	83.4	69.4	77.9	75.2	67.5	69.8	83.6

KEY TO TABLE 6.1:

1. Low-Si tholeiitic andesite (28046), Kyogle Basalt, 10 km north of Kyogle. Nimbin 9540-IV, 000440.
2. Low-Si tholeiitic andesite (28047), Kyogle Basalt, 4.5 km north-west of Kyogle. Ettrick 9440-I, 970375.
3. Low-Si tholeiitic andesite (28048), Lismore Basalt, 7 km west of Lismore. Lismore 9540-II, 329133.
4. Low-Si tholeiitic andesite (28049), Lismore Basalt, 4.5 km west-south-west of Bangalow. Rosebank 9540-I, 466253.
5. Low-Si tholeiitic andesite (28050), Lismore Basalt, 6 km north-west of Alstonville. Lismore 9540-II, 478129.
6. Low-Si tholeiitic andesite (28051), Lismore Basalt, 6 km south of Alstonville. Lismore 9540-II, 420033.
7. Low-Si tholeiitic andesite (28052), Lismore Basalt, 10 km east-south-east of Kyogle. Nimbin 9540-IV, 094291.
8. Low Si tholeiitic andesite (28053), Lismore Basalt, 13 km north of Kyogle. Nimbin 9540-IV, 001470.
9. Low-Si tholeiitic andesite (28055), Lismore Basalt, 1.5 km east of Alstonville. Lismore 9540-II, 442097.
10. Low-Si tholeiitic andesite (28057), Lismore Basalt, 6 km east of Lismore. Lismore 9540-II, 326130.
11. Low-Si tholeiitic andesite (28058), Lismore Basalt, quarry 9 km south of Lismore. Lismore 9540-II, 256042.
12. Low-Si tholeiitic andesite (28059), Lismore Basalt, Terania Creek, 7.5 km east of Nimbin. Rosebank 9540-I, 292368.
13. Low-Si tholeiitic andesite (28060), Kyogle Basalt, quarry 6 km east-north-east of Kyogle. Nimbin 9540-IV, 058355.
14. High-Al tholeiitic andesite (27290), Lismore Basalt, quarry 4 km south-south-west of Brunswick Heads. Byron Bay 9640-IV, 518397 (Duggan & Wilkinson, 1973, Table 2, Anal. 1).
15. Low-Si tholeiitic andesite (27291), Lismore Basalt, 6.5 km south of Alstonville. Lismore 9540-II, 421033.

Analysts: Nos. 1-9, 15 M.B. Duggan; 10-14 G.I.Z. Kalocsai.

Table 6.2

ANALYSES OF ROCKS OF THE HIGH-Si SERIES

	1	2	3	4	5	6	7	8	9	10	11	12	13	14
Specimen No.	28061	28062	28063	28064	28065	28066	28067	28068	28069	28070	28071	28072	28073	28074
SiO_2	61.50	59.53	58.19	61.94	57.24	58.18	63.44	62.89	62.82	62.87	62.35	65.76	68.88	69.96
TiO_2	1.50	1.60	2.15	1.20	2.02	2.40	1.25	1.25	1.64	1.42	1.00	0.90	0.60	0.66
Al_2O_3	14.77	14.75	13.90	14.45	14.54	14.13	14.03	14.12	14.78	13.99	14.67	14.77	14.31	14.14
Fe_2O_3	0.51	0.99	1.96	0.80	1.65	3.60	1.13	1.44	1.54	0.89	1.73	0.85	0.62	1.21
FeO	7.31	5.97	7.55	5.89	7.80	5.30	5.34	5.06	4.73	5.82	4.28	4.13	2.04	1.96
MnO	0.13	0.11	0.14	0.10	0.12	0.14	0.09	0.09	0.10	0.10	0.09	0.08	0.05	0.04
MgO	2.37	2.92	2.69	2.38	2.93	2.30	1.57	1.57	1.41	1.88	1.73	0.77	0.60	0.19
CaO	4.78	5.56	5.68	4.55	6.27	5.40	3.83	3.86	4.31	4.28	4.02	2.55	1.61	1.25
Na_2O	3.81	3.55	3.73	3.60	3.86	3.99	3.92	3.99	4.16	3.45	3.79	4.01	3.51	4.17
K_2O	3.01	2.89	2.34	3.22	2.59	2.56	3.80	3.70	3.35	3.72	4.17	4.29	5.31	5.06
H_2O+	0.26	1.20	1.32	1.15	0.87	0.57	1.06	1.69	0.82	0.70	1.76	2.03	1.75	1.26
H_2O-	0.16	0.39	0.24	0.02	0.23	0.68	0.32	0.20	0.18	0.34	0.29	0.16	0.18	0.37
P_2O_5	0.31	0.33	0.51	0.27	0.31	0.42	0.27	0.29	0.29	0.39	0.39	0.13	0.19	0.11
Total	100.42	99.79	100.40	99.57	100.43	99.67	100.05	100.15	100.13	99.89	100.27	100.43	99.65	100.38
							C.I.P.W. Norms							
Qz	11.61	11.06	11.00	13.86	6.56	12.33	14.81	14.53	14.72	15.65	13.44	17.71	23.27	23.09
Or	17.78	17.08	13.83	19.03	15.31	15.13	22.46	21.87	19.79	21.98	24.64	25.35	31.38	29.90
Ab	32.24	30.04	31.56	30.46	32.66	33.76	33.17	33.76	35.20	29.19	32.07	33.93	29.70	35.28
An	14.32	15.78	14.28	13.77	14.71	13.09	9.47	9.70	11.77	11.71	10.71	9.64	6.74	4.93
C	-	-	-	-	-	-	-	-	-	-	-	-	0.32	-
Di	6.22	7.99	8.83	5.90	12.02	8.88	6.56	6.36	6.43	4.87	5.56	1.84	-	0.48
Hy	13.53	11.02	11.24	11.33	11.13	4.48	7.57	7.91	5.17	9.52	6.49	6.52	4.83	1.82
Mt	0.74	1.44	2.84	1.16	2.39	5.22	1.64	2.09	2.23	1.29	2.51	1.23	0.90	1.76
Il	2.85	3.04	4.08	2.28	3.84	4.56	2.37	2.37	3.12	2.70	1.90	1.70	1.14	1.25
Ap	0.72	0.77	1.18	0.62	0.72	0.97	0.62	0.67	0.67	0.90	0.90	0.30	0.44	0.26
Rest	0.42	1.59	1.56	1.17	1.10	1.25	1.38	1.89	1.00	1.04	2.05	2.19	1.93	1.63
Total	100.43	99.81	100.40	99.58	100.44	99.67	100.05	100.17	100.12	99.85	100.29	100.42	99.66	100.40
100 an/ab+an	30.8	34.4	31.2	31.1	31.1	27.9	22.2	22.3	25.1	28.6	25.0	22.1	18.5	12.3
Diff. Index	61.6	59.3	57.1	64.4	54.9	62.2	71.3	71.4	70.3	67.6	71.5	78.4	86.4	89.4
Mafic Index	76.7	70.5	78.0	73.8	76.3	79.5	80.5	80.6	81.6	78.1	77.7	86.6	81.6	94.4

KEY TO TABLE 6.2

1. High-Si tholeiitic andesite (28061), Lismore Basalt, small quarry 7.5 km south of Nimbin. Nimbin 9540-IV, 233291.
2. High-Si tholeiitic andesite (28062), Lismore Basalt, 8 km north-north-west of Nimbin. Nimbin 9540-IV, 191442.
3. High-Si tholeiitic andesite (28063), Lismore Basalt, 6.5 km south-south-west of Mullumbimby. Rosebank 9540-I, 464351.
4. High-Si tholeiitic andesite (28064), Lismore Basalt, 1 km north of Dunoon. Rosebank, 9540-I, 314279.
5. High-Si tholeiitic andesite (28065), Lismore Basalt, quarry 7 km north of Lismore. Lismore 9540-II, 255147.
6. High-Si tholeiitic andesite (28066), Lismore Basalt, 3.5 km north-north-east of Bangalow. Byron Bay 9640-IV, 523300.
7. Icelandite (28067), Lismore Basalt, 7 km west of Nimbin. Nimbin 9540-IV, 147355.
8. Icelandite (28068), Lismore Basalt, 7 km west of Nimbin. Nimbin 9540-IV, 148358.
9. Icelandite (28069), Lismore Basalt, 9 km north of Nimbin. Nimbin 9540-IV, 200457.
10. Icelandite (28070), Lismore Basalt, quarry 7 km north of Dunoon. Rosebank 9540-I, 319338.
11. Icelandite (28071), Lismore Basalt, 5.5 km south-west of Mullumbimby. Rosebank 9540-I, 454370.
12. Icelandite (28072), boulder in pyroclastic unit with the Nimbin Rhyolite, 5 km west of Doon Doon. Rosebank 9540-I, 24855.
13. Tholeiitic rhyodacite (28073), Nimbin Rhyolite, outlier 3.5 km south-east of Nimbin. Nimbin 9540-IV, 242343.
14. Tholeiitic rhyodacite (28074), dyke intruding Lismore Basalt, 4 km south-south-west of Dunoon. Rosebank 9540-I, 291235.

Analyst: M.B. Duggan.

Table 6.3

ANALYSES OF RHYOLITIC PITCHSTONES, MICROCRYSTALLINE RHYOLITES AND RESIDUAL GLASSES

	1	2	3	4	5	6	7	8	9	10	11	12	13	14	15	16
Specimen No.	28075	28076	28076G	28077	28078	28078G	28079	28080	28081	28082	28083	28084	28085	28086	28087	28088
SiO_2	72.47	73.01	70.02	72.41	74.52	73.30	73.30	73.07	72.77	75.10	74.18	76.37	74.55	73.81	73.54	75.51
TiO_2	0.25	0.30	0.50	0.20	0.20	0.49	0.34	0.34	0.41	0.12	0.25	0.46	0.15	0.05	0.34	0.15
Al_2O_3	12.33	12.14	11.96	12.67	11.86	11.86	12.64	12.90	12.49	13.70	13.75	12.34	13.12	14.03	13.51	12.94
Fe_2O_3	0.66	0.71	0.62	0.63	0.64	0.66	0.68	0.65	0.70	0.88	0.98	0.42	0.82	0.85	0.77	0.38
FeO	1.34	1.04	0.78	0.71	0.74	0.73	0.60	0.63	1.27	0.55	0.38	0.43	0.63	0.64	0.57	0.53
MnO	0.03	0.03	0.02	0.02	0.02	0.02	0.02	0.02	0.04	0.02	0.01	0.01	0.02	0.02	0.01	0.01
MgO	0.58	0.14	0.09	0.09	0.05	0.09	0.06	0.08	0.27	0.04	0.18	0.07	0.10	0.16	0.17	0.13
CaO	1.03	0.72	0.71	0.63	0.65	0.73	0.70	0.77	0.85	0.31	0.50	0.70	0.43	0.25	0.55	0.44
Na_2O	3.05	3.04	3.15	3.09	2.76	2.88	2.77	2.45	2.85	3.39	2.67	2.97	2.84	2.72	2.89	2.84
K_2O	5.41	5.47	5.81	5.75	5.58	6.02	5.53	5.96	5.87	5.20	5.87	5.49	5.78	4.97	5.58	5.64
H_2O+	2.81	2.81	-	3.50	2.62	-	2.69	3.03	2.21	0.72	0.92	0.46	0.77	1.30	0.95	0.63
H_2O-	0.17	0.11	6.47	0.16	0.15	3.16	0.27	0.28	0.36	0.34	0.46	0.32	0.12	0.80	0.61	0.31
P_2O_5	0.09	0.05	-	-	0.07	-	0.05	0.08	0.06	-	0.03	0.03	0.03	-	0.07	-
Total	100.22	99.57	100.13	99.86	99.86	99.94	99.65	100.26	100.15	100.37	100.18	100.07	99.36	99.60	99.56	99.51
							C.I.P.W. Norms									
Qz	30.61	32.34	28.22	30.73	35.59	32.22	34.57	34.42	31.15	34.70	34.93	36.56	34.80	38.00	34.14	36.07
Or	31.97	32.32	34.33	33.98	32.98	35.58	32.68	35.22	34.69	30.73	34.69	32.44	34.16	29.37	32.98	33.33
Ab	25.81	25.72	26.65	26.14	23.35	24.37	23.44	20.73	24.11	28.69	22.59	25.13	24.03	23.01	24.45	24.03
An	3.98	3.26	1.34	3.12	2.77	1.66	3.15	3.30	3.83	1.54	2.29	3.28	1.94	1.24	2.28	2.18
C	-	0.03	-	0.22	0.27	-	0.95	1.21	0.05	1.93	2.17	0.31	1.48	3.72	1.88	1.37
Di	0.46	-	0.73	-	-	0.52	-	-	-	-	-	-	-	-	-	-
Wo	-	-	0.54	-	-	0.54	-	-	-	-	-	-	-	-	-	-
Hy	2.78	1.23	-	0.71	0.66	-	0.16	0.29	1.82	0.22	0.45	0.17	0.52	0.83	0.42	0.75
Mt	0.96	1.03	0.90	0.91	0.93	0.96	0.99	0.94	1.01	1.28	0.53	0.09	1.19	1.23	0.88	0.55
Hm	-	-	-	-	-	-	-	-	-	-	0.61	0.36	-	-	0.16	-
Il	0.47	0.57	0.95	0.38	0.38	0.93	0.65	0.65	0.78	0.23	0.48	0.87	0.29	0.10	0.65	0.29
Ap	0.21	0.12	-	-	0.16	-	0.12	0.18	0.14	-	0.07	0.07	0.07	-	0.16	-
Rest	2.98	2.92	6.47	3.66	2.77	3.16	2.96	3.31	2.57	1.06	1.38	0.78	0.89	2.10	1.56	0.94
Total	100.23	99.54	100.13	99.85	99.86	99.94	99.67	100.25	100.15	100.38	100.19	100.16	99.37	99.60	99.56	99.51
$\frac{100\ an}{ab+an}$	13.4	11.2	4.8	10.7		6.4	11.8	13.7	13.7	5.1	9.2	11.5	7.5	5.1	8.5	8.3
Diff.Index	90.9	93.6		94.5		93.8	93.8	93.3	92.2	94.7	93.3	94.7	94.4	92.7	93.5	94.8
Mafic Index	77.5	92.6		93.7		95.5	95.5	94.1	87.9	97.3	88.3	92.4	93.5	90.3	88.7	87.5

KEY TO ANALYSES IN TABLE 6.3

1. Rhyolitic pitchstone (28075), Nimbin Rhyolite, 10 km north-east of Nimbin. Rosebank 9540-I, 302425.
2. Rhyolitic pitchstone (28076), Nimbin Rhyolite, 5 km north-east of Nimbin. Rosebank 9540-I, 257391.
3. Residual glass separated from No.2.
4. Rhyolitic pitchstone (28077), Nimbin Rhyolite, 5.5 km north-east of Dunoon. Rosebank 9549-I, 353308.
5. Rhyolitic pitchstone (28078), Georgica Rhyolite Member, 4.5 km south-west of Nimbin. Nimbin 9540-IV, 182338.
6. Residual glass separated from No.5
7. Rhyolitic pitchstone (28079), Nimbin Rhyolite, 6.5 km west-south-west of Mullumbimby. Rosebank 9540-I, 423396.
8. Rhyolitic pitchstone (28080), Georgica Rhyolite Member, 9 km west-south-west of Nimbin. Nimbin 9540-IV, 137332.
9. Rhyolitic pitchstone (28081), Georgica Rhyolite Member, 6 km west-south-west of Nimbin. Nimbin 9540-IV, 162339.
10. Microcrystalline rhyolite (28082), Nimbin Rhyolite, 8.5 km east-north-east of Nimbin. Rosebank 9540-I, 296390.
11. Microcrystalline rhyolite (28083), Georgica Rhyolite Member, 7 km west of Nimbin. Nimbin 9540-IV, 147349.
12. Microcrystalline rhyolite (28084), Georgica Rhyolite Member, 7 km west of Nimbin. Nimbin 9540-IV, 148349.
13. Microcrystalline rhyolite (28085), Nimbin Rhyolite, 7 km north-east of Dunoon. Rosebank 9540-I, 355321.
14. Microcrystalline rhyolite (28086), Nimbin Rhyolite, 9.5 km east-north-east of Nimbin. Rosebank 9540-I, 305392.
15. Microcrystalline rhyolite (28087), intrusive plug (The Tower), 10.5 km south-west of Nimbin. Nimbin 9540-IV, 137296.
16. Microcrystalline rhyolite (28088), intrusive plug (Doughboy Mountain), 2 km south-east of Doon Doon. Rosebank 9540-I, 313450.

Analysts: Nos 1,2,4,5,7-16 M.B. Duggan; Nos 3,6 G.I.Z. Kalocsai.

Table 6.4

PREVIOUSLY PUBLISHED ANALYSES OF THOLEIITIC ROCKS FROM THE TWEED SHIELD VOLCANO AND ENVIRONS

	1	2	3	4	5	6	7	8	9	10	11	12	13	14	15	16	17
SiO_2	48.96	50.30	49.90	54.10	48.48	57.08	50.78	53.22	52.24	49.68	52.30	57.62	61.24	63.15	71.98	73.10	74.28
TiO_2	0.81	1.76	1.98	2.35	2.50	3.35	2.60	2.50	1.44	2.47	1.55	1.75	0.52	0.40	0.13	0.39	0.25
Al_2O_3	16.58	15.19	15.79	13.42	16.71	14.18	15.16	14.96	16.52	15.10	15.64	13.63	14.33	15.22	12.02	13.09	11.27
Fe_2O_3	1.95	1.88	4.52	4.06	5.93	2.92	2.36	1.93	4.52	1.74	3.48	5.41	1.81	0.41	1.20	1.19	1.93
FeO	8.62	9.65	6.25	7.43	5.96	9.29	10.01	8.78	6.61	7.50	4.24	5.15	6.09	5.00	1.08	1.43	0.58
MnO	0.14	0.14	0.12	0.30	0.12	0.13	0.14	0.13	tr	0.15	0.14	0.26	tr	0.08	0.06	nil	0.02
MgO	7.97	6.85	5.77	4.43	4.19	3.50	4.43	3.43	3.55	7.58	7.98	2.86	3.45	2.81	0.16	0.43	0.44
CaO	8.75	8.24	9.12	7.97	7.02	6.93	6.46	7.18	8.20	7.85	7.95	5.57	5.07	4.17	0.64	0.87	1.15
Na_2O	3.08	3.35	3.24	3.81	3.38	3.65	3.54	3.82	3.28	2.94	3.07	3.38	3.75	3.65	3.04	4.03	2.74
K_2O	0.91	0.72	0.89	1.15	1.78	1.95	2.20	1.80	1.48	0.72	1.05	3.07	3.13	3.25	5.07	4.92	4.77
H_2O+	1.18	0.56	1.36	0.88	1.44	0.96	1.32	0.66	0.65	2.40	0.56	1.54	0.28	1.10	3.86	0.54	1.01
H_2O-	0.66	1.04	1.28	nil	2.07	1.50	0.75	0.94	0.58	1.58	1.71	nil	0.17	0.10	1.02	nil	0.70
P_2O_5	0.34	0.32	0.43	0.46	0.59	0.76	0.34	0.68	0.80	0.34	0.22	0.40	0.51	0.72	0.02	0.11	0.07
Etc.	-	-	-	-	0.32	-	0.31	-	-	-	-	-	-	-	0.20	-	-
Total	99.95	100.00	100.65	100.36	100.49	100.20	100.40	100.03	99.87	100.05	99.89	100.64	100.35	100.06	100.48	100.10	99.21
								C.I.P.W. Norms									
Qz	-	-	2.04	6.60	2.46	2.76	-	3.36	6.18	1.09	3.56	12.30	11.10	14.64	32.88	28.44	37.44
Or	5.56	3.87	5.56	6.67	10.56	11.68	12.79	10.56	8.90	4.25	6.21	18.35	18.35	19.46	30.02	28.91	28.36
Ab	26.20	28.30	27.25	31.96	28.82	30.92	29.87	32.49	27.77	24.87	25.98	28.82	31.44	30.92	25.68	34.06	23.06
An	28.63	24.46	25.85	16.12	25.02	16.40	19.18	18.35	25.85	25.89	25.80	12.79	13.07	15.29	3.34	3.06	4.17
C	-	-	-	-	-	-	-	-	-	-	-	-	-	-	0.31	-	-
Di	10.42	11.84	13.34	16.75	4.64	11.07	9.00	10.64	7.48	8.74	9.62	9.61	6.90	0.68	-	0.46	0.65
Hy	6.75	18.22	12.77	9.93	10.55	12.67	15.48	13.99	11.32	23.25	17.95	5.22	14.16	14.85	1.19	1.79	0.80
Ol	15.46	4.76	-	-	-	-	2.55	-	-	-	-	-	-	-	-	-	-
Mt	2.78	2.78	6.50	5.80	8.58	4.18	3.48	2.78	6.50	2.52	5.05	7.89	2.55	0.70	1.86	1.86	1.16
Hm	-	-	-	-	-	-	-	-	-	-	-	-	-	-	-	-	1.12
Il	1.52	3.34	3.80	4.41	4.71	6.38	5.02	4.71	2.74	4.69	2.94	3.34	0.91	0.76	0.30	0.76	0.46
Ap	0.67	0.67	1.01	1.01	1.34	1.68	0.67	1.68	2.02	0.79	0.51	1.01	1.34	1.68	tr	0.34	0.34
Rest	1.84	1.60	2.64	0.88	3.83	2.46	2.41	1.60	1.23	3.98	2.27	1.54	0.45	1.20	5.08	0.54	1.71
Total	99.83	99.84	100.76	100.13	100.51	100.20	100.42	100.16	99.99	100.07	99.89	100.64	100.27	100.18	100.66	100.22	99.27
$\frac{100\ an}{ab+an}$	52.2	46.4	48.7	33.5	46.5	34.7	39.1	36.1	48.2	51.0	49.8	30.7	29.4	33.1	11.5	8.2	15.3
Diff. Index	32.4	32.7	35.6	45.4	43.1	46.4	43.4	47.1	43.5	31.4	36.8	60.0	61.0	65.7	92.7	91.8	91.2
Mafic Index	57.0	62.7	65.1	72.2	73.9	77.7	73.6	75.7	75.8	54.9	49.2	78.7	69.6	65.8	93.4	85.9	85.1

KEY TO ANALYSES IN TABLE 6.4

1. Basalt, 6 km south of Lamington (Richards, 1916, Table 6, Anal. 12).
2. Olivine tholeiite, 21 km northwest of Tabulum (Wilkinson, 1968, Table 2, Anal. 2).
3. Basalt, 3 km south of Lamington (Richards, 1916, Table 6, Anal. 10).
4. Andesite, Springbrook Plateau (Richards, 1916, Table 5, Anal. 3).
5. Olivine basalt, Black Head, Ballina (Browne 1933, Table 2, Anal. 3).
6. Potassic tholeiitic andesite, Fingal Point, Tweed Heads (Wilkinson, 1968, Table 1, Anal. 6).
7. Olivine basalt, Fingal Point, Tweed Heads (Richards, 1916, Table 6, Anal. 7).
8. Potassic tholeiitic andesite, Burleigh Heads (Wilkinson, 1968, Table 1, Anal. 8).
9. Andesitic basalt, Burleigh Heads (Richards, 1916, Table 6, Anal. 3).
10. Porphyritic basalt, Mount Tambourine (Green, 1969, Table 1, Anal. 1).
11. Porphyritic basalt, Mount Tambourine (Green, 1969, Table 1, Anal. 3).
12. Andesite, Mount Tambourine (Richards, 1916, Table 5, Anal. 2).
13. Andesite, Observation Hill, Tweed Heads (Richards, 1916, Table 5, Anal. 1).
14. Potassic icelandite, Observation Hill, Tweed Heads (Wilkinson, 1968, addendum).
15. Pitchstone, McPherson Range (Richards, 1916, Table 1, Anal. 4).
16. Rhyolite, Springbrook Plateau (Richards, 1916, Table 1, Anal. 6).
17. Rhyolite, 6 km south of Lamington (Richards, 1916, Table 1, Anal. 1).

is obvious that the Tweed Shield tholeiitic suite is relatively unique in terms of its continental environment and the spectrum of rock types developed within the Shield. Tholeiitic series, especially those in continental settings, more typically display a relatively restricted range in chemical variation, illustrated by the occurrences of tholeiitic rocks elsewhere in Australia discussed below. Typical of these is the Inverell area of New South Wales (Wilkinson and Duggan, 1973), where the tholeiitic eruptives are all closely similar in composition, straddling the basalt-andesite boundary and the plane of silica saturation. Since only the mafic end of the spectrum is typically developed in these tholeiitic associations, it is especially appropriate to compare these with the mafic representatives of the Tweed tholeiitic suite, particularly the rocks of the low-Si series.

Alkali-Silica Relations: The Tweed tholeiitic rocks have relatively high total alkali contents, compared with most typical tholeiitic suites, all mafic representatives containing greater than 3% Na_2O, with K_2O only rarely less than 1.0%. On a total alkalis vs silica (wt %) diagram (Fig. 6.1) most of the analysed rocks fall in the alkaline field relative to the dividing line separating Hawaiian alkaline and tholeiitic rocks (MacDonald and Katsura, 1964). Although widely applied to discriminate tholeiitic and alkaline volcanics on a world-wide basis, it is now clear that the MacDonald-Katsura datum line is applicable only to Hawaiian rocks and hence an alkali-silica diagram alone is inadequate to confidently distinguish the alkali and tholeiitic suites from other provinces. Indeed, several tholeiitic suites also plot in the Hawaiian alkaline field of Figure 6.1 including those of the Snake River area in Idaho, U.S.A. (Tilley and Thompson, 1970) and the Fe-rich tholeiitic

Fig. 6.1: Plot of Na_2O+K_2O against SiO_2 (wt %). Filled circles, analysed rocks of the low-Si series (Table 6.1); open circles, previously analysed rocks of the Tweed Shield (Table 6.4 Nos 1-11). The line H-H' divides the fields of Hawaiian tholeiitic and alkaline rocks (after MacDonald and Katsura, 1964). A, tholeiitic andesite, Ebor, N.S.W. (Wilkinson, 1969); B, average of 4 tholeiites, Inverell, N.S.W. (Wilkinson and Duggan, 1973); C, tholeiitic andesite, Peak Range, Qld. (Joplin, 1971); D, average of 3 tholeiites, Tasmania (Edwards, 1950); E, enstatite basalt, Kangaroo Is. (Stanley, 1910); F, tholeiite, Donnely R., W.A. (Edwards, 1938); G, tholeiite, Bunbury, W.A. (Edwards, 1938); H, tholeiite, Cape Gosselin, W.A. (Edwards, 1938); J, average chilled dolerite, Red Hill, Tas. (McDougall, 1962). 1, Average Hawaiian tholeiite (MacDonald and Katsura, 1964); 2, average of 3 Thingmuli olivine tholeiites (Carmichael, 1964); 3, average of 7 Thingmuli tholeiites (Carmichael, 1964); 4, average Izu Hakone basalt (Kuno, 1968); 5, average Izu Hakone basaltic andesite (Kuno, 1968); 6, average McKinney basalt, Snake River, Idaho (Tilley and Thompson, 1970); 7, average King Hill basalt, Snake River, Idaho (Tilley and Thompson, 1970); 8, average Hebridean tholeiite, 48-50% group (Holland and Brown, 1972); 9, average Hebridean tholeiite, 50-52% group (Holland and Brown, 1972); 10, average Deccan basalt (Sukheswala and Pldervaart, 1958); 11, average Talasea basalt (Lowder and Carmichael, 1970); 12, average of 2 least oxidised tholeiites, Tholey, Germany (Jung, 1958); 13, average Yakima basalt, Columbia R., U.S.A. (Waters, 1961); 14, average of Late Yakima and Early Ellensburg flows, Columbia R., U.S.A. (Waters, 1961); 15, average Picture Gorge basalt, Columbia R., U.S.A. (Waters, 1961); 16, average of 7 tholeiites and olivine tholeiites, Galapagos Is (McBirney and Williams, 1969); 17, average "ferrobasalt", Galapagos Is (McBirney and Williams, 1969); 18, average of 10 tholeiitic andesites, Parana Basin, S.America (Leterrier *et al.*, 1971); 19, "basalt", Lovejoy Basalt, California (Hietenan, 1972); 20, average abyssal tholeiite (Engel *et al.*, 1965).

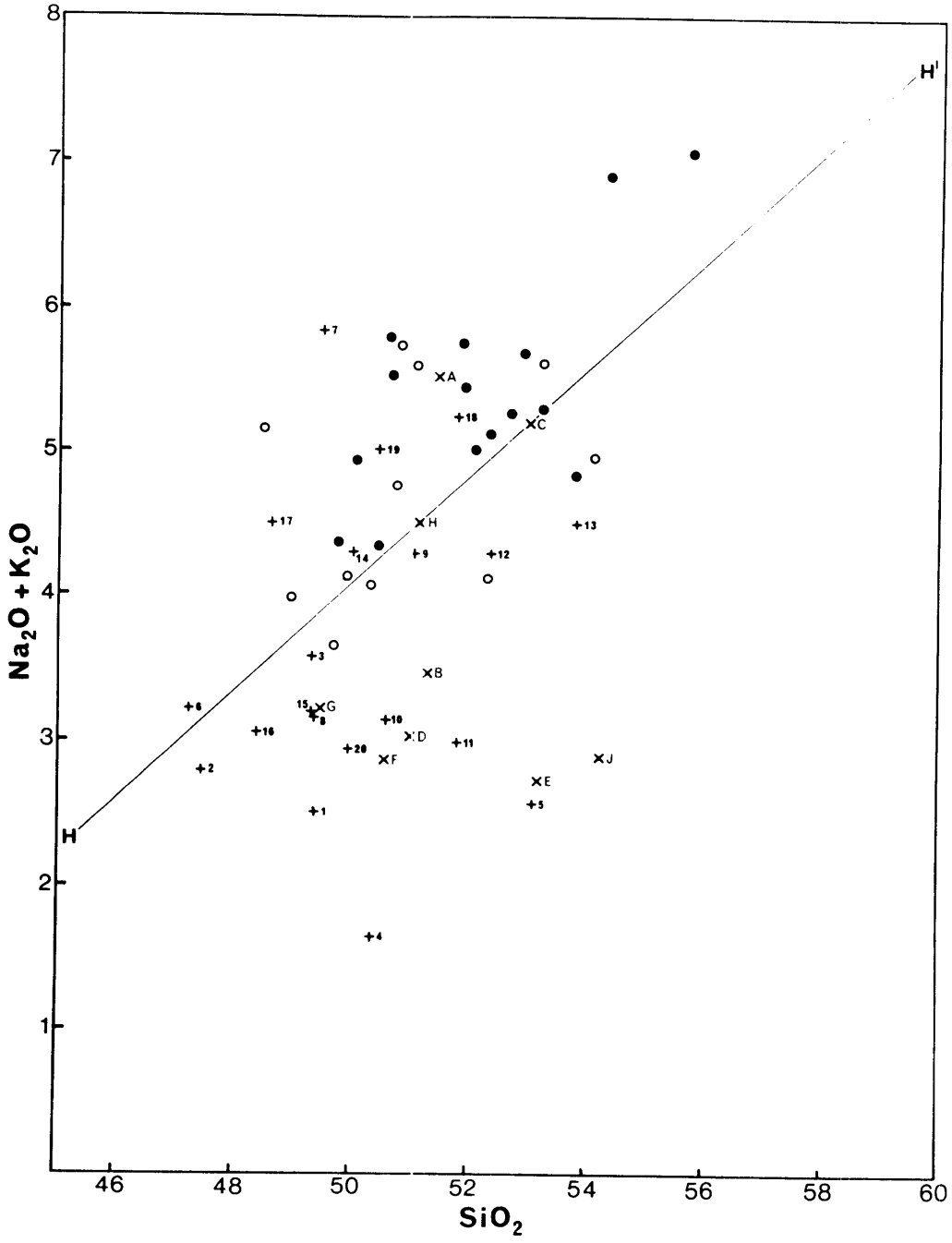

Fig. 6.1.

andesites ("ferrobasalts"; McBirney and Williams, 1969) of the Galapagos Islands. An interesting feature of Figure 6.1 is the apparent division of the tholeiitic provinces into alkali-rich and alkali-poor types with a hiatus separating the two groups. All rocks falling in the alkali-rich group contain relatively high Na_2O and high K_2O. On the other hand the alkali-poor group contains K-poor types with high Na_2O/K_2O ratios (>10; e.g. the abyssal tholeiites; Engel *et al.*, 1965; Miyashiro *et al.*, 1969) and K-rich types with quite low Na_2O/K_2O ratios (<2; e.g. the Tasmanian dolerites; McDougall, 1962).

The relatively potassic character of members of the Tweed low-Si series is evident in Figure 6.2 (K_2O vs SiO_2 wt %). They compare closely in K_2O content with several other tholeiitic suites occuring in continental environments including the Yakima "basalts"* of the Columbia River province, U.S.A. (Waters, 1961), the Karroo basalts of Basutoland (Cox and Hornung, 1966), the tholeiites of Tholey, Germany (Jung, 1958) and the Tasmanian dolerites (McDougall, 1962). The relatively potassic character of the Tweed volcanics is reflected in their strongly potassic vitric residua.

In terms of other major elements, the rocks of the low-Si series, and indeed those of the high-Si series are broadly comparable to most other tholeiitic associations. However there are some important differences between chemical trends within the two series and these are outlined in more detail below.

---

* The Yakima "basalts" are in fact more appropriate to tholeiitic andesites in composition.

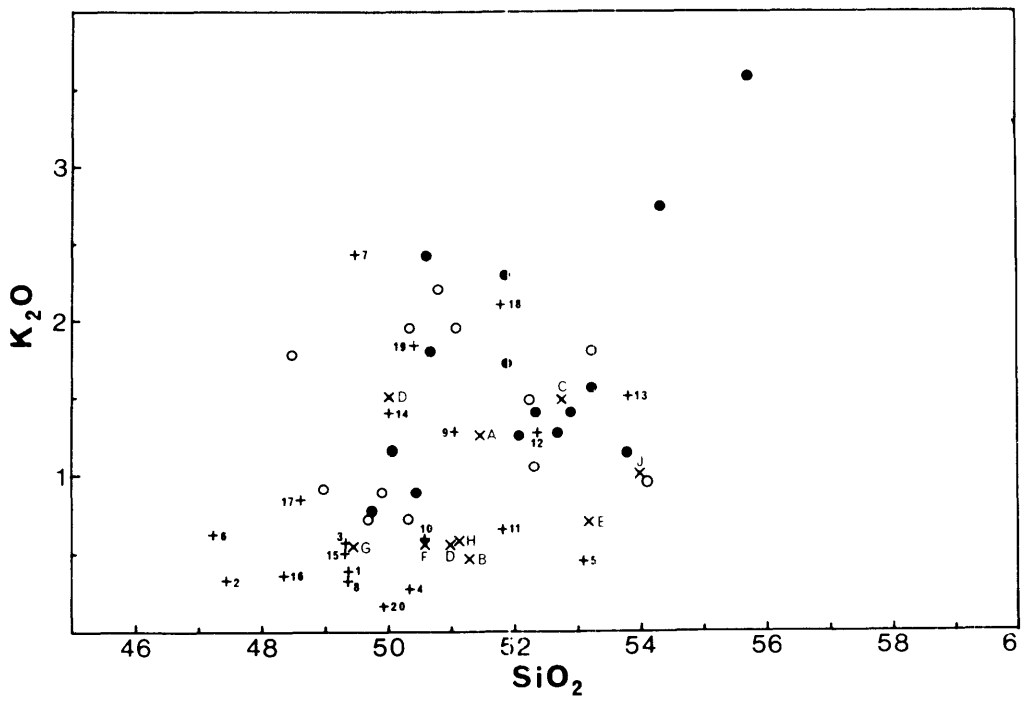

Fig. 6.2: Plot of K_2O against SiO_2 (wt %). Filled circles, analysed rocks of the low-Si series (Table 6.1); open circles, previously analysed rocks from the Tweed Shield (Table 6.4, Nos. 1-11). For explanation of other symbols see Fig. 6.1.

ii) Degree of Silica Saturation

The most mafic members of the low-Si series straddle the plane of silica saturation (Yoder and Tilley, 1962) with most falling within the qz saturated field. This is clearly illustrated in Figure 6.3 on an Ol-Di-Qz diagram (mol %; Coombs, 1963) in which the join Di-Hy corresponds to the plane of silica saturation. The plot of an analysis in a normative diagram of this type is influenced by the degree of oxidation of the rock. It has already been noted that this has probably not been a serious problem in most of the rocks plotted on Figure 6.3. The effect of readjusting Fe_2O_3 to a maximum of 1.5%, with a corresponding readjustment to FeO, is illustrated on Figure 6.3 by a horizontal line from the plotted point to the new point. It is apparent that the effect of this readjustment is quite small and therefore that the levels of silica saturation indicated by the original C.I.P.W. norms are intrinsic features of the series as a whole, thus confirming, along with mineralogical and other data, the undoubted tholeiitic character of the low-Si series in spite of their high total alkali contents and the absence of groundmass Ca-poor pyroxenes. The differing levels of silica saturation of the low-Si and high-Si series are clearly illustrated in Figures 6.4 and 6.5. The quantity qz^* represents the residual SiO_2 (wt %) after calculation of the C.I.P.W. normative components or, ab, an, di and ol (c.f. Thompson *et al.*, 1972), and is therefore a valid indicator of the level of silica saturation of a rock.

CHEMISTRY OF THE RHYOLITIC ROCKS

The rhyolites (Table 6.3), which comprise a significant proportion

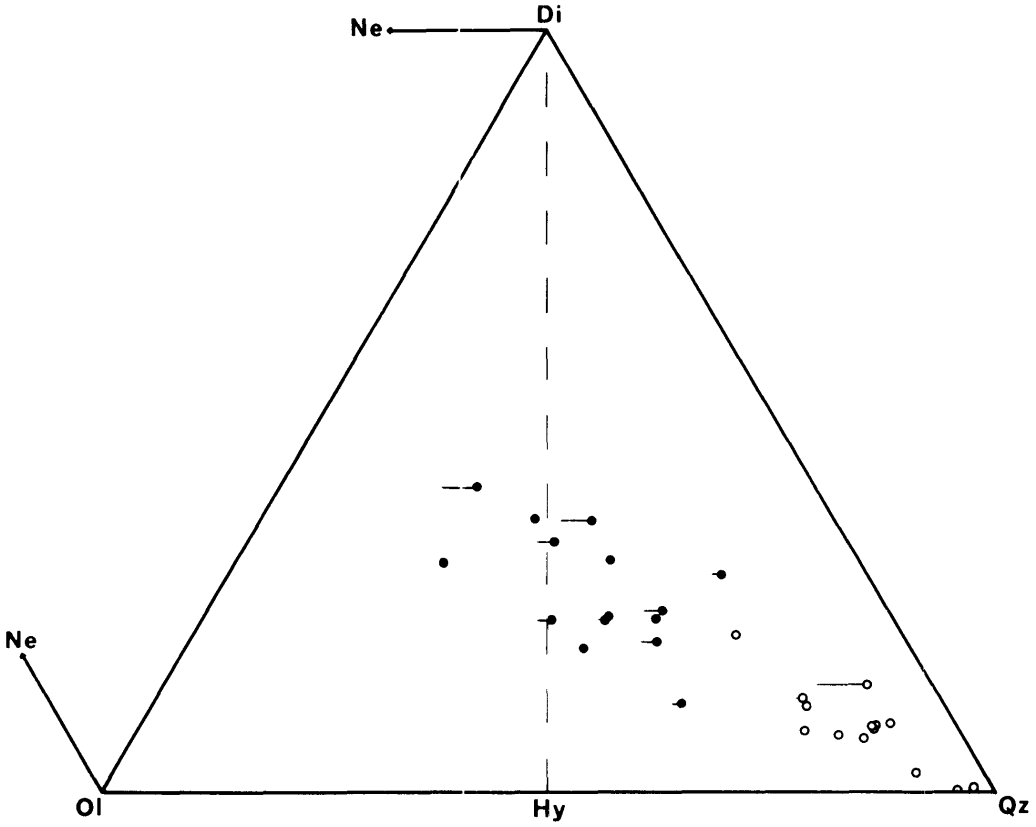

Fig. 6.3: Analysed rocks of the low-Si series (filled circles) and high-Si series (open circles) plotted on a normative Di-Ol-Qz diagram (molecular proportions; after Coombs, 1963). Horizontal lines indicate the change in the plotted position when Fe_2O_3 in the analysis is adjusted to a maximum of 1.5 wt %. The dashed line Di-Hy represents the plane of silica saturation.

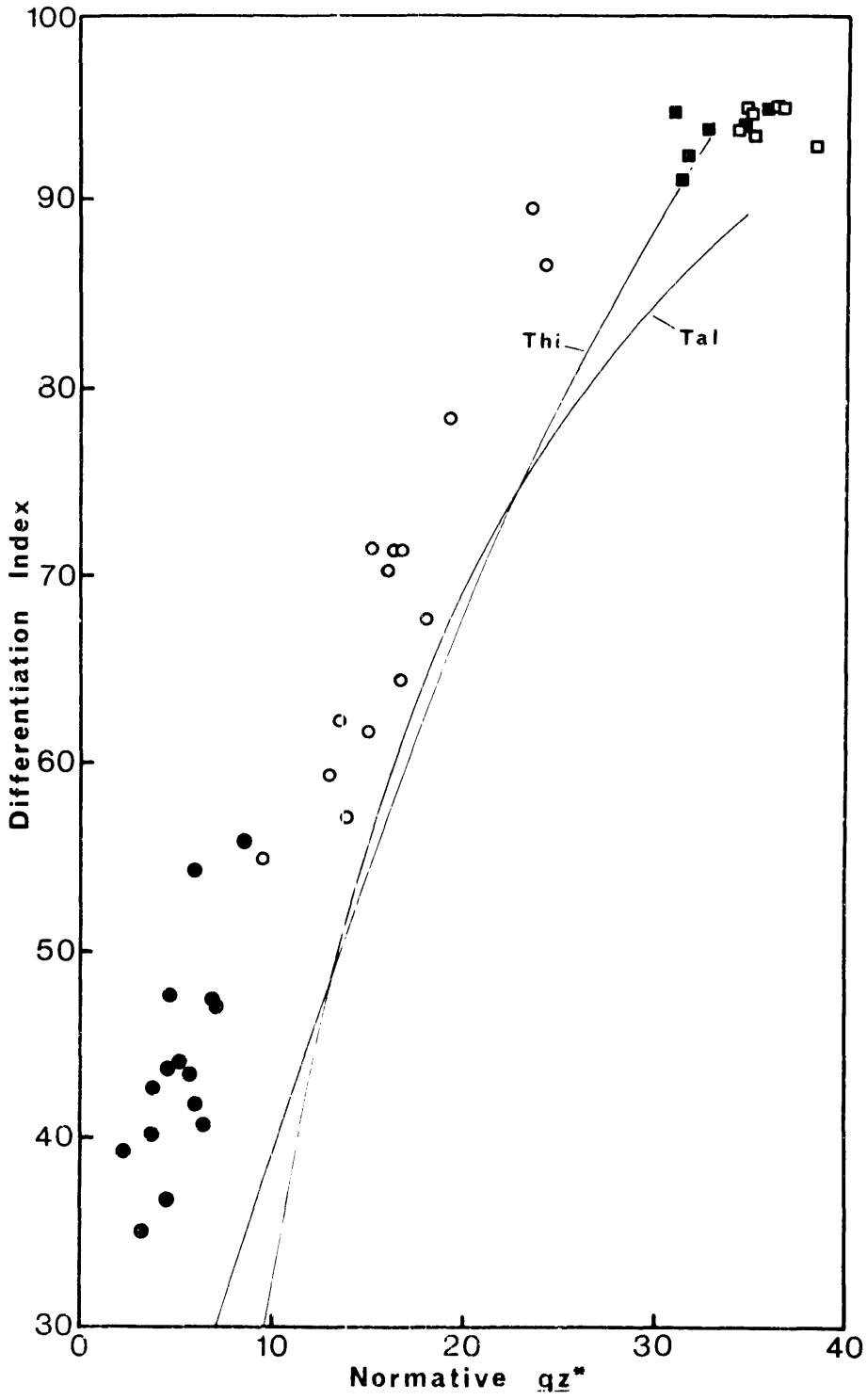

Fig. 6.4: Plot of Differentiation Index against the level of silica saturation (qz*). The quantity qz* represents the normative qz content when all hy is calculated as ol in the norm. Filled circles, members of the low-Si series; open circles, members of the high-Si series; filled squares, rhyolitic pitchstones; open squares, microcrystalline rhyolites. Generalized trends for the Thingmuli (Thi; Carmichael, 1964) and Talasea (Tal; Lowder and Carmichael, 1970) volcanic series are shown for comparison.

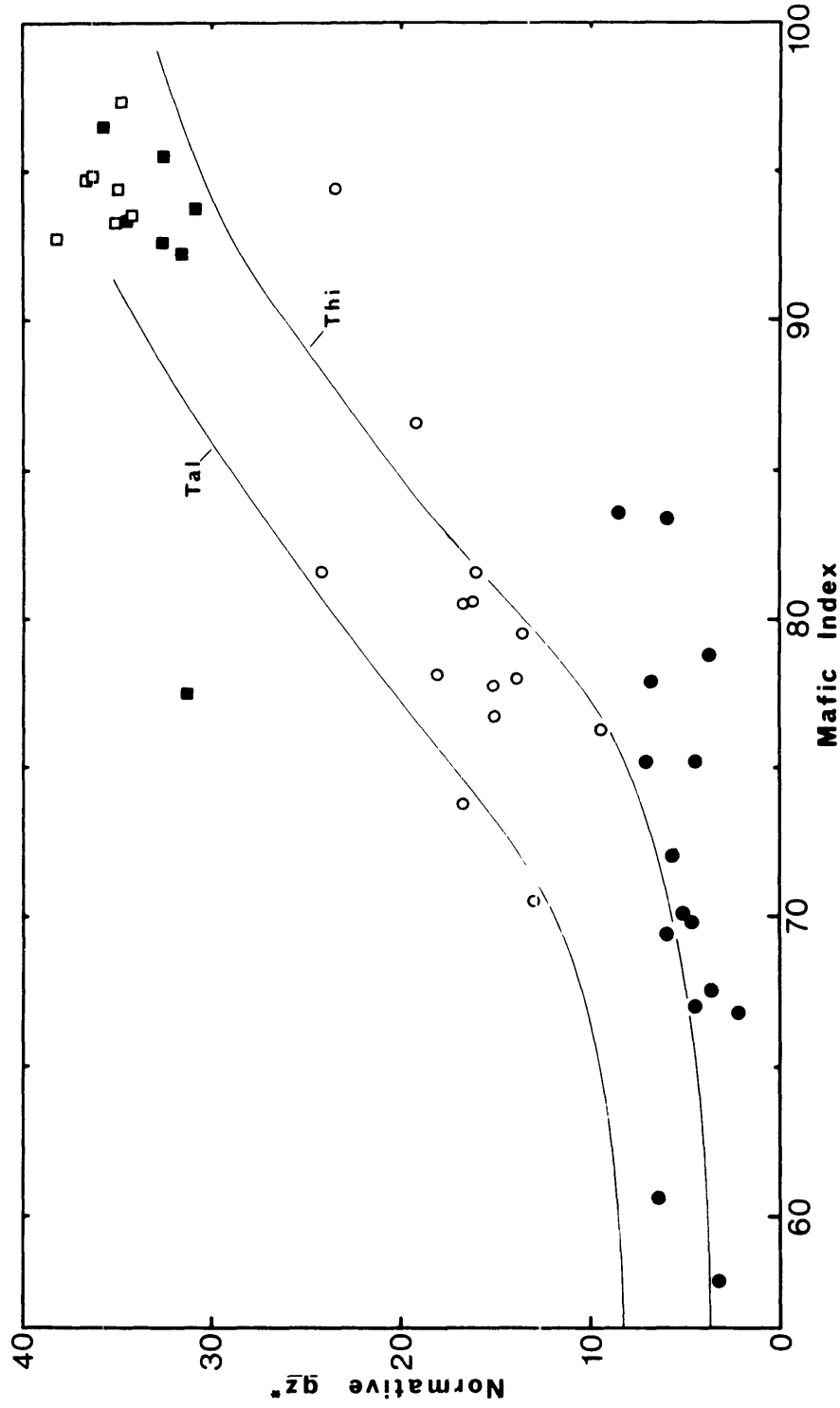

Fig. 6.5: Plot of the level of silica saturation (qz^*) against Mafic Index. The quantity qz^* represents the normative qz content when all hy is calculated as ol in the norm. Filled circles, members of the low-Si series; open circles, members of the high-Si series; filled squares, rhyolitic pitchstones; open squares, microcrystalline rhyolites. Generalized trends for the Thingmuli (Thi; Carmichael, 1964) and Talasea (Tal; Lowder & Carmichael, 1970) volcanic series are shown for comparison.

of the southern part of the Tweed Shield, are characterised by quite high K_2O contents which are reflected in the occurrence of abundant sanidine phenocrysts in porphyritic types. Na_2O is somewhat depleted relative to the more mafic rocks. The analyses listed in Table 6.3 may be divided into two groups, those of glassy lower selvages to flows and their residual glasses (Nos 1-9) and those of rocks collected from the essentially holocrystalline devitrified main body of the flows (Nos 10-16). Some interesting differences are evident between the two groups of analyses. In particular, the glassy rocks are characterised by higher CaO and H_2O + and lower Al_2O_3 and SiO_2 relative to devitrified types. These differences are reflected especially in the appearance of more an and less c in the norms of the glassy rocks.

The appearance of corundum in the norm of the rhyolites, assessed in conjunction with their depletion in Na_2O relative to the more mafic rocks, suggests that some alkali leaching may have occurred during or subsequent to solidification (Lipman, 1965; Noble, 1967). However two other observations cast doubt upon the likelihood that alkali leaching has been extensive. Firstly, normative c is more abundant in the microcrystalline rhyolites, many of which have probably crystallized directly from the rhyolitic melt than in the rhyolitic pitchstones containing abundant hydrated glass. Secondly, the analysed residual glasses (Table 6.3, Nos 2 and 6) are less peraluminous (containing normative wo) than their respective host rocks whereas their sanidine phenocrysts contain Al_2O_3 in excess of stoichiometric proportions (Section 5.4). Nevertheless it seems inevitable that at least a small amount of alkalis must have been removed during hydration of residual glasses which now contain more than 3% H_2O.

6.2 MAJOR ELEMENT VARIATION

In recent years, numerous publications have devoted considerable attention to the chemical variation exhibited by various alkaline and sub-alkaline volcanic series in which a spectrum of whole-rock compositions are developed (e.g. see Kuno, 1968; Baker, 1968; Wise, 1969; Coombs and Wilkinson, 1969; McBirney and Williams, 1969; Smith and Carmichael, 1968, 1969; Brown and Carmichael, 1971; Thompson *et al.*, 1972). It therefore seems appropriate that comments on the variation trends for individual oxides (Figs 6.6-6.13) should be adequate but concise, unless of course, petrogenetic implications demand otherwise.

For comparative purposes, generalised variation trends for Thingmuli Volcano, eastern Iceland (Carmichael, 1964) and Talasea, New Britain (Lowder and Carmichael, 1970) are also shown on the variation diagrams. These trends conveniently illustrate major element variation in typical tholeiitic (Thingmuli) and transitional to calc-alkaline (Talasea) volcanic series. Furthermore, since some Tweed volcanics show chemical characteristics more akin to typical calc-alkaline eruptives (namely low total Fe, low Fe/Mg and high Al; e.g. 27290; Duggan and Wilkinson, 1973), a curve joining the Cascade calc-alkaline averages (Carmichael, 1964) is also shown on Figures 6.6 (Al_2O_3 variation), 6.7 ($FeO+Fe_2O_3$ variation) and 6.8 (AFM diagram).

i) Variation Parameters

In depicting chemical variation within a magma series it is desirable to choose parameters which effectively reflect the major substitutions within the most important mineral phases involved in petrogenetic models. Inasmuch as any variation in a suite of volcanics resulting from crystal-liquid

equilibria will involve mainly the ferromagnesian minerals and plagioclase, the dominant substitutions will be Fe for Mg and NaSi for CaAl (Thompson, 1972a). Accordingly, parameters should be selected to reflect these substitutions. The Mafic Index (M.I. = $100(FeO+Fe_2O_3)/FeO+Fe_2O_3+MgO$; Wager and Deer, 1939; McDougall, 1962; Thompson, 1972a) and the Thornton-Tuttle Differentiation Index (D.I. = qz+or+ab+ne+lc; Thornton and Tuttle, 1960) have been chosen for this reason. The former is particularly effective in portraying variation among more mafic rocks since numerous 1 atmosphere melting studies indicate a close relationship between M.I. and the liquidus temperatures of basaltic rocks at low pressures (e.g. see Thompson, 1972a). However M.I. is rather less useful as a parameter for intermediate and acid rocks where plagioclase is commonly a liquidus phase and where separation of Fe-Ti oxides may halt or even reverse an iron-enrichment trend with falling liquidus temperature (e.g. as at Thingmuli; Carmichael, 1964). D.I. is therefore a better indicator of variation in these rocks because it provides a measure of the degree to which the salic components in a magma attain a composition appropriate to the low temperature trough in "Petrogeny's Residua System" (Ne-Ks-Qz) or in rocks with qz the "sub-system" Ab-Or-Qz (Tuttle and Bowen, 1958).

ii) Variation Trends

Aluminium: Al_2O_3 remains relatively constant throughout the two series although the high-Si series is slightly depleted in Al_2O_3 relative to the low-Si series (Fig. 6.6). The rhyolitic rocks, especially the vitric representatives, show significant depletion in Al_2O_3. Mafic members of the low-Si series are enriched in Al_2O_3 relative to comparable rocks from other

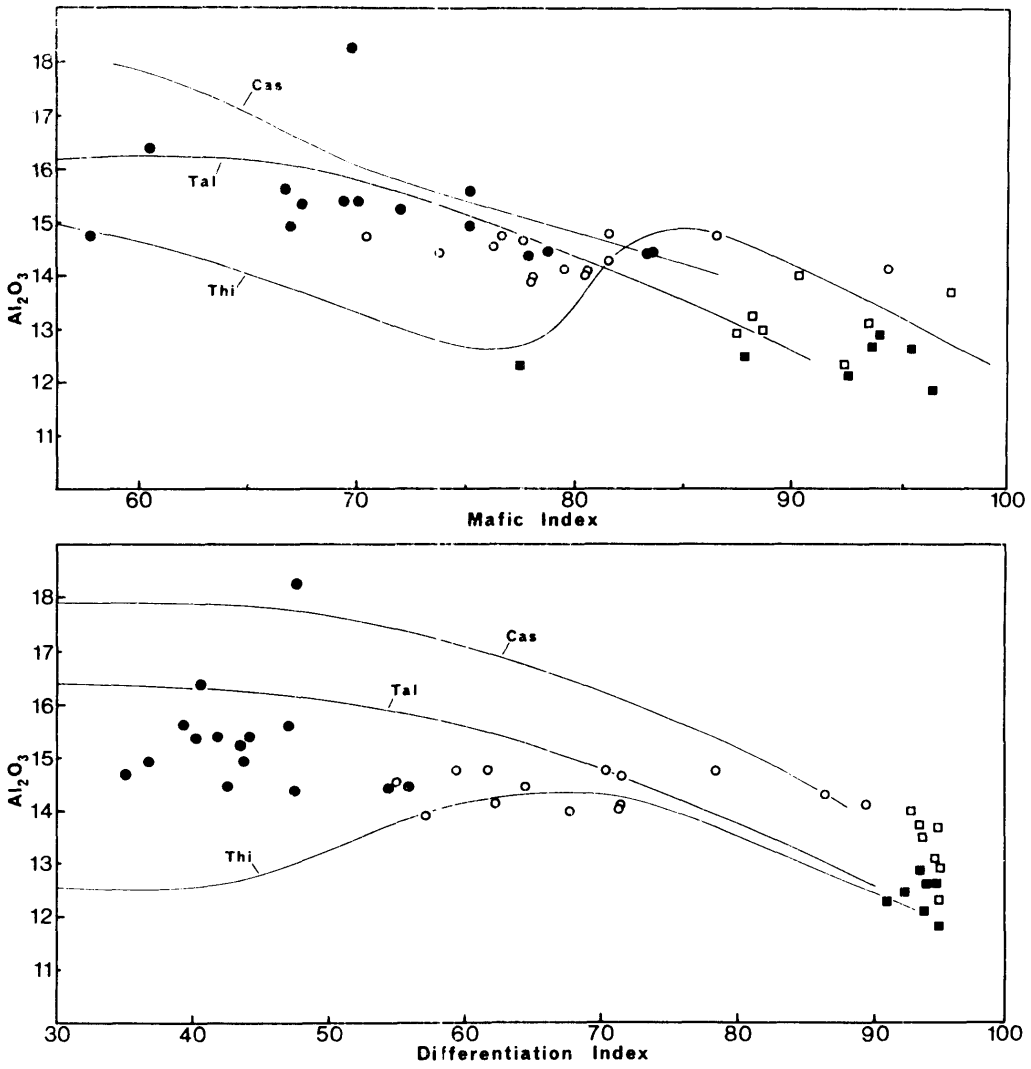

Fig. 6.6: Plot of Al_2O_3 (wt %) against Mafic Index and Differentiation Index. Filled circles, members of the low-Si series; open circles, members of the high-Si series; filled squares, rhyolitic pitchstones; open squares, microcrystalline rhyolites. Generalized trends for the Thingmuli (Thi; Carmichael, 1964), and Talasea (Tal; Lowder and Carmichael, 1970) volcanic series and a curve joining the average Cascade calc-alkaline eruptives (Cas; Carmichael, 1964) are shown for comparison.

tholeiitic series such as Hawaii (MacDonald and Katsura, 1964) and Thingmuli, Iceland (Carmichael, 1964), consistent with the appearance of plagioclase as a phenocryst phase in most of the rocks.

Iron: Total iron ($FeO+Fe_2O_3$) shows quite scattered variation in the low-Si series although a slight trend toward absolute enrichment in iron is evident (Fig. 6.7). On an AFM diagram (Fig. 6.8) this trend is more apparent. However, in a few specimens, total iron remains relatively low which results in rather low Fe/Mg ratios and a trend more akin to that of typical calc-alkaline series (e.g. Smith and Carmichael, 1968; Wise, 1969; Wilkinson, 1971). In the high-Si series, continuous alkali enrichment predominates at the expense of $FeO+Fe_2O_3$ and MgO and variation in these constituents closely parallels that of Talasea, New Britain (Lowder and Carmichael, 1970).

Magnesium: In the low-Si series, MgO decreases rapidly with increasing D.I. and M.I. from 7.5% to 2.4%, in contrast to the high-Si series where decrease in MgO is rather more gradual (Fig. 6.9). The rapid decrease in MgO in the low-Si series, coupled with an even more rapid decrease in Ni, is consistent with the fractionation of olivine as a major genetic control.

Calcium: Decrease in CaO with increasing D.I. is remarkably regular in both series from about 9.5% in the most mafic low-Si rocks to less than 1% in the rhyolites (Fig. 6.10). At equivalent D.I., the CaO content of the Tweed rocks corresponds closely to that of other subalkaline series which all show strikingly similar trends.

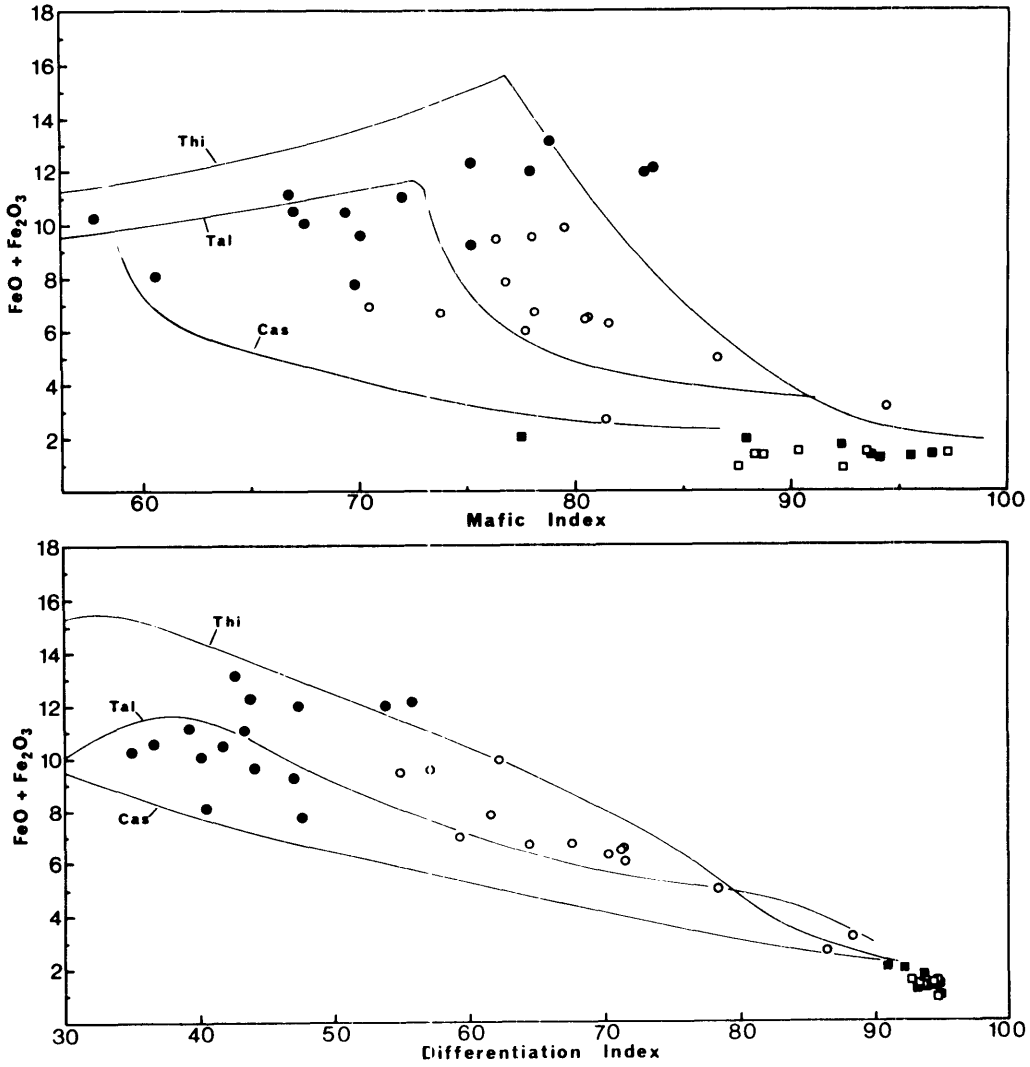

Fig. 6.7: Plot of FeO + Fe_2O_3 (wt %) against Mafic Index and Differentiation Index. Filled circles, members of the low-Si series; open circles, members of the high-Si series; filled squares, rhyolitic pitchstones; open squares, microcrystalline rhyolites. Generalized trends for the Thingmuli (Thi; Carmichael, 1964) and Talasea (Tal; Lowder and Carmichael, 1970) volcanic series and a curve joining the average Cascade calc-alkaline eruptives (Cas; Carmichael, 1964) are shown for comparison.

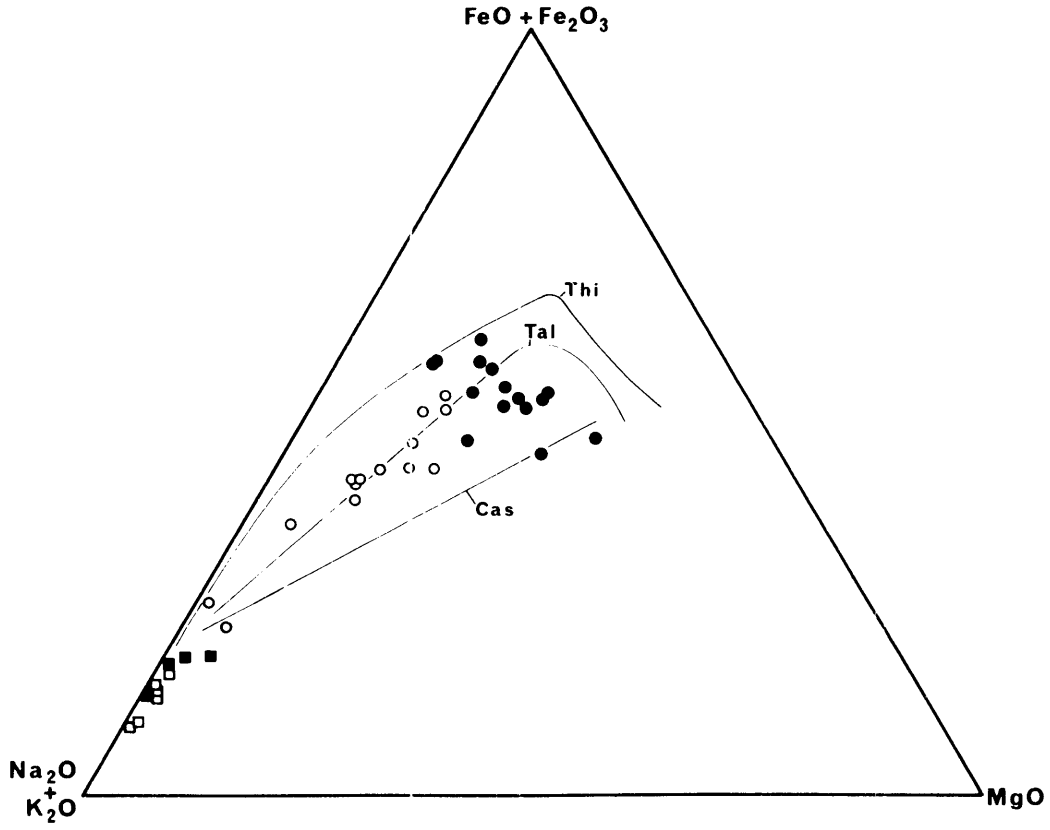

Fig. 6.8: A F M diagram (wt %) for analysed rocks from the southern portion of the Tweed Shield. Filled circles, members of the low-Si series; open circles, members of the high-Si series; filled squares, rhyolitic pitchstones; open squares, microcrystalline rhyolites. Generalized trends for the Thingmuli (Thi; Carmichael, 1964) and Talasea (Tal; Lowder and Carmichael, 1970) volcanic series and a curve joining the average Cascade calc-alkaline eruptives (Cas; Carmichael, 1964) are shown for comparison.

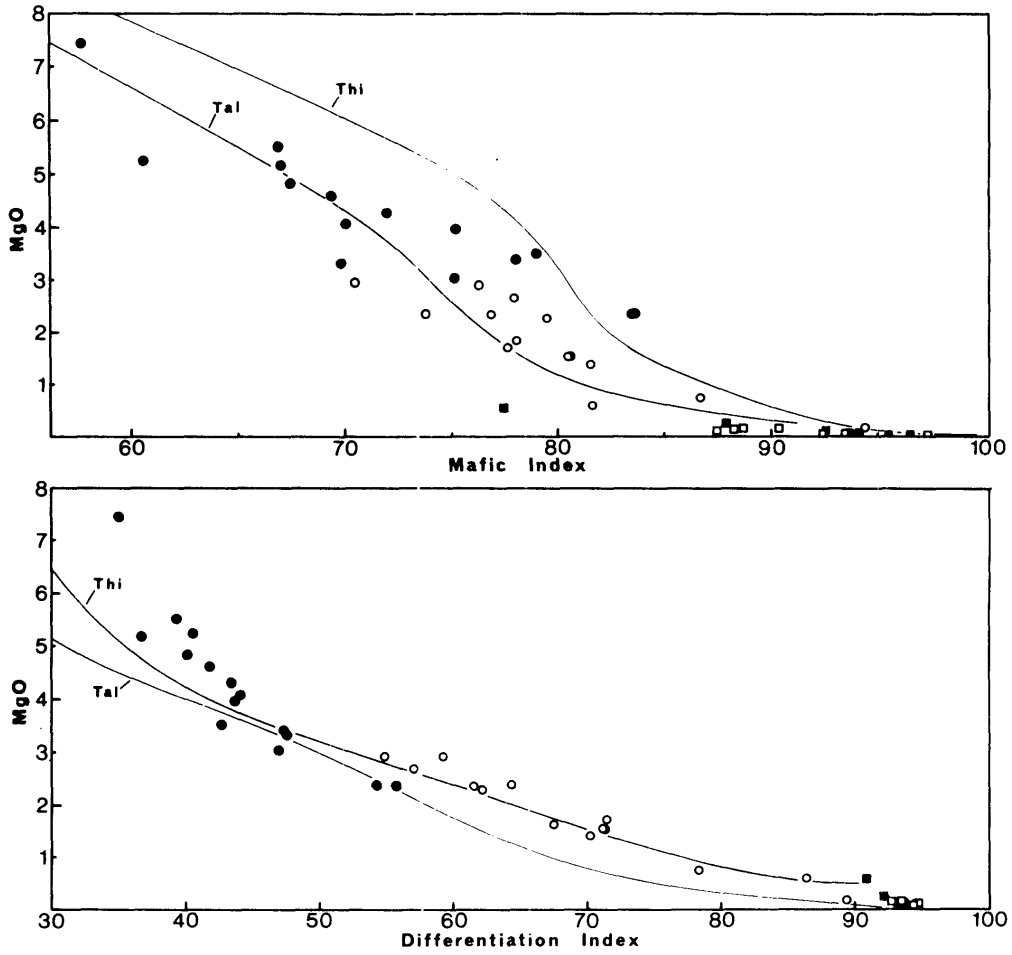

Fig. 6.9: Plot of MgO (wt %) against Mafic Index and Differentiation Index. Filled circles, members of the low-Si series; open circles, members of the high-Si series; filled squares, rhyolitic pitchstones; open squares, microcrystalline rhyolites. Generalized trends for the Thingmuli (Thi; Carmichael, 1964) and Talasea (Tal; Lowder and Carmichael, 1970) volcanic series are shown for comparison.

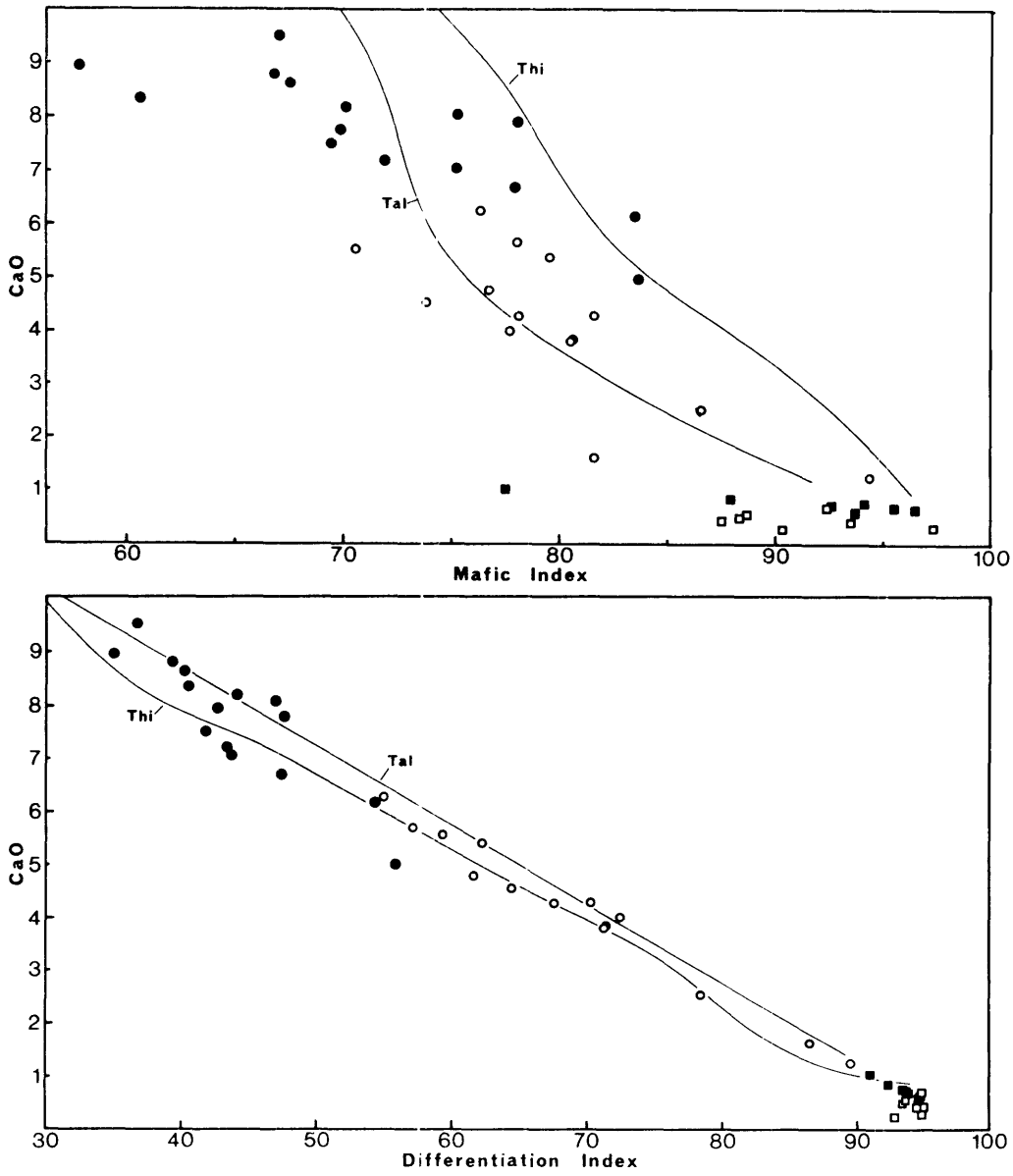

Fig. 6.10: Plot of CaO (wt %) against Mafic Index and Differentiation Index. Filled circles, members of the low-Si series; open circles, members of the high-Si series; filled squares, rhyolitic pitchstones; open squares, microcrystalline rhyolites. Generalized trends for the Thingmuli (Thi; Carmichael, 1964) and Talasea (Tal; Lowder and Carmichael, 1970) volcanic series are shown for comparison.

Alkalis: Na_2O remains relatively constant at between 3 and 4% throughout both series (Fig. 6.11) except in the rhyolitic rocks where Na_2O becomes somewhat depleted (2.5-3.1% Na_2O). This trend is similar to established trends for other subalkaline volcanic suites and contrasts with variation in many alkaline lava series where Na_2O rises progressively with increasing D.I. leading to the development of alkali-rich trachytes, phonolites and alkali rhyolites (e.g. see Coombs and Wilkinson, 1969), K_2O increases steadily throughout both series (Fig. 6.12). The rhyolitic rocks contain greater than 5% K_2O. As a consequence there is a progressive decrease in Na_2O/K_2O ratio from 4-5 in the most mafic rocks to about 0.5 in the rhyolites.

Other Oxides: The minor oxides, TiO_2 P_2O_5 and MnO increase slightly with D.I. and M.I. in the low-Si series but decrease throughout the high-Si series (Fig. 6.13). TiO_2 is also somewhat depleted in the most evolved low-Si series rocks.

6.3. TRACE ELEMENT DATA

Trace element data for the tholeiitic rocks are listed in Tables 6.5-6.7 together with various element ratios cited below and in subsequent discussion. The data, although only available for a limited number of elements, nevertheless provide some valuable insights into various petrogenetic aspects of the rocks, in particular the relationship between the low-Si and high-Si series and between the high-Si series and the rhyolites.

Although it is not desirable at this stage to prejudge a fractional crystallization origin for any of the tholeiitic rocks (the genesis of which will be considered fully in Chapter 7), the chemical data outlined below and

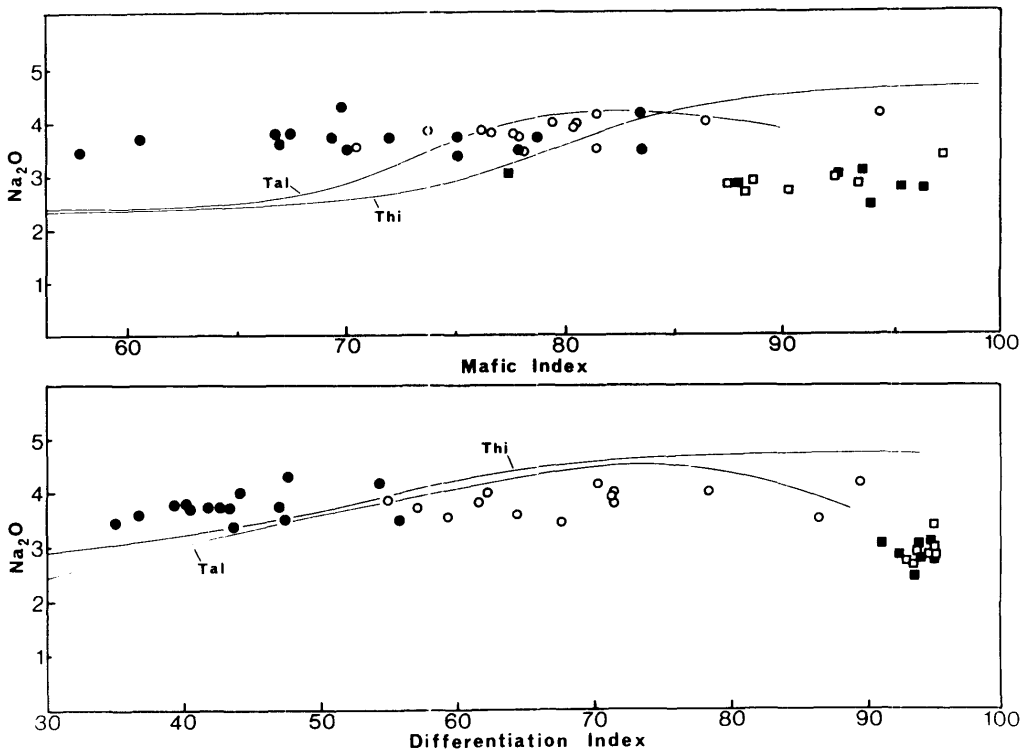

Fig. 6.11: Plot of Na_2O (wt %) against Mafic Index and Differentiation Index. Filled circles, members of the low-Si series; open circles, members cf the high-Si series; filled squares, rhyolitic pitchstones; open squares, microcrystalline rhyolites. Generalized trends for the Thingmuli (Thi; Carmichael, 1964) and Talasea (Tal; Lowder and Carmichael, 1970) volcanic series are shown for comparison.

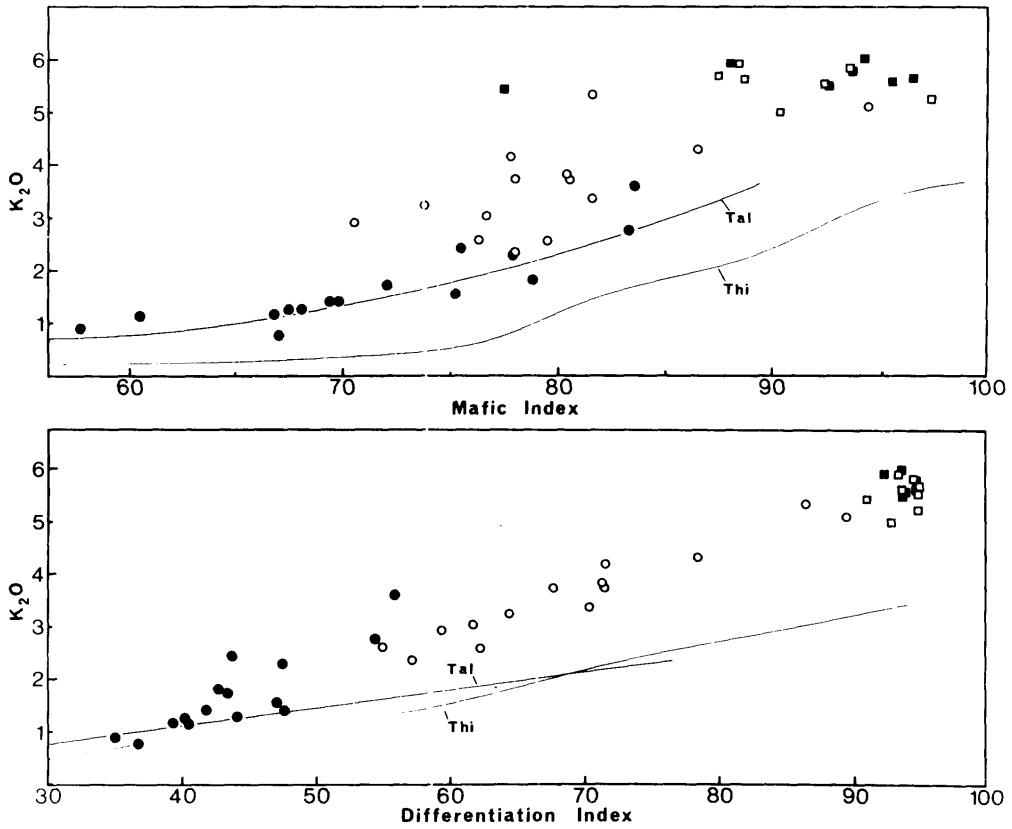

Fig. 6.12: Plot of K_2O (wt %) against Mafic Index and Differentiation Index. Filled circles, members of the low-Si series; open circles, members of the high-Si series; filled squares, rhyolitic pitchstones; open squares, microcrystalline rhyolites. Generalized trends for the Thingmuli (Thi; Carmichael, 1964) and Talasea (Tal; Lowder and Carmichael, 1970) volcanic series are shown for comparison.

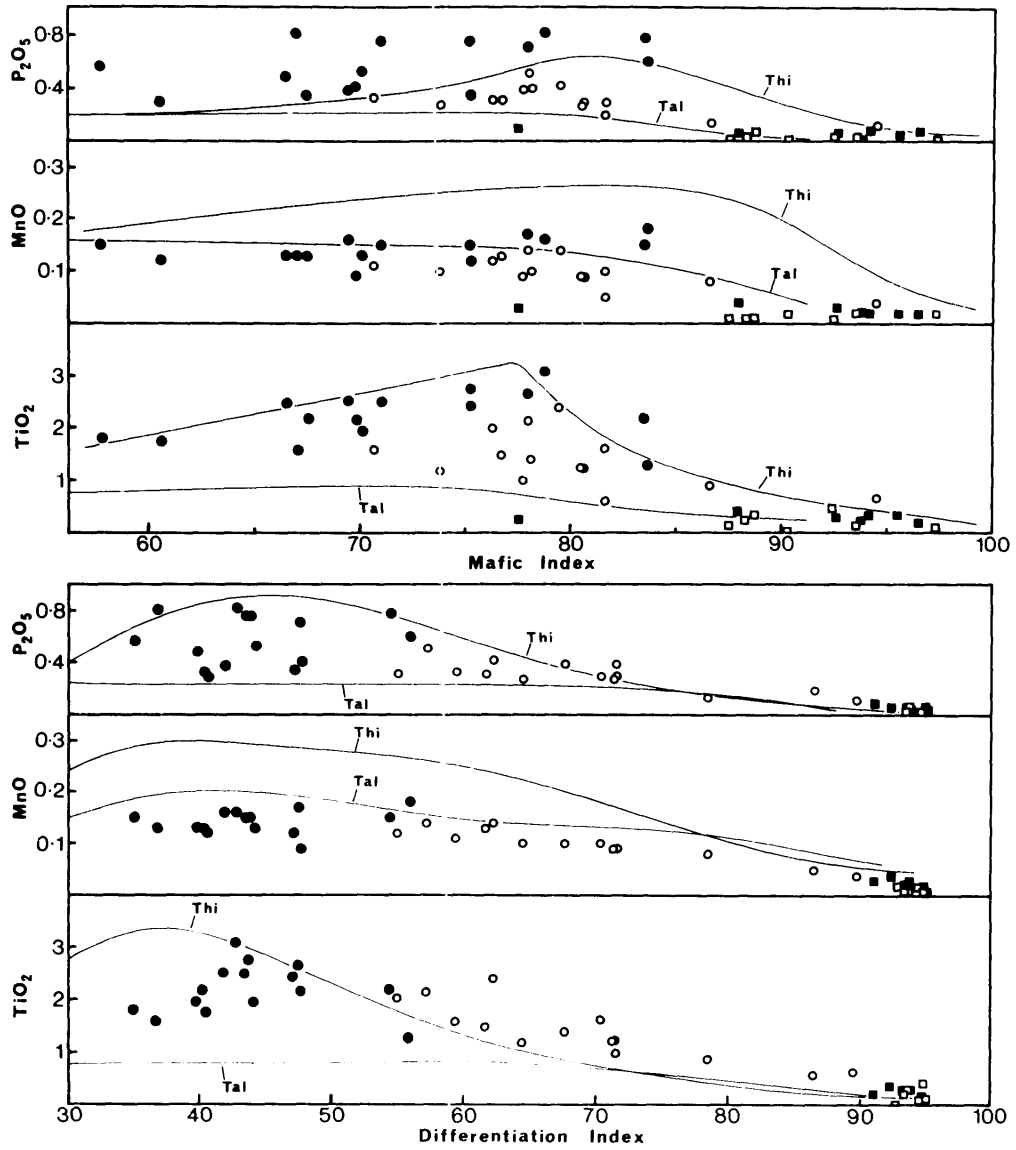

Fig. 6.13: Plots of the oxides P_2O_5, MnO and TiO_2 (wt %) against Mafic Index and Differentiation Index. Filled circles, members of the low-Si series; open circles, members of the high-Si series; filled squares, rhyolitic pitchstones; open squares, microcrystalline rhyolites. Generalized trends for the Thingmuli (Thi; Carmichael, 1964) and Talasea (Tal; Lowder and Carmichael, 1970) volcanic series are shown for comparison.

TABLE 6.5

TRACE ELEMENT ANALYSES OF ROCKS OF THE LOW-Si SERIES (PPM)

Analysis No	1	2	3	4	5	6	7	8	9	10	11
Specimen No	28046	28047	28048	28049	28050	28051	28052	28053	28055	27290	27291
V	140	134	129	130	147	148	164	158	88	92	36
Ni	183	120	78	89	39	15	24	55	10	37	31
Co	37	39	30	46	47	35	31	39	30	21	28
Ba	214	228	277	558	543	490	293	-	664	412	838
Rb	20	16	31	34	46	38	29	24	62	20	81
Sr	439	565	516	541	511	491	442	445	389	837	271
K/Rb	441	494	365	510	527	472	446	405	443	697	440
Ba/Rb	10.6	14.6	8.8	16.6	11.1	12.9	10.3	-	10.7	20.5	10.3
Ca/Sr	146	120	116	95	99	116	133	141	113	67	81

For key to specimen localities see Table 6.1.

Element ratios calculated before rounding off data.

Analyst: M.B. Duggan.

TABLE 6.6

TRACE ELEMENT ANALYSES OF ROCKS OF THE HIGH-Si SERIES (PPM)

Analysis No	1	2	3	4	5	6	7	8	9	10	11	12
Specimen No	28061	28062	28063	28064	28065	28066	28067	28070	28071	28072	28073	28074
V	89	106	164	75	147	153	72	64	36	36	26	10
Ni	32	33	14	22	13	61	13	16	16	6	11	9
Co	20	23	29	19	28	26	15	15	14	9	5	4
Ba	481	453	494	494	414	445	513	539	399	589	496	720
Rb	84	86	69	85	66	69	113	99	146	139	187	155
Sr	292	346	348	258	364	328	231	236	288	164	119	92
K/Rb	358	336	338	377	394	374	336	376	286	309	284	326
Ba/Rb	5.72	5.26	7.14	5.79	6.30	6.50	4.54	5.45	2.73	4.24	2.65	4.65
Ca/Sr	117	115	117	126	123	118	118	130	94	111	97	98

For key to specimen localities see Table 6.2.

Element ratios calculated before rounding off data.

Analyst: M.B. Duggan.

TABLE 6.7

TRACE ELEMENT ANALYSES OF RHYOLITIC PITCHSTONES AND MICROCRYSTALLINE RHYOLITES (PPM)

Analysis No	1	2	3	4	5	6	7	8
Specimen No	28075	28076	28077	28078	28079	28082	28083	28088
V	12	7	5	5	8	0.3	11	3
Ni	18	8	6	17	6	4	7	7
Co	3	3	2	2	2	2	2	1
Ba	70	140	<100*	<100*	<100*	<100*	-	70
Rb	246	221	252	215	203	560	215	259
Sr	48	28	33	27	40	n.d.	44	17
K/Rb	220	248	228	260	272	93	273	218
Ba/Rb	0.29	0.62	-	-	-	-	-	0.28
Ca/Sr	154	186	138	170	108	-	81	187

For key to specimen localities see Table 6.3.

Element ratios calculated before rounding off data.

* Determined by atomic absorption spectrophotometry. nd = not detected.

Analyst: M.B. Duggan.

in the previous section provide strong support to fractionation processes as a major petrogenetic control. Consequently, it is more convenient, merely for ease of presentation, to consider the trace element data predominantly in the light of such processes. Variation in trace element contents is therefore assessed in terms of the observed phenocryst phases insofar as these will normally be the phases available for fractionation.

Variation in the trace elements with Differentiation Index is illustrated in Figures 6.14 and 6.15 and the principle features of this variation are now summarised.

Vanadium. Vanadium is relatively constant in the more mafic rocks of the low-Si series at between 130 and 160 ppm. However in the most evolved members of the low-Si series V is significantly depleted (as low as 36 ppm). In the high-Si series V decreases rapidly with increasing D.I. (Fig. 6.14) and variation closely parallels the trend for Talasea, New Britain (Lowder and Carmichael, 1970).

Vanadium substitutes for Fe^{3+} in crystal lattice sites and therefore readily enters titanomagnetite and to a lesser extent ilmenite and clinopyroxene but it is virtually excluded from olivine because of charge balance difficulties (Taylor, 1965; Prinz, 1967). The relatively constant V in all but the most evolved members of the low-Si series is therefore consistent with the late appearance of Fe-Ti oxides in the crystallization sequence of these rocks. Depletion of V in the most evolved rocks of the series coincides with the appearance of titanomagnetite as an early crystallizing phase and therefore probably reflects incorporation of some titanomagnetite in the

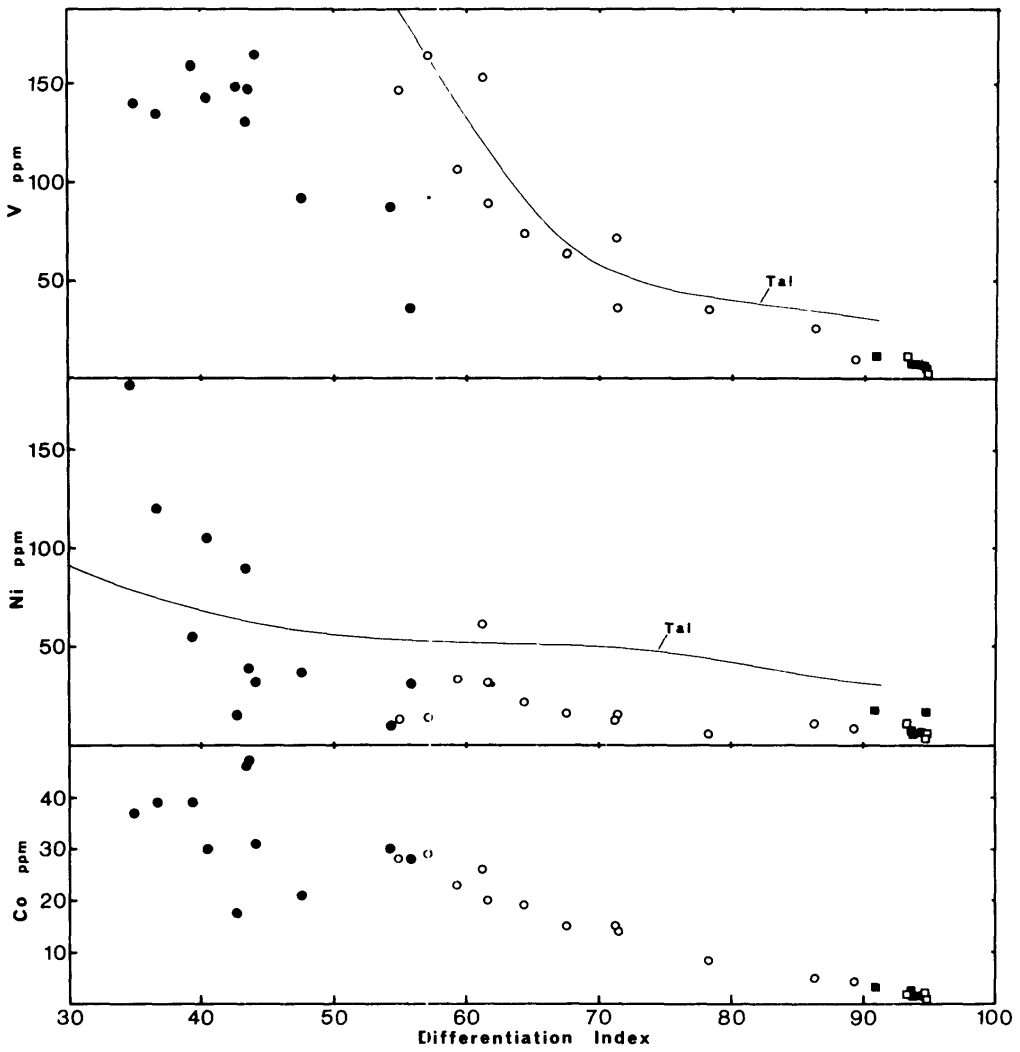

Fig. 6.14: Plots of the trace elements V, Ni and Co (ppm) against Differentiation Index. Filled circles, members of the low-Si series; open circles, members of the high-Si series; filled squares, rhyolitic pitchstones; open squares, microcrystalline rhyolites. Generalized trends for the Talasea volcanic series (Tal; Lowder and Carmichael, 1970) with respect to V and Ni are shown for comparison.

crystal assemblage being removed during fractionation. It is notable that these rocks are also depleted in TiO_2 relative to the more mafic members of the series (Fig. 6.13).

Nickel. Ni decreases rapidly with increasing D.I. in the mafic rocks of the low-Si series. In the high-Si series, Ni varies considerably in the mafic members and then decreases slowly through the series to the acid rocks.

The geochemical behavior of Ni is relatively complex (Ringwood, 1955; Taylor, 1965). However it enters most readily into the olivine structure and less readily into pyroxenes and Fe-Ti oxides. In the low-Si series, the strong depletion in Ni with increasing D.I. (180 down to 10 ppm) corresponds to a similar decrease in the abundance of olivine phenocrysts, these being absent from the most evolved rocks of the series. This variation is therefore consistent with fractional crystallization processes with olivine as an important phase.

A small amount of Ni contamination during the crushing process cannot be excluded in the rhyolitic rocks which show relatively high Ni (3-15 ppm) for rocks of this type.

Cobalt. In the low-Si series, variation is rather scattered in the range 15-50 ppm (Fig. 6.14). However in the high-Si series there is a progressive decrease in Co with increasing D.I. from about 25 ppm down to 5 ppm.

Co shows a strong coherence with total Fe+Mg (Carr and Turekian, 1961) and it is therefore preferentially incorporated in olivine and

pyroxenes but with lower abundances than Ni (Prinz, 1967). The scattered variation of Co in the low-Si series is therefore somewhat aberrant. However it is consistent with proposals, which will be detailed in Chapter 7, that these rocks are not directly related by a single liquid line of descent and the scatter may reflect the variable importance in their genesis of high pressure fractionation of ortho- and clinopyroxene in addition to olivine.

In the high-Si series, the regular decrease in Co through the series is quite consistent with proposals that these rocks evolved along a single liquid line of descent by fractionation of pyroxenes and plagioclase with minor olivine and ilmenite (Chapter 7).

Barium. Ba increases quite rapidly with increasing D.I. in the low-Si series but rather less rapidly in the high-Si series (Fig. 6.15). However increase in Ba in the latter series is steady through to rhyodacite. In the rhyolitic rocks, strong depletion of Ba (usually <100 ppm) is evident relative to more mafic rocks, in direct contrast to the Thingmuli rhyolites which are strongly enriched in Ba (1000 ppm; Carmichael *et al.*, 1974, p.75).

Ba substitutes for K in mineral lattices and is therefore preferentially incorporated in K-bearing minerals, especially K-feldspar and to a very much smaller extent, plagioclase (Prinz, 1967). Consequently, Ba will increase in a fractionating liquid until the final stages where either the fractionating plagioclase becomes sufficiently potassic to enable entry of significant amounts of Ba into the structure or else a discrete K-feldspar phase begins to separate. The latter case seems especially relevant to the genesis of the Ba-depleted Tweed rhyolites in which K-feldspar is a common phenocryst phase. This will be discussed further in Chapter 7.

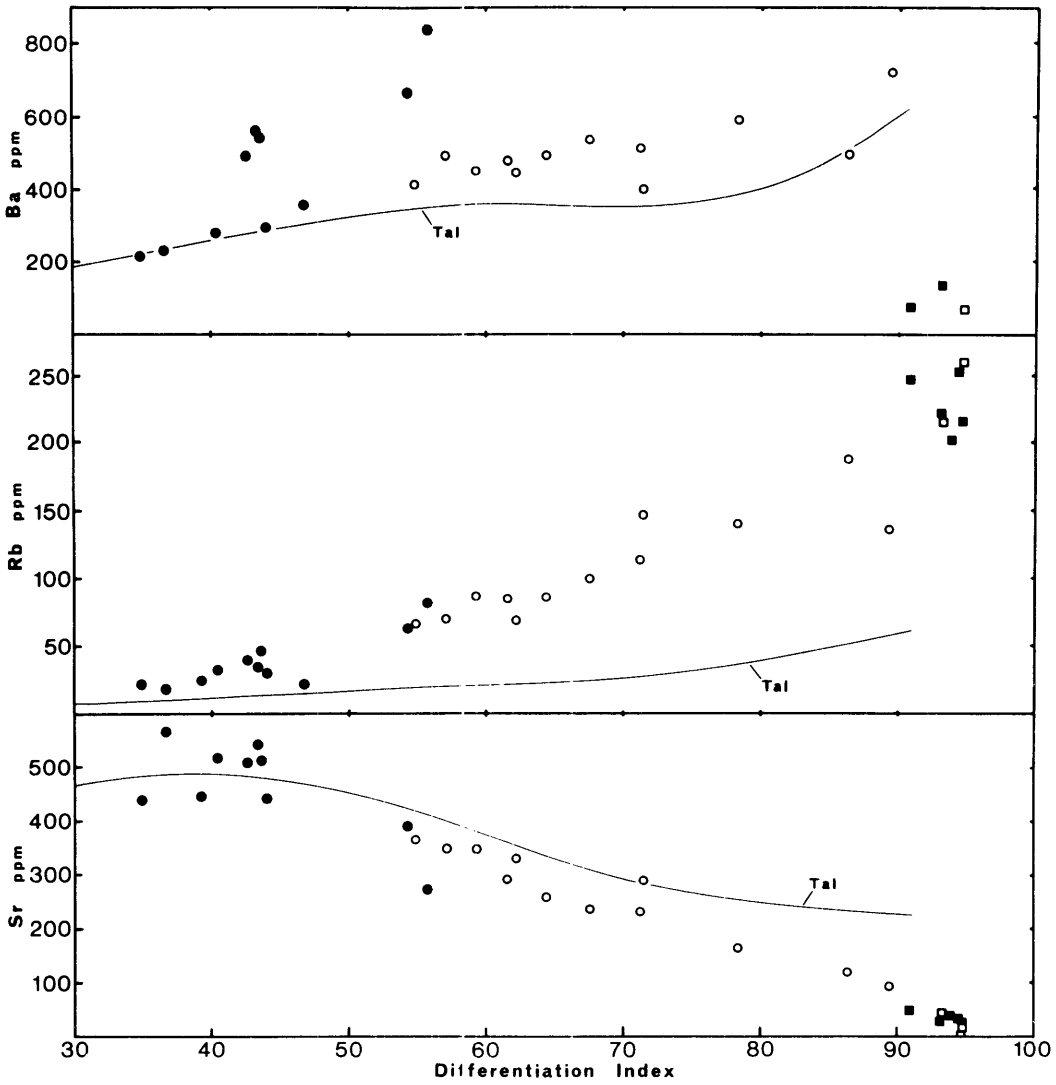

Fig. 6.15: Plots of the trace elements Ba, Rb and Sr (ppm) against Differentiation Index. Filled circles, members of the low-Si series; open circles, members of the high-Si series; filled squares, rhyolitic pitchstones; open squares, microcrystalline rhyolites. Generalized trends for the Talasea volcanic series (Tal; Lowder and Carmichael, 1970) are shown for comparison.

The apparently divergent Ba trends in the low-Si and high-Si series may reflect a high component of (? more sodic) plagioclase involved in fractionation processes in the high-Si series. Ba/Rb ratios (Fig. 6.16) are quite distinct in each group of rocks, being lower in the high-Si series (2-8) than in the low-Si series (10-20) and lower again in the rhyolites (<0.5).

Rubidium. Throughout both series Rb increases regularly with increasing D.I. (Fig. 6.15) in accordance with its rejection by all the major mineral phases. A significantly higher Rb content is evident in the rhyolitic rocks compared with the salic rocks of the high-Si series. K/Rb ratios are relatively distinct in each of the three rock groups. They are rather high (400-550) in the low-Si series, somewhat lower (275-400) in the high-Si series and lower again (200-275) in the rhyolites. However variation in K/Rb ratios within each group is quite unsystematic.

A marked coherence in geochemical behavior is evident between Rb and K although entry of Rb into K lattice sites is hampered by the larger size of the Rb^+ ion (1.48Å) relative to the K^+ ion (1.33Å). However this difference only becomes important in cases of extreme fractionation where K-bearing phases (notably K-feldspar) are fractionating from the liquid. In this case significant enrichment in Rb and lowering of the K/Rb ratio may occur. The strong Rb enrichment in the rhyolites relative to the icelandites and rhyodacites of the high-Si series is therefore consistent with a proposal that the rhyolites represent extreme fractionates of a more basic tholeiitic magma (Chapter 7). One analysed rhyolite (28082) shows extreme Rb enrichment which, when assessed in conjunction with a total depletion in Sr and a very

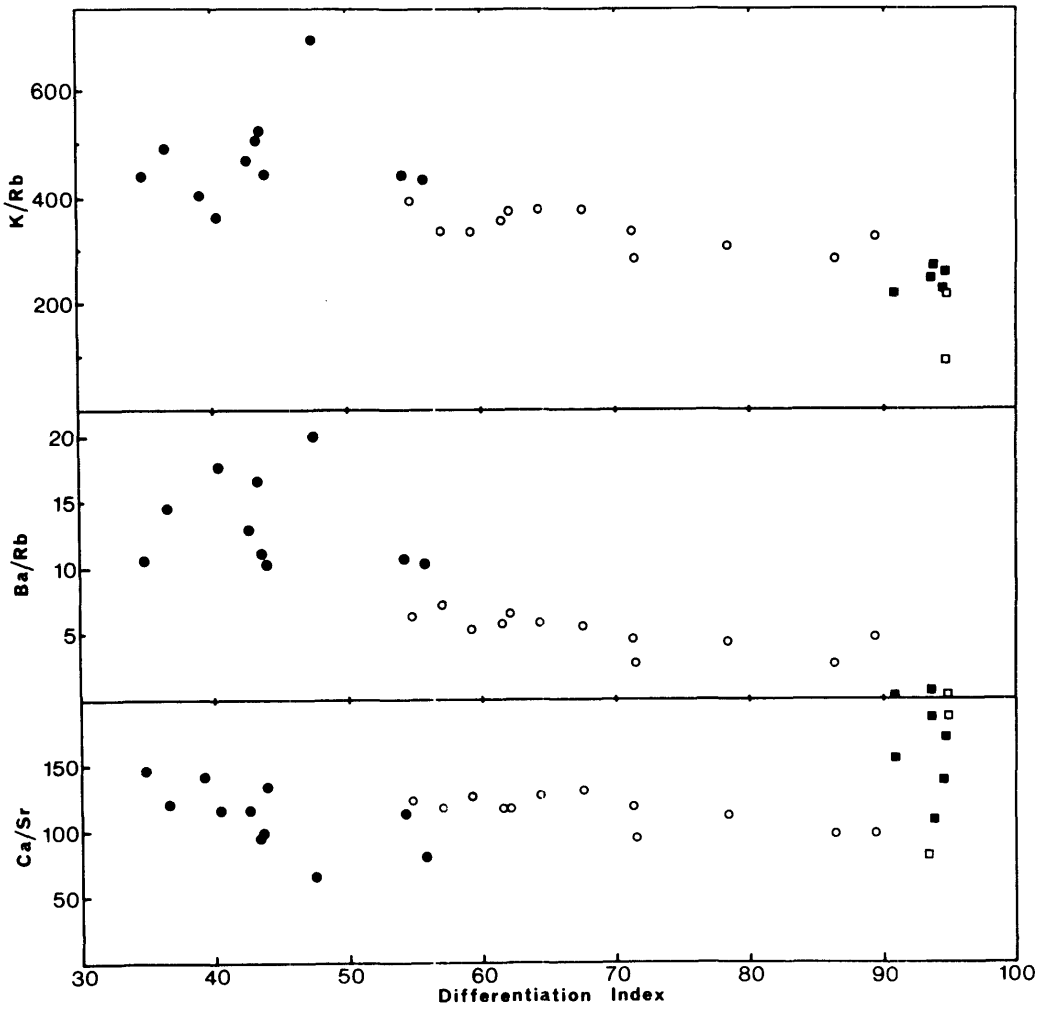

Fig. 6.16: Plots of K/Rb, Ba/Rb and Ca/Sr ratios against Differentiation Index. Filled circles, members of the low-Si series; open circles, members of the high-Si series; filled squares, rhyolitic pitchstones; open squares, microcrystalline rhyolites.

low K/Rb ratio (93), suggests extreme fractionation of the parent liquid relative to the other rhyolitic rocks. Similar rhyolites also occur on the northern flanks of the Shield (A. Ewart, personal communication, 1973).

Strontium. Among the more mafic members of the low-Si series, Sr variation is rather unsystematic. However in the most evolved members of the low-Si series, and throughout the high-Si series, there is a progressive decrease in Sr with increasing D.I.

Sr enters Ca lattice sites in plagioclase with some difficulty but is virtually exluded from the pyroxene structure (Taylor, 1965). Consequently the Ca/Sr ratio may fall slightly with fractionation of these minerals. On the other hand Sr is readily incorporated into the K-feldspar lattice and therefore fractionation of this mineral will significantly increase the Ca/Sr ratio. Hence the wide variation in Ca/Sr ratios of the rhyolites is especially significant and is compatible with the previous proposal that some fractionation of K-feldspar from the parent liquid has occurred during their formation.

CHAPTER 7

DISCUSSION

7.1 GENERATION OF PARENT MAGMAS AND THE POTASSIUM CONTENT OF THOLEIITIC ROCKS

Low pressure experimental data on basaltic compositions indicate the presence of a thermal divide corresponding to the critical plane of silica undersaturation in the "basalt tetrahedron" Di-Fo-Ne-Qz (Yoder and Tilley, 1962). This divide effectively precludes a direct genetic relationship between hypersthene normative and nepheline normative magmas at low pressures, a relationship which had been widely proposed in earlier studies (Bailey *et al.*, 1924; Bowen, 1928; Tilley, 1950). However at higher pressures (>9 kb) the thermal barrier no longer persists (Green and Ringwood, 1967). Therefore the continuum of basaltic compositions across the thermal divide strongly suggests that these rocks derive at pressures >9 kb (35-40 km) and thus within the upper mantle. Seismic data (Powers, 1955; Eaton and Murata, 1960) recorded prior to and during Hawaiian volcanic eruptions indicate direct ascent of magma from depths of 55-60 km.

Large cognate phenocrysts (megacrysts) of high pressure origin preserved in alkaline (Kuno, 1964; Binns *et al.*, 1970; Frisch and Wright, 1971) and tholeiitic (Jamieson, 1966; Nicholls and Lorenz, 1973; Duggan and Wilkinson, 1973) volcanics indicate rapid transportation to the surface from their sites of crystallization within the upper mantle or from near the crust-mantle boundary. In addition, alkaline rocks containing ultramafic xenoliths must have ascended rapidly from mantle depths (at rates of the order of 1-10 cm/sec) in order to prevent settling of these inclusions

(Maaløe, 1973a). It is therefore obvious that many basaltic lavas must represent essentially unmodified magma derived from upper mantle depths and may be considered as primary magmas. The chemical characteristics of primary magmas will be dependent upon the degree of partial melting and the nature of the source rock. It is upon the composition of this source rock that conflict of opinion exists among experimental petrologists.

Green and Ringwood (1967) have proposed a hypothetical "pyrolite" model for the upper mantle; the most recently proposed composition for pyrolite is one part typical Hawaiian olivine tholeiite and three parts peridotite (Pyrolite III; Ringwood, 1966). Green and Ringwood envisage 30% partial melting of "pyrolite" producing olivine tholeiitic liquids, with lower degrees of melting producing alkaline liquids and very small degrees of melting producing ultra-alkaline (nephelinitic) liquids. A petrogenetic grid based on this model was recently proposed (Green, 1970, 1971) which relates magma type and degree of melting to depth of melting of pyrolite in the presence of small amounts of water (~0.1% H_2O).

As an alternative to the Green-Ringwood model, O'Hara (1965, 1968) proposed a garnet peridotite mantle in which up to 15% of picritic hy-normative liquid may be derived by partial melting. He proposed that high pressure eclogite fractionation of Ca-pyroxene and garnet from this liquid coupled with low pressure olivine fractionation could produce the spectrum of silica saturation levels observed in natural basaltic magmas.

A more detailed evaluation of these models is not relevant to this discussion because the tholeiitic lavas in the Tweed Shield are all quite evolved relative to demonstable primitive magmas in terms of their

Mg/Mg+Fe ratios (Roeder and Emslie, 1970; Green, 1973a,b) and normative plagioclase compositions. In fact, the most mafic tholeiitic rock analysed from the southern part of the Tweed Shield has 100 Mg/Mg+Fe = 57 and a normative plagioclase 100 an/ab+an = 43 in contrast to typical basalts which have 100 Mg/Mg+Fe = 63-73 (Green, 1971) and 100 an/ab+an = 50-65. It is therefore most important to investigate possible processes which may have produced the chemical features of the low-Si series, especially in view of the presence in some of these lavas of high pressure cognate phases (plagioclases and pyroxenes) indicating rapid rise of magma from near the crust-mantle boundary (Duggan and Wilkinson, 1973).

The significance and origin of the high K contents and associated elements (e.g. the incompatible elements, including P, Ba, Rb and Sr which do not substitute readily in major silicate phases; Green and Ringwood, 1967) of many volcanic rock series is a major petrogenetic problem, especially for K-rich tholeiitic sequences. Various hypotheses for enrichment in K have been reviewed recently by Jamieson and Clark (1970) and proposed models are briefly reviewed in relation to the Tweed low-Si series below.

1. Degree of Melting of Mantle Material

Although small degrees of melting of quite K-poor peridotite (K_2O <0.2%) may produce significant K enrichment in the derivative liquids, it is doubtful whether tholeiitic liquids can be produced by the small degrees of melting (~5%) required to produce the appropriate degree of K enrichment. Experimental data (Bultitude and Green 1971; Green, 1970,1971,1973a,b) indicate that small degrees of melting of peridotite (pyrolite) source rocks will produce highly undersaturated nephelinitic liquids so that although

this process may adequately explain alkali enrichment in many alkaline rocks it appears to be of little significance in tholeiitic magma generation where significant degrees of partial melting at the source region are inferred.

2. Crystal-Liquid Fractionation

Jamieson and Clark (1970) show that low pressure fractionation alone is incapable of producing the range of K contents (K_2O = 0.1-2.5%) observed in tholeiitic volcanic suites. They suggest that a process of "eclogite fractionation" i.e. fractionation of aluminous clinopyroxene and garnet (O'Hara and Yoder, 1967) at pressures in excess of 25 kb may produce a wide range in K_2O contents without significantly altering other major element abundances. However, eclogite fractionation should produce a calc-alkaline trend (T.H. Green and Ringwood, 1968; Ringwood, 1974), in contradistinction to the overall character of the low-Si series, especially with respect to iron and qz enrichment.

3. Upper Mantle Wall Rock Alteration

This model includes the wall rock alteration process envisaged by Green and Ringwood (1967) and the closely similar "zone refining" concept of Harris (1957) whereby continuous dissolution of mantle peridotite accompanied by precipitation of the major peridotite phases produces enrichment of the incompatible elements in the melt. The effectiveness of these processes during repeated episodes of melting has been questioned on the grounds that their efficiency will rapidly decrease with progressive depletion of the mantle in K_2O and also as the magma conduits coalesce to

form larger channels (O'Hara, 1968; Jamieson and Clark, 1970). Its applicability in the Tweed Shield where a large volume of volcanic material has been erupted in a relatively localised area is especially doubtful.

4. Crustal Wall Rock Alteration

Large scale enrichment of basaltic rocks in potassium and associated elements by magmatic assimilation (Engel *et al.*, 1965) or wall rock leaching seems unlikely for several reasons. Firstly, Jamieson and Clark (1970) show that enrichment factors for these elements in a sequence of K-rich olivine tholeiites from Rhodesia relative to abyssal tholeiites vary widely and are not reflected in any enrichment in SiO_2. Secondly, not all basalts erupted in a continental environment are enriched in K (e.g. Baffin Bay, Greenland; Clark, 1972). Furthermore, it seems likely that successive batches of magmas should be progressively depleted in K_2O if some "magmatic leaching" process were operative as the crustal material was progressively depleted in potash and that this depletion should be reflected in progressively increasing Na/K ratios. No such depletion with time is evident. On the other hand if wholesale assimilation of sialic material had taken place one would expect an abundance of partially fused sialic material (cf. Steiner, 1958) in the rocks and perhaps a trend of strong qz enrichment with increasing K_2O. Neither feature is observed to any significant extent in the Tweed sequence. Addition of low melting sialic material would also produce an aberrant qz enrichment trend. Finally, high pressure phases preserved in many rocks similarly enriched in K_2O in the low-Si series indicate relatively rapid ascent of the host liquids from the depths at which these phases precipitated (cf. Maaløe, 1973a), which is thought to be broadly equivalent to the crust-mantle boundary

(Duggan and Wilkinson, 1973). A similar argument is valid for the potassic olivine-rich lavas of the Nuanetsi igneous province in Rhodesia (Jamieson, 1966) and the Saar Nahe Trough tholeiites (Nicholls and Lorenz, 1973).

5. Mantle Inhomogeneity

While the above processes assume a homogeneous K-poor zone of magma generation, the possibility remains that the mineralogical and geochemical constitution of the mantle is quite heterogeneous and that gross variations observed between magmatic series in different areas reflect this variation.

Phlogopitic mica and pargasitic amphibole, stable phases at upper mantle depths (Kushiro, 1970), are not uncommon accessory phases in many peridotite nodules in alkali volcanics (Varne, 1968,1970; Dawson *et al.*, 1970; Frey and Green, 1974). As such they represent a potential source of K even if only present in minor amounts. For example, a peridotite source rock containing 1% phlogopite could, providing the phlogopite were completely incorporated in the melt phase, yield about 20% of liquid containing 0.5% K_2O. Assuming a peridotite source rock with small amounts (1-5%) of phlogopite, essential features of the melting process are illustrated by phase equilibrium studies in the system forsterite-diopside-silica (Bowen, 1914, Kushiro and Schairer 1963; Kushiro, 1964) and on the assemblage phlogopite-enstatite (Modreski and Boetcher, 1972). At 20 kb under water deficient conditions phlogopite + enstatite would begin to melt at about 1050-1100°C to produce Fo + water deficient liquid. The nature of this liquid will depend upon the amount of En involved in the melting. A substantial quantity of enstatite must be melted with phlogopite in order

to produce a K-bearing liquid which is sufficiently hy-normative to be capable of fractionating to oversaturated compositions.

Another model for mantle inhomogeneity has been proposed by Green (1970), in which the low velocity layer is envisaged as the principal zone of magma generation and is vertically zoned with respect to the incompatible elements which concentrate towards the top of this zone. Thus the K-poor abyssal tholeiites of the mid-ocean ridges may represent melted material (20% melting) from the K-depleted portion of the low velocity zone while the relatively more K-rich tholeiites of, for example, the Hawaiian Islands represent a similar degree of melting within the K-enriched zone.

It has recently been proposed that the Tweed Shield Volcano, together with many other eastern Australian Cainozoic volcanic provinces, originated during lithospheric plate passage over a mantle melting source (Wellman and McDougall, 1974a; see Section 7.7). This model partially alleviates problems of element depletion in successive magma batches since a volcanic province of limited areal extent would continually tap a different portion of the melting source. In fact if one accepts a proposed spreading rate of 66 mm/year (Wellman and McDougall, 1974a) the plate may move some 240 km during the eruption span of the Tweed Shield Volcano (3.0 m.y., Wellman and McDougall, 1974b).

In summary, of the five models for K enrichment discussed above, the first (small degrees of melting) and fourth (crustal wall rock reaction, including contamination) appear to have little applicability. On available evidence the second (crystal liquid fractionation, especially ecologite fractionation) and fourth (mantle wall rock alteration) may have been of

minor importance. However, mantle inhomogeneity, either in a lateral or vertical sense, is probably the most significant factor. It is not possible to determine however whether this inhomogeneity is brought about by vertical zonation in the partially liquid low velocity zone or by the presence of small amounts of mica and/or amphibole in the source area.

7.2 EVOLUTION OF THE LOW-Si SERIES

A fractional crystallization origin has commonly been ascribed to the more evolved members of tholeiitic volcanic associations, with olivine tholeiite or, more rarely, tholeiitic picrite as the favoured parent magma (e.g. Carmichael, 1964). Fractional crystallization is generally assumed to have taken place in relatively high level magma chambers beneath eruptive centres and only recently has it become apparent that moderately high pressure fractionation processes may also be important (Maaløe, 1973b). In the following discussion, the importance of both low and moderately high pressure fractionation will be assessed in the light of available field, chemical and petrographic data on the Tweed low-Si series.

7.2.1 Summary of Pertinant Data

Any petrogenetic model for the evolved members of the low-Si series must be compatible with the following data:

1) Basalts s.s., are absent or extremely rare in this part of the Shield and tholeiitic andesites (which nevertheless may be ol-normative) predominate as the most mafic representatives of the series.

2) The rocks do not show the type of compositional variation

characteristic of a single liquid line of descent but rather show considerable scatter in variation diagrams (Figs. 6.4-6.15).

3) Major element variation is dominated by enrichment in Fe and K, depletion in Mg and Ca and relatively constant Na and Al contents throughout.

4) Among trace elements, Ni initially decreases very rapidly, V is steady at first but decreases in the most evolved rocks of the series. Ba and Rb increase while the K/Ba and K/Rb ratios remain steady and the Ca/Sr ratio falls significantly through the series.

5) Some lavas contain moderately high pressure phases (pyroxenes and plagioclase) indicating rapid transportation from crust-mantle boundary depths with little time for modification by low pressure processes. So far as can be ascertained the respective host rocks are geochemically identical to other rocks of the series lacking any obvious high pressure phases.

6) Olivine and/or plagioclase are the only phases occurring as phenocrysts throughout the low-Si series except in very rare members at the iron-rich end of the series where pyroxene and titanomagnetite phenocrysts may be present. However only one example of this particular type of rock has been found (an iron-rich tholeiitic andesite; 28055). With this exception clinopyroxene apparently has not been a liquidus phase in members of the series at low pressures so that clinopyroxene, as a significant liquidus or near liquidus phase, did not participate in low pressure fractionaton.

7.2.2 Low Pressure Fractionation

Fractional crystallization, implicitly at relatively low pressures, has been invoked or inferred for the evolved members of most tholeiitic

series. These include Thingmuli (Carmichael, 1964) and Hekla (Baldridge *et al.*, 1974) in Iceland, the Hawaiian tholeiitic series (Tilley, 1960; MacDonald and Katsura, 1964; Thompson and Tilley, 1970; Bauer *et al.*, 1973), the Hebridean tholeiitic series (Holland and Brown, 1972), the Karroo Basalts in South Africa (Cox and Hornung, 1966), the Galapagos Islands (McBirney and Williams, 1969), the Deccan Basalts in India (Sukheswala and Poldervaart, 1958; Konda, 1971) and the Hachimantai and surrounding volcanoes (Kawano and Aoki, 1960) and Izu Hakone and Huzi volcanic zones (Tsuya, 1937; Tilley, 1950; Isshiki, 1963; Kuno, 1954,1968) in Japan. Several lines of evidence offer strong support for the general concept of low pressure fractionation and these are briefly summarized below.

Fractional crystallization within high level tholeiitic dolerite sills produces a spectrum of rock compositions appropriate to the more common evolved members of tholeiitic associations in the range quartz dolerite (= quartz tholeiite) to granophyre (= tholeiitic rhyodacite or rhyolite; F. Walker, 1940; McDougall, 1962; Gunn, 1966; K.R. Walker, 1969). Similar trends are observed in segregation veins and schliere in tholeiitic volcanics and dolerites (Kuno *et al.*, 1957; Kunc, 1965,1968).

The intersertal residua in many tholeiitic rocks have compositions appropriate to more evolved liquids along a tholeiitic liquid line of descent; i.e. inninmorite → rhyolite. Studies of these residua have closely documented the fractionation process at low pressures (Walker *et al.*, 1952; Elliot, 1956; Evans and Moore, 1968; Tilley and Thompson, 1970; Wilkinson and Duggan, 1973). Thus separation of olivine and plagioclase from olivine tholeiite or tholeiite yields Fe-rich andesitic liquids. With addition of

clinopyroxene to the fractionation assemblage, the derivative liquids become progressively more evolved producing icelandite and dacite compositions. The ultimate fractionation product is a small amount of rhyolitic glass (Evans and Moore, 1968; Wilkinson and Duggan, 1973).

The close proximity of many tholeiitic eruptives to a four phase curve (Ol, Pl, Cpx, Liq) at low pressures (as evidenced by appearance of the three major silicate phases over a small cooling interval in numerous one atmosphere melting experiments, together with the appearance of all three phases as phenocrysts) has been widely cited as strong evidence favouring low pressure fractionation as an important control of their genesis (Yoder and Tilley, 1962; Tilley *et al.*, 1963,1964,1965). For example, in Kilauean lavas (Thompson and Tilley, 1970) clinopyroxene and plagioclase join olivine as liquidus or near liquidus phases in rocks with Mafic Index ~62. However Thompson (1972a) has shown that the Kilauea lavas are somewhat more ideal than most other rock series in their one atmosphere melting behaviour and that clinopyroxene does not always join olivine and plagioclase on the liquidus of more evolved members of volcanic series.

If a magma series develops through low pressure fractionation processes along a single liquid line of descent then ideally the composition of successive batches of liquid should be capable of being derived by extraction of appropriate quantities of the phenocryst phases occurring in more mafic members which are presumed to be parental to these rocks. Thus if rocks of the low Si series are interrelated by low pressure fractionation, successive magma compositions should derive by removal of olivine and plagioclase (the principal phenocryst phases) in varying proportions from

more mafic representatives.

To test this possibility, the compositions of crystal extracts required to produce various more evolved compositions have been calculated assuming that the crystal extract is essentially potash-free and therefore that any increase in K_2O represents residual concentration during fractionation. The calculations have been performed using analyses of rocks of the low-Si series recalculated 100% anhydrous (Table 7.1). Some examples of these calculations are set down in Table 7.2 together with their C.I.P.W. norms, calculated where necessary after readjustment of Fe_2O_3/FeO ratios to avoid appearance of ne in the norm. The precise significance of these data is limited but one point is quite clear, namely that it is necessary for clinopyroxene to be a significant component of the crystal extract regardless of whether successive liquids lie on a single liquid line of descent or whether they derive independantly from a common parent magma. This is also clearly shown on a Di-Ol-Qz diagram (Fig.7.1; after Coombs; 1963) where it is evident that at least Ca-rich pyroxene in addition to olivine must be removed from the more mafic liquids to produce the more evolved rock types trending toward the Qz apex. In some tholeiitic series where clinopyroxene actually appears in the more mafic rocks as a phenocryst phase, a low pressure fractionation scheme is quite feasible. However, their absence from the Tweed low-Si series virtually excludes low pressure fractionation from playing a major role in their genesis. The almost constant Na_2O content throughout the series also places constraints on the composition of the plagioclase component of any extract. For example, to maintain a constant Na_2O of about 3.5% an extract containing about 50% plagioclase must have

Table 7.1

ANALYSES AND C.I.P.W. NORMS OF ROCKS OF THE LOW-Si SERIES RECALCULATED ANHYDROUS

	1	2	3	4	5	6	7	8	9	10	11	12	13	14	15
	28046	28047	28048	28049	28050	28051	28052	28053	28055	28057	28058	28059	28060	27290	27291
SiO_2	51.16	51.38	54.42	52.65	51.46	51.01	53.86	50.72	54.75	53.12	53.11	54.66	52.77	53.78	56.40
TiO_2	1.83	1.64	1.77	2.53	2.80	3.11	1.99	2.00	2.21	2.56	2.71	2.50	2.21	2.19	1.31
Al_2O_3	14.91	15.43	16.58	15.46	15.19	14.57	15.73	15.84	14.53	15.63	14.73	16.03	15.58	18.56	14.62
Fe_2O_3	1.61	3.96	1.05	1.93	2.68	2.68	1.96	3.80	2.79	2.01	2.93	2.33	1.66	2.54	2.38
FeO	8.74	6.90	7.10	9.29	9.82	10.53	7.83	7.50	9.27	8.61	9.35	7.15	8.54	5.32	9.89
MnO	0.15	0.13	0.12	0.15	0.15	0.16	0.13	0.13	0.15	0.16	0.17	0.12	0.13	0.09	0.18
MgO	7.56	5.35	5.31	4.37	4.05	3.54	4.17	5.60	2.40	4.69	3.49	3.13	4.90	3.40	2.41
CaO	9.07	9.83	8.45	7.32	7.18	8.00	8.38	8.92	6.22	7.63	6.85	8.30	8.76	7.92	5.05
Na_2O	3.50	3.72	3.74	3.78	3.44	3.76	4.09	3.83	4.20	3.79	3.57	3.84	3.85	4.36	3.53
K_2O	0.90	0.80	1.15	1.75	2.46	1.81	1.30	1.18	2.76	1.42	2.35	1.60	1.27	1.42	3.62
P_2O_5	0.58	0.85	0.29	0.77	0.77	0.83	0.54	0.50	0.79	0.39	0.73	0.35	0.33	0.42	0.61
							C.I.P.W. Norms								
Qz	-	1.25	1.95	1.09	0.14	0.16	1.76	-	3.00	1.75	3.28	5.09	-	1.90	4.41
Or	5.33	4.70	6.82	10.31	14.54	10.71	7.67	6.95	16.32	8.39	13.86	9.47	7.49	8.41	21.41
Ab	29.65	31.46	31.67	32.02	29.07	31.77	34.61	32.41	35.04	32.03	30.24	32.49	32.59	36.91	29.88
An	22.30	23.09	25.04	20.06	18.77	17.55	20.75	22.56	12.91	21.47	17.23	21.78	21.49	26.85	13.36
Di	15.39	16.35	12.23	9.28	9.81	13.98	14.29	14.96	10.81	11.43	10.12	14.12	16.29	7.86	6.59
Hy	11.90	12.33	16.70	17.86	16.68	14.11	13.04	8.48	11.85	16.26	14.30	8.13	13.92	8.89	17.01
Ol	8.28	-	-	-	-	-	-	4.18	-	-	-	-	0.84	-	-
Mt	2.34	5.73	1.51	2.80	3.89	3.89	2.84	5.51	4.05	2.91	4.25	3.38	2.41	3.69	3.45
Il	3.47	3.12	3.36	4.80	5.31	5.91	3.78	4.86	4.19	4.86	5.15	4.73	4.20	4.15	2.48
Ap	1.34	1.97	0.70	1.79	1.79	1.91	1.26	0.89	1.82	0.89	1.68	0.81	0.78	0.97	1.41
$\frac{100\ Mg}{Mg+Fe}$	56.9	47.7	54.0	41.4	37.1	32.8	43.6	47.7	26.6	44.5	34.2	37.6	46.5	44.3	26.3
Equilibrium olivine compositions															
$K_D = 0.3$	81.5	75.2	79.7	69.9	66.3	61.9	72.1	75.2	54.8	72.8	63.4	66.8	74.4	72.7	54.3
$K_D = 0.33$	80.0	73.4	78.1	67.8	64.1	59.5	70.1	73.4	52.4	70.8	61.1	64.6	72.5	70.7	52.0

For key to specimen numbers see Table 6.1.

TABLE 7.2

COMPOSITIONS, C.I.P.W. NORMS AND AMOUNTS OF K-POOR CRYSTAL EXTRACTS REQUIRED TO BE REMOVED TO DERIVE SOME OF THE MORE EVOLVED MEMBERS OF THE LOW-Si SERIES FROM MORE MAFIC PARENTS

Parent	28046	28046	28046	28046	28049	28049	28048
Derivative	28049	28048	28050	27290	28055	28050	28050
% Extract	50%	23%	65%	38%	38%	30%	70%
SiO_2	47.0	40.3	51.0	46.9	49.2	55.4	53.4
TiO_2	1.1	2.0	1.3	1.2	3.1	1.9	2.0
Al_2O_3	14.4	9.2	14.8	9.0	17.0	16.1	17.4
Fe_2O_3	0.3	3.4	-	-	-	0.2	-
FeO	9.1	14.4	9.1	14.2	10.0	8.1	6.6
MnO	0.2	0.3	0.2	0.3	0.2	0.2	0.1
MgO	10.8	15.1	9.5	14.4	7.6	5.1	6.6
CaO	10.8	6.4	10.1	11.0	9.1	7.7	9.9
Na_2O	3.2	2.7	3.5	2.1	3.1	4.6	3.8
K_2O	0.1	0.1	0.1	0.1	0.1	0.1	0.1
P_2O_5	0.4	1.6	0.5	0.8	0.7	0.8	0.2
Qz	-	-	-	-	-	3.5	0.1
Or	0.5	0.3	0.3	0.3	0.6	0.6	0.6
Ab	27.3	22.9	29.9	17.8	26.2	38.7	32.4
An	24.5	13.1	24.3	14.9	32.2	22.8	30.4
Di	21.5	6.8	18.5	27.8	6.8	8.3	14.4
Hy	-	-	7.4	2.8	20.5	20.4	18.2
Ol	22.8	39.9	16.0	32.1	6.4	-	-
Mt	0.4	4.9	-	-	-	0.3	-
Il	2.1	3.9	2.5	2.4	5.8	3.6	3.8
Ap	0.9	3.6	1.1	1.9	1.7	1.8	0.4

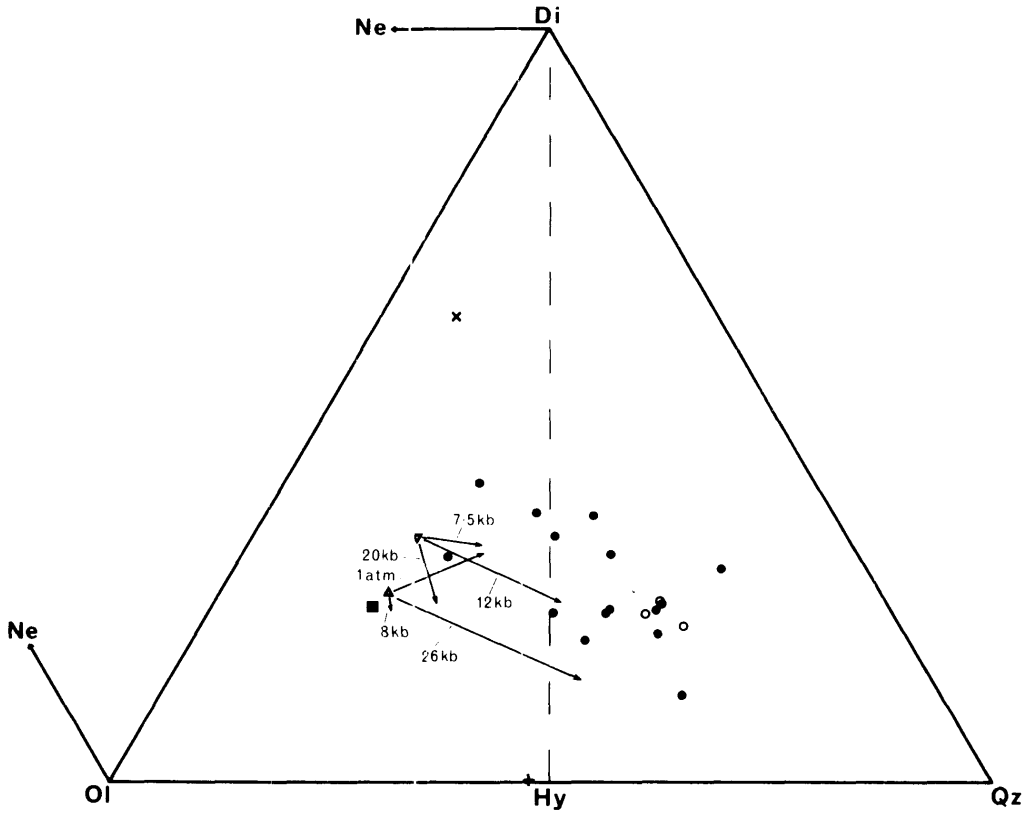

Fig. 7.1: Members of the low-Si series, some calculated derivative liquid compositions and relevant experimental data plotted on a Di-Ol-Qz (normative mol %) diagram. Filled circles, members of the low-Si series (Table 7.1); open circles, some sample derivative liquids obtained by crystal-extract calculations (Table 7.4, Nos. 3-5); square, proposed parent magma composition (Table 7.4, No.1); ×, subcalcic aluminian augite in high-Al tholeiitic andesite 27290 (Duggan & Wilkinson, 1973); +, aluminian augite in high-Al tholeiitic andesite 27290 (Duggan & Wilkinson, 1973); triangle, Snake River lava 59-P-13 (Thompson, 1972b); inverted triangle, abyssal tholeiite T-87 (Kushiro, 1973b). Arrows indicate the experimentally determined fractionation trends at the stated pressures under anhydrous conditions. Note that all Fe is calculated as FeO in the experimental trends.

100 an/ab+an ~50 or even less. Lesser amounts of plagioclase in the extract would require even more sodic plagioclase compositions whereas greater amounts of more An-rich plagioclase would excessively deplete residual liquids in Al_2O_3 beyond the levels observed in the low-Si series. Phenocrysts interpreted as low pressure crystallization products in these volcanics are generally considerably more An-rich (An_{60-70}; e.g. 28048) and therefore unlikely to produce this trend.

On the basis of this evidence, together with the occurrence of pyroxene and plagioclase megacrysts of relatively high pressure derivation which are undoubtedly unstable at low pressure in their host liquid (itself chemically undistinguishable from megacryst-free rocks), low pressure fractionation is considered to play only a minor role in the derivation of the low-Si series. This does not imply that some fractionation has not occurred during source to surface travel of the lavas. In most cases upward movement has been sufficiently slow to allow resorption or settling out of remanent high pressure phases which are found in only a small percentage of the rocks.

7.2.3 High Pressure Fractionation

The possibility that some tholeiitic andesites and more evolved types may have originated at higher (moderate) pressures has only recently been explored. In the Tweed low-Si series, feldspars and aluminian pyroxenes (bronzite and subcalcic augite) interpreted as products of moderately high pressure crystallization near the crust-mantle boundary (Duggan and Wilkinson, 1973) occur sporadically and unsystematically throughout the lava sequence. Rocks bearing these phases are otherwise petrographically and chemically

indistinguishable from other rocks of the low-Si series and it is evident that the entire series is essentially cogenetic.

Documented occurrences of demonstrably high pressure phases in tholeiitic rocks outside the Tweed Shield are rare. Jamieson (1966) reported large aluminous orthopyroxene crystals in some Karroo Basalts which he interpreted as products of crystallization at high pressures and Nicholls and Lorenz (1973) have experimentally duplicated the conditions of formation of aluminous orthopyroxene and clinopyroxene megacrysts in tholeiites from the Saar Nahe Trough in Germany (P_{total} = 6-10 kb; T = 1280-1080°C; 2-4 wt % H_2O). However a feature of both the Saar Nahe and Karroo occurrences is the relatively magnesian nature of the host rocks (100 $Mg/Mg+Fe^{total}$ = 68-75 and 61-76 respectively) suggesting little ferromagnesian mineral fractionation subsequent to separation of the liquids from their upper mantle parent.

In contrast, megacryst-bearing lavas of the Tweed Shield are significantly depleted in Mg (100 Mg/Mg+Fe = 26-45; Table 7.1, Nos 10,14,15) and are therefore unlikely to represent unmodified equilibrium partial melts of mantle peridotite. Instead they may be interpreted as either liquids that have already undergone significant fractionation at relatively high pressures or alternatively as partial melt products of "basaltic" parents near the crust-mantle boundary. In terms of major element trends these two processes will be essentially identical and therefore indistinguishable on petrological grounds.

Liquidus temperatures of 1100-1200°C are indicated for members of the low -Si series by the Kudo-Weill plagioclase geothermometer (Kudo and

Weill, 1970) and compare well with one atmosphere liquidus temperatures on rocks of comparable composition (e.g. Tilley and Thompson, 1970; see also Section 5.4). These will therefore represent the absolute minimum temperatures of melting. Attainment of these temperatures near the crust-mantle boundary would seem to require unreasonably high geothermal gradients in excess of 30°C/km assuming a crustal thickness of 35-40 km in this part of Eastern Australia (Finlayson, 1968; Cleary, 1973). Furthermore, under the water-deficient conditions which were probably operative during formation of these magmas, actual liquidus temperatures were probably somewhat higher than 1200°C. It would seem then that this hypothesis has little relevance to the Tweed situation unless large quantities of material of basaltic composition (eclogite) were available for melting within the upper mantle at perhaps 60-100 km depth. Although an eclogite model for the upper mantle has been suggested from time to time (Holmes, 1927; Lovering, 1958; Kennedy, 1959) the existence of large amounts of material of basaltic composition at such depths within the upper mantle is quite at variance with seismic data and modern petrogenetic theory (e.g. O'Hara, 1968; Green, 1970).

The alternative hypothesis, involving fractionation near the crust-mantle boundary is compatible with field, mineralogical and chemical data on the low-Si series and finds support in several high pressure experimental studies on melting of basaltic rocks under anhydrous conditions (Thompson, 1972b, 1974; Kushiro, 1973b). This experimental data will be considered later.

The striking dominance of andesites and absence of basalts is compatible with fractionation at considerable depth. If each successive

batch of magma underwent substantial fractionation near the crust-mantle boundary (for example; in response to heat loss to surrounding rocks during passage through the upper mantle), then no rocks of strictly basaltic composition need necessarily appear in the volcanic pile. In other words virtually no eruptive would retain the characteristics of a primary basaltic magma.

The mafic members of the low-Si series correspond closely in composition to the "basaltic andesite gap" proposed by Thompson (1972c) who suggested that the gap resulted from eruption of some unmodified basalts coupled with *in situ* closed system high pressure partial crystallization of basaltic material at depth with subsequent release of the andesitic liquid at an advanced stage of crystallization. If this mechanism were operative then it is evident that little or no unmodified material has been erupted but rather that all have undergone some fractionation at considerable depth to produce the spectrum of rocks forming the low-Si series.

The genesis of high pressure feldspars and pyroxenes in members of the low-Si series has already been discussed in detail and further detailed discussion is unwarranted (see Chapter 5 and Duggan and Wilkinson, 1973). Crystallization of these phases at moderately high pressures (approximately 9 kb) near the crust-mantle boundary was followed by relatively rapid transport to surface conditions and eruption. Preservation of these high pressure phases, potentially unstable at low pressures, effectively precludes significant low pressure fractionation. Megacryst-free low-Si rocks may, on mineralogical grounds, have undergone some low pressure fractionation. They commonly contain phenocrysts of plagioclase and olivine and more rarely,

scattered sieved plagioclase phenocrysts. However the close compositional similarity of megacryst-bearing and megacryst-free rocks suggests that accompanying chemical variation has been minimal and that the low pressure processes were restricted to reaction and resorption leading to removal of all traces of high pressure phases with the exception of an occasional strongly sieved and resorbed plagioclase phenocryst.

Evaluation of high pressure fractionation trends by conventional crystal extract mass-balance calculations is made difficult by the limited analytical data on the high pressure phases in these rocks. However some sample calculations carried out using mineral compositions listed in Table 7.3 are presented in Table 7.4. In making these calculations, it was necessary to select some composition as a potential parent magma for the series. The most Mg-rich rock so far found in the low-Si series (28046) has 100 $Mg/Mg+Fe^{total}$ = 57 and would be in equilibrium with olivine having $\frac{100\ Mg}{Mg+Fe}$ = 82-80 using distribution coefficients for iron and magnesium between olivine and liquid of

$K_D[(Fe/Mg)_{Ol}/(Fe/Mg)_{liq}]$ of 0.3 (Roeder and Emslie, 1970) and 0.33 (Thompson, 1974).

This andesite is too Fe-rich to have been in equilibrium with any presently accepted peridotitic upper mantle composition. Current estimates of this composition are 100 Mg/Mg+Fe = 89-92 (Green, 1971) and 85 (Kushiro, 1973b; Thompson, 1974). Addition of 10% of olivine of composition Fo_{80} to the composition 28046 yields a liquid composition capable of being in equilibrium with an upper mantle of $\frac{100\ Mg}{Mg+Fe}$ = 85 (Table 7.4, No.1). This ratio is calculated using total iron calculated as FeO to enable direct

TABLE 7.3

COMPOSITIONS OF MINERALS USED IN CRYSTAL EXTRACT CALCULATIONS IN TABLE 7.4

	(1) Olivine (Fo_{80})	(2) Olivine (Fo_{70})	(3) Clinopyroxene	(4) Plagioclase An_{50}
SiO_2	39.2	37.6	49.9	56.0
TiO_2	-	-	1.2	-
Al_2O_3	-	-	5.2	27.9
Fe_2O_3	-	-	-	0.5
FeO	18.5	26.7	11.4	-
MnO	0.2	0.3	0.2	-
MgO	42.0	35.3	14.5	-
CaO	0.1	0.1	16.5	9.1
Na_2O	-	-	0.9	5.8
K_2O	-	-	-	0.7
P_2O_5	-	-	-	-

1 and 2. Olivines - compositions estimated from microprobe data listed in Table II.1 (Appendix II).

3. Clinopyroxene from high-Al tholeiitic andesite 27290 (Duggan and Wilkinson, 1973 Table 1, No.3).

4. Plagioclase from high-Al tholeiitic andesite 27290 (Duggan and Wilkinson, 1973).

TABLE 7.4

COMPOSITIONS AND C.I.P.W. NORMS OF DERIVATIVE LIQUIDS OBTAINED BY CRYSTAL-EXTRACT CALCULATIONS USING MINERAL COMPOSITIONS LISTED IN TABLE 7.3

	(1)	(2)	(3)	(4)	(5)	(6)	(7)
SiO_2	50.1	52.0	52.6	52.3	53.2	52.8	52.9
TiO_2	1.7	2.0	2.8	3.2	2.6	3.1	2.4
Al_2O_3	13.6	15.9	16.4	15.6	18.4	14.6	15.5
Fe_2O_3	1.5	1.7	2.6	3.0	2.6	3.4	2.3
FeO	9.6	8.1	6.2	6.7	5.1	7.6	8.5
MnO	0.2	0.1	0.1	0.1	0.1	0.1	0.1
MgO	10.7	5.2	4.4	4.6	3.1	4.9	4.3
CaO	8.3	9.7	8.4	7.8	8.1	7.4	8.1
Na_2O	3.2	3.7	4.1	4.1	4.5	3.7	3.8
K_2O	0.8	1.0	1.4	1.5	1.4	1.7	1.6
P_2O_5	0.5	0.6	1.0	1.1	1.0	0.6	0.6
Qz	-	-	2.2	2.5	2.7	3.4	1.6
Or	4.8	5.7	8.0	8.9	8.2	10.2	9.4
Ab	26.9	31.6	35.0	34.8	38.4	31.6	31.8
An	20.2	23.9	22.0	19.6	25.7	17.8	20.7
Di	13.9	16.6	10.5	9.5	6.7	11.2	12.8
Hy	10.7	13.1	10.8	11.7	7.5	12.4	14.4
Ol	16.8	1.5	-	-	-	-	-
Mt	2.1	2.5	3.8	4.4	3.7	4.9	3.4
Il	3.1	3.7	5.4	6.1	5.0	5.9	4.5
Ap	1.2	1.5	2.3	2.6	2.2	1.4	1.4
$\frac{100Mg}{Mg+Fe}$	63.5	49.0	47.9	46.6	42.6	45.0	42.0
Equilibrium Olivine compositions							
$K_D = 0.30$	85	76	76	74	72	76	74
$K_D = 0.33$	84	74	74	73	70	74	72

KEY TO TABLE 7.4

(1) 28046 + 10% Fo_{80} - proposed parent magma composition.

(2) Composition (1) less 15% Fo_{80}. Compare Table 7.1 Nos (2) and (8).

(3) Composition (1) less 15% Pl + 15% Cpx followed by 25% Fo_{70}. Compare with Table 7.1 No. (7).

(4) Composition (1) less 20% Pl + 17.5% Cpx followed by 27.5% Fo_{70}. Compare with Table 7.1 Nos (4) and (14) and average low-Si tholeiitic andesite (This Table, No. 7).

(5) Composition (1) less 45% of an extract containing 20% Pl + 40% Cpx + 40% Fo_{70}. Compare with high Al tholeiitic andesite 27290 (Table 7.1, No. 15).

(6) High-Al tholeiitic andesite 27290 less 30% An_{50}. Compare with average low-Si tholeiitic andesite (This Table, No. 7).

(7) Average low-Si tholeiitic andesite - average of 10 analyses (28047, 048, 049, 050, 051, 052, 057, 058, 059, 060).

---

comparison with microprobe data on experimentally produced glasses (see below). The presence of some of the Fe as Fe_2O_3 will make the Mg/Mg+Fe ratio closer to the preferred value (100 Mg/Mg+Fe = 89-92) of Green (1971).

Derived compositions listed in Table 7.4 are broadly comparable with intermediate members of the low-Si series in most major elements and in terms of level of silica saturation. They therefore illustrate the

general feasibility of deriving these rocks by removal of plagioclase and aluminian clinopyroxene together with, or followed by, olivine from the proposed parent magma composition (Table 7.4, No. 1).

It is appropriate to consider whether fractionation of these particular phases is compatible with experimental data. In this context the anhydrous melting relations of an olivine tholeiite from the Snake River Plain (Thompson, 1972b; see Table 7.5, No 1) and an abyssal olivine tholeiite (Kushiro and Thompson, 1972; Kushiro, 1973b; Table 7.5, No. 2) are especially relevant. At 7-10 kb, clinopyroxene and plagioclase are near liquidus phases joined later by olivine in both compositions. Orthopyroxene also occurs near the liquidus of the abyssal tholeiite at 7.5 kb. At lower pressures olivine crystallizes earlier, appearing on the liquidus at about 5 kb in the Snake River lava and 7 kb in the abyssal tholeiite. Plagioclase is also a liquidus or near liquidus phase throughout the pressure range 0-10 kb in the Snake River lava. Nicholls and Ringwood (1972, 1973) show that the maximum pressure limit for the stability of olivine on the liquidus of olivine tholeiite (Table 7.5, No. 3) and silica saturated tholeiite (Table 7.5, No. 4) expands considerably with increasing P_{H_2O}.

These results collectively indicate that the proposed fractionation scheme is feasible, either under anhydrous conditions or in the presence of small amounts of water. Fractionation of the clinopyroxene component at depth under these conditions effectively prevents the liquidus reaching a low pressure four phase (Ol, Pl, Cpx, liq) curve attained by many tholeiitic lavas as previously discussed and therefore clinopyroxene does not constitute a phenocryst phase. The single exception to this (28056) which contains low

TABLE 7.5

ANALYSES AND C.I.P.W. NORMS OF SOME ROCKS FOR WHICH EXPERIMENTAL DATA AT HIGH P AND T ARE AVAILABLE

	(1)	(2)	(3)	(4)	(5)	(6)	(7)
SiO_2	47.76	49.68	45.9	51.5	51.7	51.6	46.4
TiO_2	3.03	1.55	0.1	1.8	1.97	1.64	4.66
Al_2O_3	14.93	15.49	14.4	13.8	14.7	15.8	13.2
Fe_2O_3	1.36	0.92	1.0	2.2	-	-	-
FeO	12.37	8.25	11.9	8.9	9.91*	8.22*	17.4*
MnO	0.20	0.18	0.3	0.1	0.22	0.19	0.40
MgO	6.70	9.17	12.4	9.4	7.45	8.07	5.28
CaO	9.41	10.61	12.9	8.9	9.62	10.4	8.37
Na_2O	2.62	2.88	0.8	2.5	3.39	2.56	2.64
K_2O	0.75	0.11	0.01	0.7	0.15	0.12	1.25
P_2O_5	0.53	0.14	0.03	0.2	-	-	0.91
H_2O	0.03	0.56	-	-	-	-	-
Total	99.70	99.54	99.74	100.00	99.15	98.65	100.51
Qz	-	-	-	0.2	-	0.5	-
Or	4.45	0.56	0.1	4.1	0.9	0.7	7.4
Ab	22.01	24.63	6.8	21.4	28.7	21.7	22.3
An	26.69	28.91	35.7	24.2	24.5	31.3	20.5
Di	13.57	18.48	23.0	15.4	19.1	16.6	12.7
Hy	15.49	10.60	9.7	27.8	16.0	24.7	11.5
Ol	8.37	11.08	22.7	-	6.2	-	15.1
Mt	2.09	1.39	1.5	3.2	-	-	-
Il	5.78	3.04	0.1	3.3	3.7	3.1	8.9
Ap	1.34	0.34	0.1	0.4	-	-	2.1
Rest	0.07	0.56	0.3	-	-	-	-

* Total Fe as FeO.

KEY TO TABLE 7.5

(1) Ol tholeiite 59-P-13 (Tilley and Thompson, 1970). Total includes CO_2 0.01%.

(2) Abyssal olivine tholeiite T-87 (Miyashiro, Shido and Ewing, 1969; Table 3).

(3) Olivine tholeiite (Nicholls and Ringwood, 1973). Total includes Cr_2O_3= 0.2%.

(4) SiO_2 saturated tholeiite (Nicholls and Ringwood, 1973).

(5) Glass from melting of (2) at 7.5 kb, 1200°C (Kushiro, 1973b). Total includes Cr_2O_3 0.05%.

(6) Glass from melting of (2) at 12 kb 1250°C (Kushiro, 1973b). Total includes Cr_2O_3 = 0.05%.

(7) Glass from melting of (1) at 8 kb, 1150°C (Thompson, 1972).

---

pressure clinopyroxene phenocrysts is therefore probably a rare example of a liquid that has undergone substantial near surface fractionation.

The glasses produced in the 7.5 and 12 kb runs on the abyssal tholeiite have been analysed by Kushiro (1973b; see Table 7.5, Nos 5 and 6). The proportion of glass produced in these runs (50-75%) is sufficiently high to minimise any modification by quench crystallization and they may therefore be considered as close to equilibrium compositions. Since the major element compositions (K_2O excepted) are close to those of the more basic representatives of the low-Si series, then the results are especially relevant. When plotted on a Di-Ol-Qz diagram (mol %; Coombs, 1963) the trends

produced in the 7.5 and 12 kb melting runs are broadly appropriate to the low Si series trend (Fig. 7.1). Similarly on an AFM diagram, (Fig. 7.2) the iron enrichment trends closely parallel that of the Tweed low-Si series rocks. The glass from the Snake River tholeiite at 8 kb (Table 7.5, No.7) does not trend towards silica saturation but subsequent fractionation of olivine from this liquid would produce a trend closely matching that of the Tweed rocks.

Having determined the general feasibility of moderately high pressure fractionation processes, a critical test of its application is provided by some of the trace element data. The wide variation in nickel contents (Fig. 6.14) of the more magnesian rocks attest to the role played by olivine in their fractionation. On the other hand, vanadium (Fig. 6.14) which is strongly partitioned into oxide phases (especially titanomagnetite) remains more or less constant except in the most evolved rocks where titanomagnetite has become an early crystallizing phase and has therefore probably taken some part in the fractionation.

One other rock with a somewhat lower V content is the high alumina tholeiite andesite 27290 (Duggan and Wilkinson, 1973). This and other trace element data now available on this rock permit a more confident assessment of the genesis of this particular rock type. A very high K/Rb ratio (697) and Sr content (837 ppm) together with lower Co, V, Rb, and Ca/Sr, Rb/Sr ratios (Figs. 6.14-6.16) assessed in conjunction with the mineralogical data, suggest that this particular rock may well have been derived from a low-Si tholeiitic andesite magma principally by accumulation of plagioclase megacrysts from the fractionating magma under the conditions previously

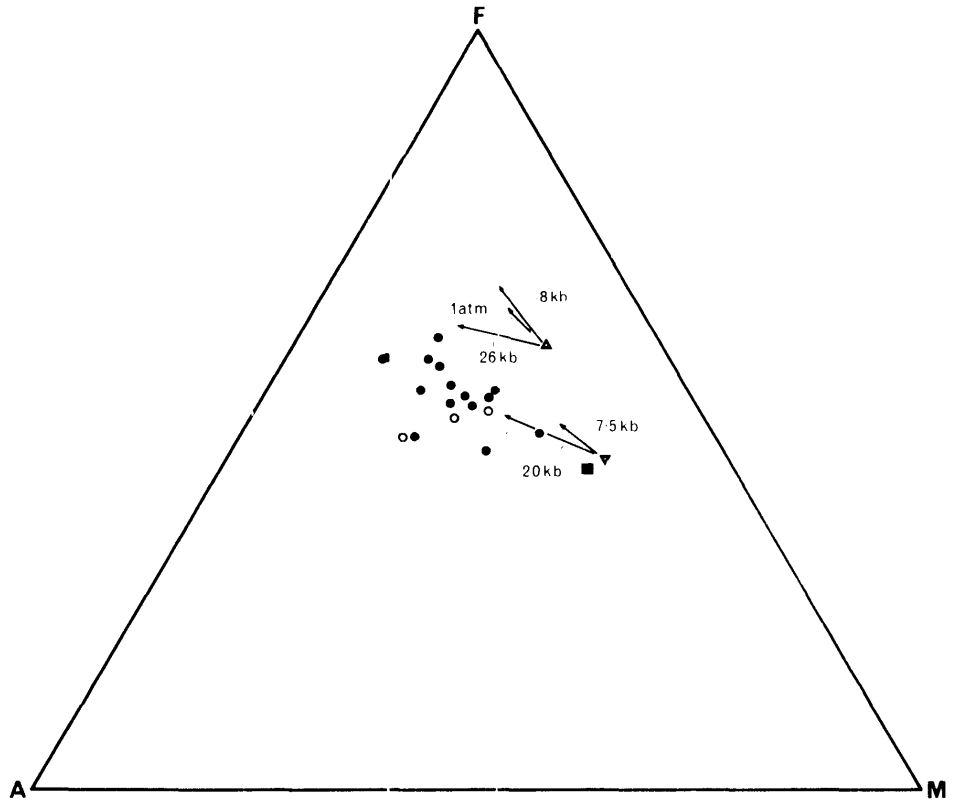

Fig. 7.2: An A F M diagram depicting members of the low-Si series, some calculated derivative liquid compositions and relevant experimental data. Filled circles, members of the low-Si series (Table 7.1); open circles, some derivative obtained by crystal extract calculations (Table 7.4, Nos. 3-5); square, proposed parent magma composition (Table 7.4, No.1); triangle, Snake River lava 59-P-13 (Thompson, 1973b); inverted triangle, abyssal tholeiitic T-87 (Kushiro, 1973b). Arrows indicate the experimentally determined fractionation trends at the stated pressures under anhydrous conditions. Note that all Fe calculated as FeO in the experimental trends.

proposed (~9 kb). To test this hypothesis the residual composition after removal of 30% plagioclase An_{50} (similar in composition to the plagioclase megacrysts) has been calculated (Table 7.4, No 6) and is in fact remarkably similar to the average low-Si tholeiitic andesite (Table 7.4, No 7).

Other trace element data, notably the significant increase in Rb and especially Ba and fairly constant Sr and K/Rb ratio are all consistent with the hypothesis that variation in the low-Si series is brought about by separation of Ca-pyroxene and some plagioclase, either accompanied or followed by olivine.

Returning to the role played by limited subsequent low pressure fractionation of olivine and plagioclase, there is evidence of a very strong and quite localised gravity high located more or less below the Mount Warning Central intrusive complex (B.M.R. Bouger Anomoly map 1 : 500,000; 1971). It is tentatively suggested that some low-Si lavas have paused at quite shallow depths for a suitable time to allow limited fractionation of olivine and plagioclase, probably resulting in some development of olivine-plagioclase cumulates at relatively shallow depths. In fact olivine-plagioclase cumulates of an appropriate composition are occasionally observed in some low-Si rocks (Plate 2, No.6).

7.3 EVOLUTION OF THE HIGH-Si SERIES

In contrast to the rather complex chemical variation among members of the low-Si series, rocks of the high-Si series display well-defined trends consistent with evolution more or less along a single liquid line of descent. This is clearly evident in plots of major and trace elements against

Differentiation Index (Figs. 6.4 to 6.16). The more irregular variation of these elements when plotted against Mafic Index reflects the variable effect of the separation of ilmenite on whole rock Fe/Mg ratios.

The principal chemical and petrographic features of the high-Si series are summarized below.

1) Alkali enrichment predominates throughout the series and variation on an AFM diagram (Fig. 6.8) simulates a calc-alkaline trend, although it must be noted that the high-Si trend is relatively more iron-rich at the intermediate end and also relatively Al-poor throughout (Fig. 6.6).

2) Enrichment in qz is continuous with increasing D.I. (Fig. 6.4).

3) Variation of the major elements closely follows that of the Talasea (New Britain) series although the high-Si trend for K_2O is consistently relatively higher. For both series CaO, $FeO+Fe_2O_3$, MgO, TiO_2 and P_2O_5 fall steadily, Na_2O and Al_2O_3 remain relatively constant and K_2O and SiO_2 increase (Figs 6.6-6.13).

4) Olivine, ferroaugite, plagioclase and ilmenite are early crystallizing phenocryst phases in various members of the series. Hypersthene, pigeonite and a more magnesian augite form later phenocrysts.

5) In terms of relative volumes, rocks of the high-Si series comprise only a minor (< 5%) component of the tholeiitic succession; low-Si tholeiitic andesites and rhyolites are far more voluminous in this portion of the Shield.

The origin of the high-Si series must be assessed in the light of these data and the following proposals will be examined, most of which have

at some time been proposed for the genesis of the calc-alkaline igneous rock suite. These are:

1) Direct partial melting in the upper mantle of either mantle peridotite under hydrous conditions (Kushiro, 1969; Yoder, 1969a; Myson and Kushiro, 1974) or quartz ecologite under anhydrous conditions (Green and Ringwood, 1968).

2) Partial melting in the lower crust (Turner and Verhoogen, 1960); compare the model based on melting of amphibolite under hydrous conditions at 30-40 km as proposed by Green and Ringwood (1968).

3) Mixing of separate acid and basic magmas in varying proportions (Holmes, 1932).

4) Fractional crystallization of subalkaline magmas at low to moderate pressures. The parental magmas may have been originally modified by sialic contamination (Tilley, 1950).

i) Partial Melting in the Upper Mantle

Direct partial melting of upper mantle periodotite under hydrous conditions can be discounted for the genesis of the Tweed high-Si series on a number of grounds. Firstly, abundant mineralogical data indicate that the high-Si series evolved as a strongly water-deficient magma (Section 5.4). Secondly, the principal grounds upon which Kushiro and co-workers base their hypothesis are the high SiO_2 and Al_2O_3 contents of experimental partial melts of aluminous peridotite. These geochemical characteristics are not observed in the Tweed rocks and in any case it has been argued that the glasses analysed by Kushiro were metastable quench products rather than

equilibrium melt compositions (Green, 1970; Nicholls and Ringwood, 1974; Nicholls, 1974). In addition, the members of the high-Si series are far too iron-rich (100 Mg/Mg+Fe < 43) to represent primitive melts separated from a peridotitic residuum and erupted without any significant compositional modifications (Nicholls and Ringwood, 1974).

Dry melting of quartz eclogite at upper mantle depths also produces a range of liquid compositions characteristically rich in Al (Green and Ringwood, 1968). Furthermore, the production of magmas by partial melting of quartz eclogite at such depths is dependant upon the availability of sufficient quantities of material of basaltic composition. This can be considered unlikely in view of the apparent absence of any evidence for tectonic processes capable of carrying basaltic material into the upper mantle either now or during the later half of the Cainozoic in this part of eastern Australia (see Section 7.6).

ii) Partial Melting in the Lower Crust

Partial melting of basaltic material under hydrous conditions or of amphibolite at lower crustal depths has been suggested by Green and Ringwood (1968) as a possible mode of origin for the calc-alkaline rock suite. However the highly aluminous nature of the derived liquids and hydrous conditions involved render the process of little relevance to the present discussion. Furthermore, it is unlikely that geothermal gradients would be sufficient to produce melting of basaltic material under anhydrous conditions (see previous section) within the lower crust.

iii) Mixing of Magmas

The relative paucity of rocks comprising the high-Si series compared

with the abundant and more mafic low-Si series on one hand and rhyolitic rocks on the other, invites an examination of the possible role of magma mixing processes in producing these intermediate magmas. The mixing should be reflected in the chemical trends within the high-Si series and, unless adequate time was available for equilibration, by clear evidence of disequilibrium among the phenocryst phases.

Apart from the occurrence of sieved plagioclase and ferroaugite phenocrysts, both of which can be satisfactorily explained as early moderate pressure phases (see Sections 5.3,5.4), most analysed high-Si rocks exhibit little evidence of mineralogical disequilibria. Sieved plagioclase and ferroaugite are absent as phenocryst phases in the voluminous rhyolitic rocks.

Chemical variation within the series is also strongly at variance with a magma mixing hypothesis. Firstly the sharp decrease in Na_2O and Al_2O_3 between the rhyodacitic rocks and the rhyolites should be noted. A magma mixing model would require essentially continuous variation joining the more mafic high-Si rocks and the rhyolites. The trend for Ba (Fig. 6.15) also argues strongly against this model. Strong Ba depletion in the rhyolites would indicate that mixing with more mafic magma, whether it was low-Si or high-Si type, should give a trend of decreasing Ba with increasing D.I. which is opposite to that observed.

A model based on magma mixing on a scale necessary to produce the high-Si series is therefore rejected. On a local scale however it may have been of minor importance. For example, one icelandite (28071) contains phenocrysts of olivine (Fo_{80}), plagioclase (An_{27}), augite ($Ca_{38}Mg_{46}Fe_{16}$), ferrohypersthene (Fe_{59-69}), sanidine ($Ab_{60}An_5Or_{35}$) and quartz. Significantly,

this rock lies off the major trend of the high-Si series, especially with respect to Ba (low), Rb and Sr (both high). These data are consistent with mixing of phenocryst-bearing rhyolite and a relatively mafic magma of the high-Si series.

iv) Fractional Crystallization

A brief review of the role of low and moderate pressure fractionation in producing the evolved members of tholeiitic series has already been presented (Section 7.2).

If a series of lavas have been derived entirely by a process of closed system fractional crystallization, then analyses of its members should define an unique liquid line of descent. It should then be possible to interrelate the chemistry of the various rock types by addition or subtraction of varying proportions of the phenocrysts found in the lavas. When this procedure is applied to the Tweed high-Si series the overall picture is clouded by a number of factors. For example, the lavas of the high-Si series, although a relatively minor component of the total volcanic pile, were extruded throughout the eruptive span of the Lismore Basalt and over a wide area. It is therefore difficult to assess possible parent-daughter relationships by addition or subtraction calculations. Nevertheless the calculated compositions of some residual liquids derived by removal of observed phenocryst phases from representative members of the high-Si series (Table 7.6) show a striking similarity to more evolved members, assuming that these lie along a common liquid line of descent. The phases used in these calculations (olivine, ferroaugite, relatively sodic plagioclase, ilmenite) are those

TABLE 7.6

CRYSTAL-EXTRACT CALCULATIONS ON ROCKS OF THE HIGH-Si SERIES

	(1)	(2)	(3)	(4)	(5)	(6)	(7)
SiO_2	61.50	64.9	64.30	66.9	66.94	71.0	70.49
TiO_2	1.50	1.3	1.27	0.9	0.92	0.5	0.61
Al_2O_3	14.77	14.3	14.22	14.8	15.03	14.4	14.64
Fe_2O_3	0.51	0.5	1.15	1.3	0.87	1.0	0.63
FeO	7.31	6.4	5.41	3.7	4.20	1.7	2.09
MnO	0.13	0.09	0.09	0.05	0.08	0.03	0.05
MgO	2.37	1.5	1.59	0.8	0.78	0.4	0.61
CaO	4.78	3.1	3.88	2.7	2.60	1.6	1.65
Na_2O	3.81	3.7	3.97	4.1	4.08	3.7	3.59
K_2O	3.01	3.9	3.85	4.4	4.37	5.4	5.43
P_2O_5	0.31	0.4	0.27	0.3	0.13	0.2	0.19
Qz	11.61	17.1	15.02	18.4	18.03	25.0	23.81
Or	17.78	22.8	22.76	26.2	25.81	31.7	32.11
Ab	32.23	31.3	33.62	34.7	34.54	30.9	30.39
An	14.32	11.0	9.60	9.0	9.81	6.7	6.90
C	-	-	-	-	-	0.1	0.33
Di	6.22	1.3	6.65	2.2	1.87	-	-
Hy	13.53	12.5	7.67	5.3	6.64	2.6	4.94
Mt	0.74	0.8	1.66	1.9	1.25	1.5	0.92
Il	2.85	2.4	2.40	1.6	1.74	1.0	1.17
Ap	0.72	1.0	0.63	0.8	0.31	0.4	0.45
Total Fe as FeO	7.77	6.8	6.44	4.9	4.98	2.6	2.66
100 an/ab+an	30.8	26.0	22.2	20.6	22.1	17.8	18.5
D.I.	61.6	71.2	71.4	79.3	78.4	87.6	86.3

KEY TO TABLE 7.6

(1) 28061 (Table 6.2, No 1).

(2) Composition of residual liquid after extraction from composition 1 of 15% plagioclase (Table II.3b, No 5) + 7% ferroaugite (Table II.2b, No 10) + 2% olivine (Table II.1, No 28) + 1% ilmenite (Table 5.5, No 6). Compare with column 3.

(3) 28067 (Table 6.2, No 7).

(4) Composition of residual liquid after extraction from composition 3 of 6% plagioclase (Table II.3b, No 37) + 7% ferroaugite (Table II.2b, No 63) + 1% olivine (Table II.1, No 35) + 1% ilmenite (Table 5.5, No 10). Compare with column 5.

(5) 28072 (Table 6.2, No 12).

(6) Composition of residual liquid after extraction from composition 5 of 17% plagioclase (Table II.3b, No 70) + 3% ferroaugite (Table II.2b, No 94) + 3% olivine (Table II.1, No 40) + 1% ilmenite (Table 5.5, No 13). Compare with column 7.

(7) 28073 (Table 6.2, No 13).

All calculations performed prior to rounding off numbers in columns 2, 4 and 6.

Compositions normalised to 100% anhydrous.

which, on textural grounds, have been interpreted as *early* phenocrysts and therefore the phases most likely to participate in fractionation. The calculations adequately demonstrate that it is not unreasonable to derive the more evolved members of the high-Si series by fractionation of more mafic "parents".

The viability of fractional crystallization processes in producing the Thingmuli and Talasea series has been clearly demonstrated (Carmichael, 1964,1967a; Lowder, 1970; Lowder and Carmichael, 1970). In the latter example, Lowder and Carmichael (1970) showed that variation within the series can be adequately explained by subtraction of appropriate proportions of the phenocrysts in the various lavas. A notable feature of both the Thingmuli and Talasea series has been the important role played by a Fe-Ti oxide phase in the differentiation process. In both series the appearance of an Fe-Ti oxide (titanomagnetite) as a liquidus or near liquidus phase coincides with a sudden change in trend of the liquid line of descent from predominant iron enrichment to predominant alkali enrichment. In the Tweed high-Si series, a somewhat similar role is attributed to ilmenite which occurs as phenocrysts in most rocks. Inclusion of a relatively small proportion of these phenocrysts in a crystal fractionation assemblage (~5% of the assemblage; *see* Table 7.6) would be sufficient to inhibit an iron-enrichment trend and initiate a trend of qz enrichment within the derivative liquids.

Levels at which the fractionation processes might have occurred are difficult to estimate. Somewhat tenuous evidence suggests that they may have been operative at intermediate depths in the crust *i.e.* at pressures in

the vicinity of 5 kb. Firstly, pyroxenes which are clearly high pressure phases are apparently absent from the high-Si series even when sieved feldspars are abundant; Al-poor ferroaugites coexist with these particular feldspars (see Section 5.4). At 9 and 13.5 kb the high pressure characteristics of liquidus and near-liquidus clinopyroxenes are well established, compared with their lower pressure analogues, even for relatively evolved host rock compositions (e.g. T.H. Green, 1972); furthermore these pyroxenes are Mg-rich throughout the range of investigated host rock compositions. It is therefore likely that the sodic feldspars and Al-poor ferroaugites crystallized at pressures substantially lower than 9 kb. On the other hand, the sieved and reverse zoned nature of the early plagioclase phenocrysts suggests elevated pressures of formation but under relatively anhydrous conditions (see Section 5.4).

It is therefore suggested that the high-Si series evolved by fractional crystallization of a more mafic magma at intermediate crustal depths where the liquid reached a five phase (olivine, pyroxene, plagioclase, ilmenite, liquid) curve and fractionation proceeded with separation of these phases. The common occurrence of relict phenocrysts of olivine (or its pseudomorphs) mantled by pigeonite indicates that olivine persisted as a near liquidus phase throughout the sequence and only reacted with liquid at intermediate compositions (in andesites and icelandites) with fall in temperature.

The nature of the parent magma to the high-Si series and its relationship to the low-Si series will be discussed in the following section.

7.4 RELATIONSHIP BETWEEN THE LOW-Si SERIES AND THE HIGH-Si SERIES

Up to this point, the low-Si series and the high-Si series have been considered as separate magma series which evolved under differing pressure regimes. It now remains to assess possible relationships between the two series and to speculate on the controls of their differing characteristics. In summary, the low-Si series is considered to be a product of fractionation processes near the crust-mantle boundary involving olivine, aluminian pyroxenes and plagioclase. The dominant trend was one of iron enrichment with only slight increase in qz. On the other hand the high-Si series developed at somewhat lower pressures through fractionation which involved ilmenite in addition to olivine, plagioclase and Al-poor pyroxenes. A trend of alkali and qz enrichment is predominant.

The overall chemical characteristics of both series in terms of major and trace elements are closely comparable, especially when the respective mafic members are compared. It is only when chemical variations within each series are assessed in detail that subtle chemical differences emerge. The broad chemical similarities strongly suggest that the two series are related, possibly to the extent of sharing a common parent magma. A more detailed assessment of this proposal would require detailed experimental data on comparable rocks at pressures up to about 9 kb and under anhydrous and water deficient conditions.

Unfortunately the experimental data presently available provide little assistance on this problem. Either the rock compositions studied to date are inappropriate (e.g. O'Hara *et al.*, 1970) or the results are inconclusive because ilmenite does not appear until well below the liquidus

(e.g. Thompson, 1972b). In other studies, no details are given of the opaque mineral assemblage crystallizing during experimental runs (e.g. Green and Ringwood, 1968; Green, 1969). Nevertheless it is quite clear from the size and widespread distribution of ilmenite phenocrysts in the high-Si series that this oxide phase was available for fractionation during evolution of this series. It is almost equally certain that ilmenite was not a fractionating phase in the low-Si magmas where Fe and Ti increase with fractionation. The reasons why ilmenite phenocrysts should have crystallized from rocks of the high-Si series but not from the low-Si series are unclear. Certainly the higher Fe and Ti contents of the low-Si series relative to the high-Si series (see Tables 6.1, 6.2) make it extremely unlikely that it has been a function of host rock chemistry. However the significantly different pressure regimes proposed for the evolution of the low-Si series (~9 kb) and the high-Si series (~5 kb) suggest that the crystallization of ilmenite may be in part pressure dependant.

It is suggested that the two series may have developed from a common parent by fractionation under differing pressure regimes. On one hand the low-Si series developed near the crust-mantle boundary by fractionation involving a substantial proportion of clinopyroxene thus leading to enrichment in iron and suppression of qz enrichment. On the other hand, some magma ascended to intermediate crustal depths where ilmenite quickly became a fractionating phase together with olivine, augite and plagioclase. This supressed further iron enrichment and set the liquids upon a course of alkali and qz enrichment. As discussed in the following section, the

ultimate product of this fractionation has probably been a substantial volume of relatively dry rhyolitic magma.

7.5 GENESIS OF THE RHYOLITIC ROCKS

7.5.1 Water Content and Eruption Temperatures

Before discussing the genesis of the rhyolites, it is desirable to obtain an estimate of their volatile contents and temperatures of eruption. These variables will have an important bearing upon the depth of origin and the nature of the parent material, both of which are relevant to genetic interpretations. Are the rhyolites products of crustal anatexis or do they represent extreme fractionates of more mafic parents?

Experimental data on melting relations of granitic magmas place stringent constraints on the volatile contents (in particular H_2O) of magmas reaching the surface as lava flows (Cann, 1970; Harris *et al.*, 1970). A generalized outline of liquidus and solidus relations of acid magma with varying water content is shown in Figure 7.3. A water-bearing granitic magma, even if not water saturated will eventually reach its own water saturated solidus, following upward movement and crystallization. At this point the magma becomes immobile and further upward movement is impossible

As it nears the surface a rather less hydrous magma with some crystallization either encounters its water saturated solidus and freezes or else reaches the surface at a temperature above its solidus. In the first case spontaneous expulsion of the volatile phase will occur upon solidification resulting in violent eruption of pyroclastic material (Harris *et al.*, 1970) while in the latter case volatiles will be lost from the

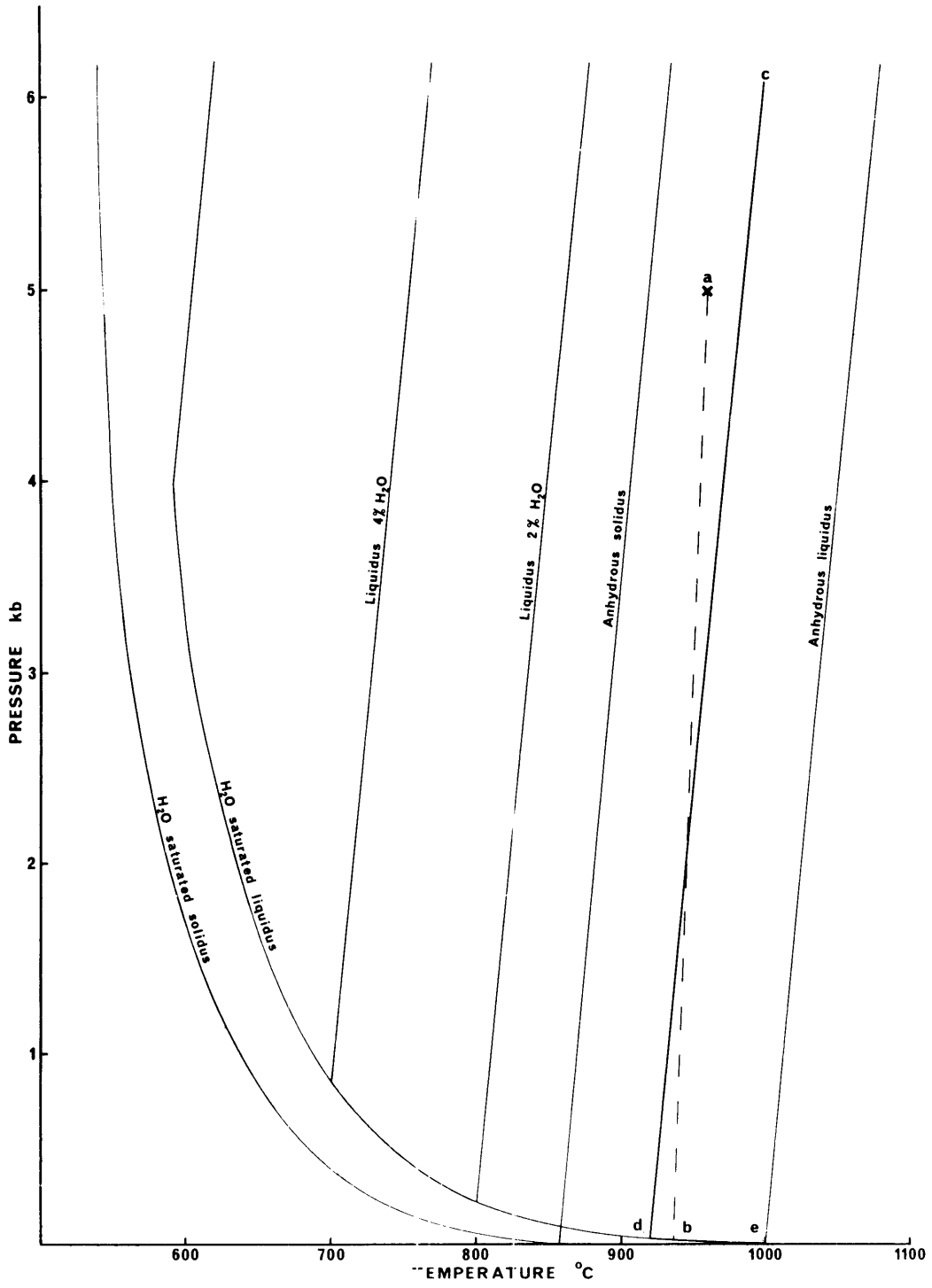

Fig. 7.3: P-T diagram illustraing generalized melting relations of a hypothetical acid magma. See text for discussion.

liquid with decrease in confining pressure causing substantial vesiculation and an increase in viscosity. Consequently the acid magma will tend to form exogenous lava domes with little lateral flow. A classic example of hydrous rhyolitic volcanism is provided by the lava domes, ignimbrites, pumice and ash deposits and rare acid lava flows of the Central Volcanic Zone of the North Island of New Zealand (Ewart, 1963,1965,1966,1969; Ewart *et al.*, 1971).

Considering now water-deficient magma (which will of necessity have a significantly higher liquidus temperature than more hydrous magmas; see Fig. 7.3) this may reach the surface as a liquid. As an example, in Figure 7.3 consider the case of an acid liquid at 5 kb and 1050°C containing a trace (say 0.5%) of H_2O (point a) with a hypothetical liquidus curve c-d-e as shown. Disregarding the minor femic component of such a melt it will consist largely of liquid with some crystals of quartz and feldspar. On rising the melt + crystals may follow a path a-b similar to that depicted. Whether or not the liquidus is actually crossed will depend upon several factors including the amount of heat lost to surrounding rocks and the degree of adiabatic cooling brought about by falling pressure during ascent (the latter is 1°C/km on Fig. 7.3). If the magma moves toward or crosses the liquidus then some resorption of previously formed phenocrysts will occur as evidenced by the widespread occurrence of resorption phenomena in quartz and feldspar phenocrysts in many of the Tweed rhyolitic rocks. Obviously crystallization will recommence when the magma reaches the water saturated liquidus (point b on Fig. 7.3) but as shown this will not occur until very shallow depths. The important point to note is that at no time

does the magma encounter the solidus curve so that upon reaching the surface it is capable of existing as a liquid and therefore forming a flow.

An interesting feature of the Tweed rhyolite flows, at least in the southern part of the Shield, is the considerable lateral extent of many of the flows. Many flows must have covered several square kilometers but have an average thickness of only about 100 m thus suggesting relatively low viscosities during and subsequent to eruption. It therefore seems that there has been little increase in viscosity through loss of volatiles during eruption and therefore eruption occurred under conditions of very low volatile contents but at relatively high temperatures. Low volatile contents are also strongly supported by the relatively minor pyroclastic component of the acid eruptives (<10%), by the rarity of vesiculation within the rhyolite flows, and by the absence of any evidence of hydrothermal activity associated with the erupted rhyolites. Other evidence in support of this proposal includes the lack of significant oscillatory zoning in plagioclase phenocrysts (cf. Yoder, 1969a; Morashi *et al.*, 1974), the absence of primary hydrous phases, and appearance of ilmenite as the sole Fe-Ti oxide phase in the rhyolites.

Eruption temperatures of 970-1040°C for the rhyolites have been estimated on the basis of the Kudo-Weill plagioclase geothermometer (Kudo and Weill, 1970; see Section 5.4) assuming a dry magma. Using the Kudo-Weill equation for P_{H_2O} = 0.5 kb the estimated eruption temperatures are a little lower (920-990°C) but still relatively high for rocks having essentially minimum melting compositions i.e. with respect to the Ab-Or-Qz system. The usefulness of this approach is limited to some extent by the

necessity for an accurate estimate of water pressures during crystallization. Nevertheless the geothermometric data are consistent with other field and mineralogical criteria in suggesting relatively high temperatures and low volatile contents for the rhyolite magmas at the time of eruption.

7.5.2 Origin of the Rhyolite Magmas

The rhyolite flows and associated acid pyroclastics of the Tweed Shield, erupted through several vents on its southern flanks, constitute an important component of the volcanic succession. Voluminous flows of rhyolite also occur on the northern slopes of the Shield, particularly in the Binna Burra and Springbrook areas in south-eastern Queensland.

Significant developments of acid volcanics or small high level intrusions often accompany subalkaline (especially tholeiitic) volcanic activity and the genesis of the acid magmas has been the subject of considerable debate. In essence it may be argued that acid magmas originate either by partial melting of crustal rocks or by extreme fractionation of basic parent magmas. Two examples suffice to illustrate this debate. Firstly, numerous minor felsite, granophyre and high level granite intrusions on Skye and Rhum have been attributed to localised partial fusion of sediments by the large basic intrusions which are a feature of the region (Wager *et al.*, 1953; Brown, 1963; Bell, 1966; Dunham and Thompson, 1967). However Kleeman (1965) has argued that these bodies represent the end product of fractionation of basic magma, probably accompanied by considerable contamination by siliceous sediments. The second example is Iceland, where underlying sialic material is apparently absent and manifestations of acid volcanism are confined to areas of central volcanic activity (Carmichael,

1964). Here the acid rocks are generally regarded as fractionates derived from more basic magma (e.g. Carmichael, 1962,1964; Moorbath and Walker, 1965; Sigurdsson, 1970) although Gibson (1969) has suggested that the mineralogical and chemical data are equally consistent with a process of partial fusion of basaltic material.

The end products of all these processes may be essentially identical, at least in terms of major element chemistry and mineralogy. For example, although a series of rhyolites may plot within the low temperature regions of the systems Ab-Or-Qz or Ab-An-Or it is not possible to discriminate between the various processes of rhyolite genesis outlined above. It only indicates that the rhyolitic magmas have acquired compositions appropriate to low melting liquids under their conditions of formation. It is therefore necessary to critically examine all aspects of the field, mineralogical and chemical data to ascertain the most likely mode of origin of the Tweed rhyolitic rocks and their relationship to the low-Si and high-Si series.

Field Data. In at least the southern portion of the Tweed Shield, rhyolitic volcanism was confined to two principal eruptive episodes. The first eruptive phase, producing the Georgica Rhyolite, preceded major outpourings of tholeiitic rocks belonging to both the low-Si and high-Si series. The Nimbin Rhyolite, the second rhyolitic eruptive phase, followed a period of prolonged and widespread outpourings of lavas of both series and apparently marked the cessation of eruption of the high-Si series. Within the Nimbin Rhyolite, some of the most evolved members of the high-Si series occur as boulders in certain pyroclastic horizons. For example, 28072, an

evolved icelandite (Table 6.2, No.12) occurs as large boulders in a typical rhyolitic pyroclastic matrix.

The field associations therefore suggest some genetic link between the tholeiitic andesites, icelandites and rhyodacites of the high-Si series and the rhyolitic rocks.

The relative volumes of acid to intermediate and basic rocks erupted during development of the Shield is also fundamental to this discussion. It is commonly contended that, if crystal fractionation is a valid control in rhyolite genesis, the rhyolites should constitute only a small proportion (~10% or less) of the total volume of eruptives, assuming basaltic parents. An estimate of relative abundances in the Tweed sequence is made especially difficult by the deeply dissected nature of the Shield. For example, assuming a relatively conical shape for the original Shield and a thickness of 1.5-2.0 km of lavas at the summit (this estimate accords well with the estimated elevation of the summit of 1920 m given by Solomon, 1964) the total volume of the Shield is estimated at 3000 km^3 and the volume of material removed to form the central erosion caldera represents at least 25% of the original volume; perhaps no more than 40% of the original volume remains. On the other hand the outcrop pattern of the rhyolites suggests that they have been more resistant to erosion than the more basic eruptives. On the basis of the outcrop pattern and the present spatial distribution of flows about proposed eruptive centres (accompanying map; see also McTaggart, 1961) the original outcrop area of the rhyolites is estimated at approximately 1000 km^2. Since the average thicknesses of the Nimbin Rhyolite in the southern parts of the Shield and the Binna Burra Rhyolite in the northern

part are probably about 150 m then the original volume of rhyolite is unlikely to have exceeded about 200 km^3 or only about 7% of the total volcanic pile. Two points suggest that this figure is not incompatible with fractionation. Firstly, in terms of their normative salic constituents, even the most primitive Tweed volcanics have relatively high Na_2O+K_2O (~4%) and are therefore capable of producing substantial volumes of rhyolitic liquid by extreme fractionation. More specifically, magmas with similar K contents to the most mafic tholeiitic volcanics found in the southern part of the Shield ($K_2O>0.7\%$; Table 6.1) could, with extreme fractionation, yield more than 10% of rhyolite magma containing 5.5% K_2O (cf. Table 6.3). Secondly, a major positive gravity anomoly centred beneath the Tweed Shield (B.M.R. Bouger anomoly map, 1971) suggests that a large amount of mafic material remains as intrusives beneath the Shield area and hence the erupted mafic magma may represent only a small proportion of the original amount available for fractionation.

Chemical Data. Several aspects of the chemistry of the rhyolitic rocks, especially with respect to specific trace elements, appear more consistent with an origin by fractional crystallization rather than by differential anatexis. Many of the major oxides *e.g.* $FeO+Fe_2O_3$ (Fig. 6.7), MgO (Fig. 6.9), CaO (Fig. 6.10) and K_2O (Fig. 6.12), show essentially continuous variation from the most salic rocks which can be confidently assigned to the high-Si series through to the rhyolites. Admittedly a discontinuity in the trends for Na_2O and Al_2O_3 is evident. However the Na_2O trend may be due to alkali leaching during hydration and/or devitrification and the Al_2O_3 trend may be explained by continued fractionation after the residual liquid acquires a rhyolitic composition and alkali feldspar begins to separate

(cf. the whole rock-groundmass trend for these rocks, Section 7.5.4. Perhaps the most important evidence in favour of their origin by extreme fractionation is provided by the strong Ba depletion in the rhyolites. Early formed rhyolitic liquids derived from partial melting, either of sediments or of basaltic material, should be strongly enriched in Ba since the K-bearing phases into which Ba is strongly partitioned will be among the first to break down to produce these relatively potassic liquids. A similar enrichment could be expected during fractionation (e.g. McBirney and Williams, 1969) until the liquid reaches the two feldspar surface in the system An-Ab-Or-Qz (Carmichael, 1963) and potash feldspar becomes a liquidus phase. Subsequent fractionation will then rapidly deplete the liquid in Ba (Nockolds and Allen, 1954; Siedner, 1965) through the strong tendency for Ba to preferentially enter K lattice sites. On the other hand Rb would continue to be partitioned into liquid relative to phenocryst phases even during fractionation of K-feldspar, thereby producing a residual increase in Rb and a lowering of the K/Rb ratio during extreme fractionation (Heier and Adams, 1963).

As a consequence the rhyolites are characterised by extremely low Ba/Rb ratios (<0.5; Table 6.7) closely comparable with those of late stage granites in the Snowy Mountains region of N.S.W. (average Ba/Rb = 0.7; Kolbe and Taylor, 1966; Taylor *et al.*, 1968) which have been interpreted as products of extreme fractionation of a granodioritic magma. On the other hand the Tweed rhyolites contrast strongly with North Island, New Zealand, calc-alkaline rhyolites (average Ba/Rb = 8.1; Ewart *et al.*, 1969; Taylor *et al.*, 1968), considered to be derived by partial fusion of the underlying sedimentary pile (Ewart and Stipp, 1968).

It is believed that the above geochemical features are inconsistent with a partial melting origin for the rhyolite magmas. They are also inconsistent with fractionation processes unless a K-feldspar phase has been involved in the latter stages of fractionation, thereby depleting the liquid in Ba. On chemical grounds it seems that fractionation has proceeded up to and beyond the point where the fractionating liquid has reached the cotectic line de in the system Ab-An-Or-Qz (Fig. 7.4; James and Hamilton, 1969, modified from Carmichael, 1963). The nature and behavior of the rhyolitic liquids with respect to phase relations within this system will be discussed in some detail below.

7.5.3 Rhyolites in Relation to the Ab-An-Or-Qz System

In terms of their normative chemistry the rhyolites are strongly enriched in the salic low melting components (ab,or,qz), indicated by their high D.I. (>90); however an is also an important minor normative constituent. It is therefore appropriate to consider the crystallization relations of the rhyolitic rocks in terms of phase relations in the system Ab-An-Or-Qz (Carmichael, 1963), especially in view of the detailed experimental data now available on various parts of the system (e.g. Tuttle and Bowen, 1958; Luth *et al.*, 1965; James and Hamilton, 1969; Luth, 1969). In this system at 1 kb P_{H_2O} (Fig. 7.4), two curved divariant surfaces, the quartz-feldspar surface a b c d (James and Hamilton, 1969) and the two-feldspar surface d e f g (Carmichael, 1963) separate liquidus primary phase fields of plagioclase, alkali feldspar, and a silica polymorph and intersect along a cotectic line d e which traces the path of liquids in equilibrium with three solid phases. A primary phase field of leucite near the Or apex, of little relevance

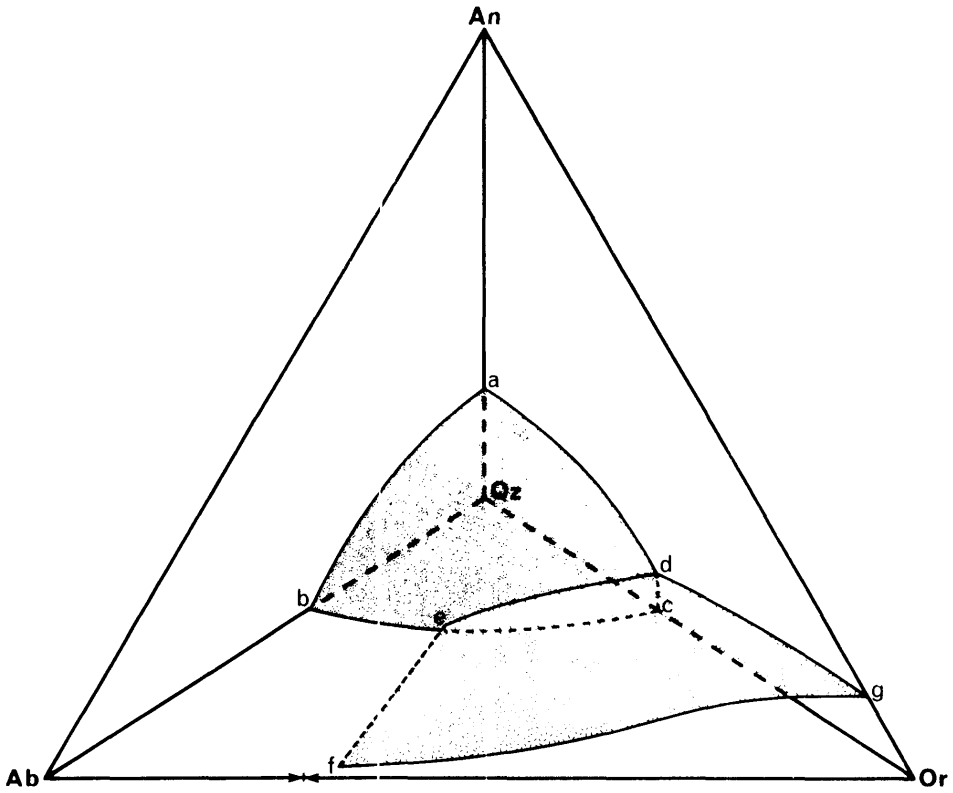

Fig. 7.4: The quaternary system Ab-An-Or-Qz at 1 kb P_{H_2O} (after James and Hamilton, 1969). The quartz-feldspar boundary surface a b c and the two-feldspar boundary surface d e f g intersect along the cotectic line d e. This line traces the path of liquids in equilibrium with two feldspars and quartz and terminates at the invarient point e which is located within the tetrahedron above the Ab-Or-Qz face.

to the present discussion, need not be considered.

In Figure 7.5 the rhyolites are plotted on an Ab-Or-Qz diagram together with residual glasses separated from two phenocryst-rich vitric rhyolites. The presence of phenocrysts of two feldspar species and quartz in all but the most aphyric rhyolites, together with chemical evidence presented in the previous section suggesting that K-feldspar has been a fractionating phase, indicate that during fractionation the rhyolitic liquids have reached the low temperature trough in the Ab-Or-Qz system under the conditions prevailing during fractionation. In this projection, compositions cluster on the feldspar side of the quartz-feldspar surface determined at 1 kb P_{H_2O} and have Ab/Or ratios appropriate to An contents of approximately 3-5%, values consistent with those found in the rocks themselves, especially the vitric representatives. The presence of abundant quartz phenocrysts, in addition to feldspar, in rhyolites whose normative ab, an and or components plot well within the experimentally determined feldspar field suggests that the primary phase volume of quartz was considerably greater during phenocryst precipitation than is indicated by the experimental data. However most data presently available on this system have been obtained under conditions of $P_{H_2O} = P_{total}$ and therefore must be applied with caution to the water-deficient acid magmas under discussion. Data on the joins Ab-SiO_2 and Or-SiO_2 (Luth, 1969) indicate that P_{H_2O} and P_{total} must be treated as separate variables but that they have similar effects at pressures up to about 10 kb. Furthermore, experimental data on natural rocks show that the primary phase field of quartz expands with increasing "dry" load pressure in the same manner as with increasing P_{H_2O} (Green and Ringwood, 1968; Ringwood, 1974).

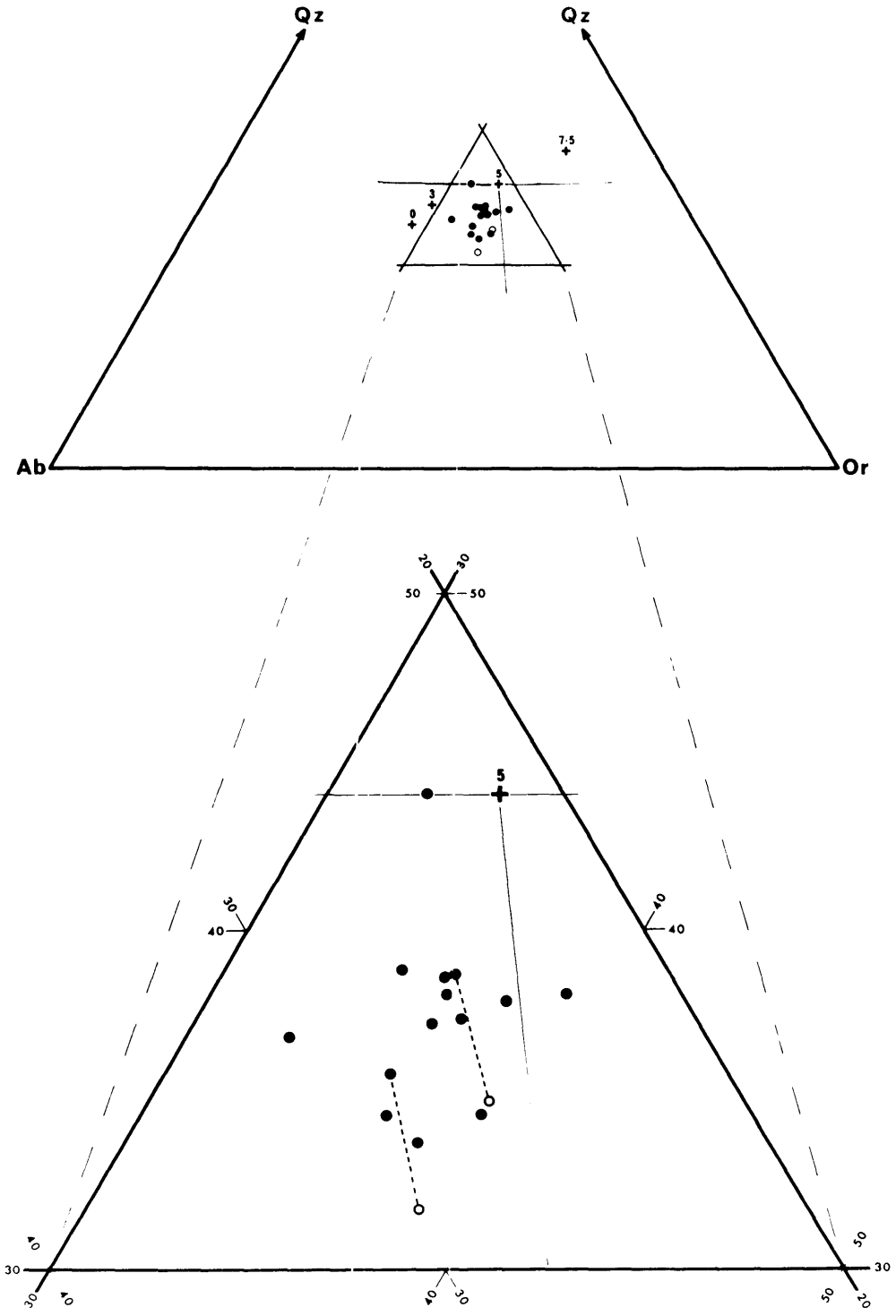

Fig. 7.5: Compositions of the rhyolites (filled circles) and 2 residual glasses (open circles) plotted in terms of the normative components ab, or and qz (wt %). Tie lines join whole rock-residual glass pairs. Crosses indicate the piercing points at 0, 3, 5 and 7.5 wt % An projected from the An apex onto the Ab-Or-Qz face. The lower diagram is an enlargement of the small triangle in the upper diagram.

For example, quartz replaces plagioclase on the liquidus of a dacite composition at 9 kb anhydrous (Green and Ringwood, 1968).

The presence of quartz phenocrysts in the rhyolites and the displacement of the rhyolites away from the Qz apex relative to the quartz-feldspar boundary surface therefore suggest that fractionation may have taken place at moderate pressures. It is proposed that the rhyolites formed by extreme fractionation of a relatively dry, more basic magma at intermediate crustal depths (~5 kb).

The normative feldspar components have been plotted on an Ab-An-Or diagram in Figure 7.6. The line d'-e' represents the projection of the 1 kb P_{H_2O} isobaric univariant curve (= two feldspar boundary curve) d e Figure 7.4 projected from the quartz saturation surface on to the ternary feldspar face.

Relative to the 1 kb P_{H_2O} boundary curve, the rhyolites are displaced towards the Ab-Or join. If, as has been argued, these rhyolites are extreme fractionates then it is possible that under water deficient conditions either the univariant two feldspar boundary curve moves towards more An-poor compositions or else the invariant point e (in essence, the end point of complete fractionation) moves towards more Or-rich compositions. The positions of both the curve and the invariant point may also be affected by minor components in the natural acid liquids not present in the synthetic system. Alternatively the rocks may have been somewhat depleted in CaO by some post-eruptive process, especially in view of the consistently lower CaO (and hence lower an since they are corundum normative) of the devitrified rhyolites relative to vitric types which indicates at least some mobility

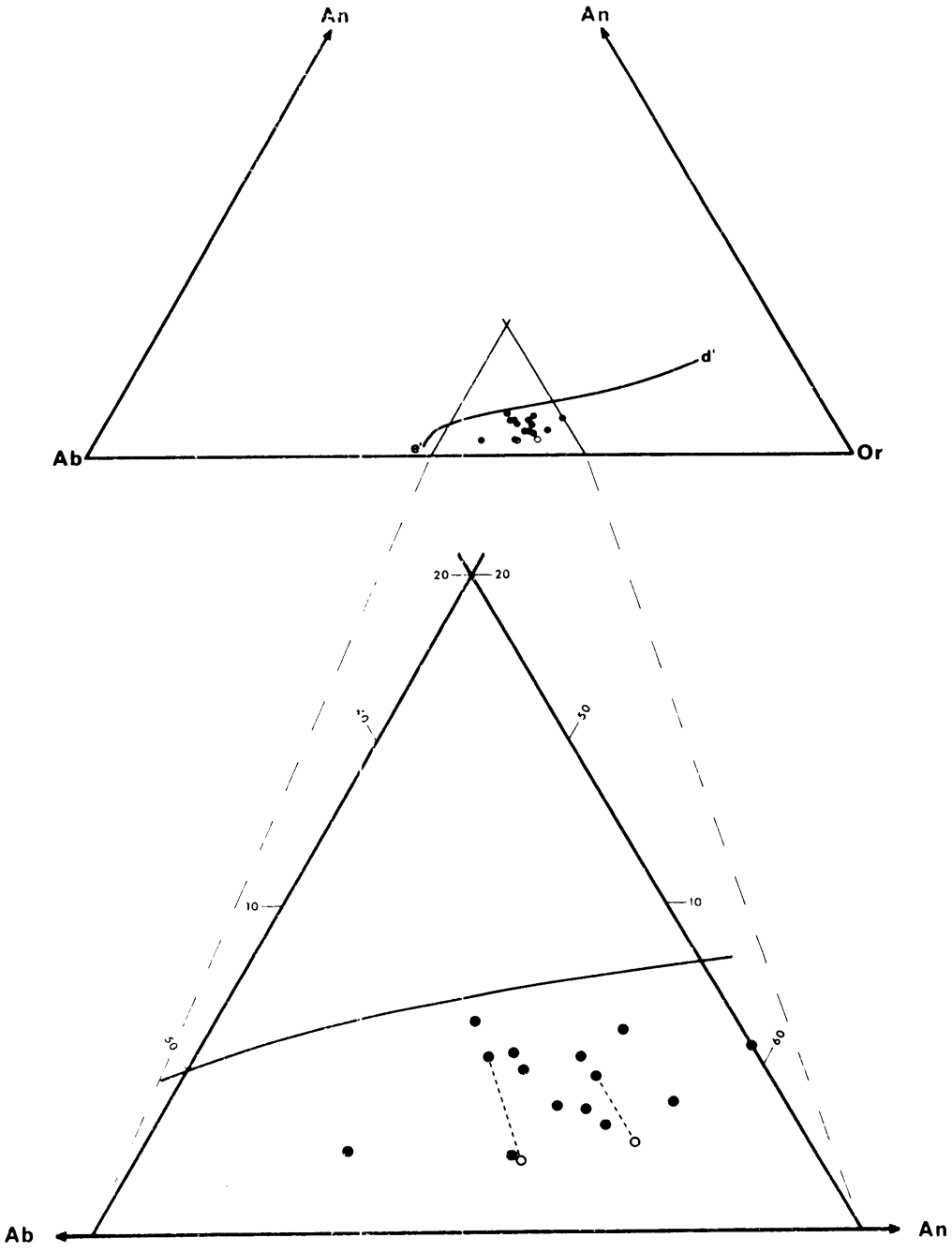

Fig. 7.6: Compositions of the rhyolites (filled circles) and 2 residual glasses (open circles) plotted in terms of the normative components ab, an and or (wt %). Tie lines join whole rock-residual glass pairs. The line d'e' represents the cotectic line de in Fig. 7.4 projected from the Qz apex onto the Ab-An-Or face. The lower diagram is an enlargement of the small triangle in the upper diagram.

of Ca at this time. The better known process of alkali leaching would actually have the reverse effect.

The above discussion is based predominantly upon experimentally determined phase relations in the H_2O-saturated Ab-An-Or-Qz system. A more rigorous assessment of the applicability of phase relations in this system to the rhyolites may become possible after examination of the system under water-deficient conditions.

7.5.4 Whole Rock-Residual Glass Trends in the Rhyolites

Residual glasses from two porphyritic rhyolitic pitchstones have been plotted on the Ab-Or-Qz (Fig. 7.5) and Ab-An-Or (Fig. 7.6) diagrams, the tie lines joining the glasses and their respective host rocks. The overall chemistry of these glasses has already been discussed (Chapter 6). The glasses closely resemble the rhyolitic host rocks in most respects despite the removal from the latter of about 30% by volume of phenocrysts of quartz and two feldspars. The residual glasses differ principally from their hosts in containing slightly lower qz, slightly higher K_2O and a small amount of wo in the norm.

The lower qz of the residual glasses suggests that a slight expansion of the primary phase volume of quartz has occurred between the period of fractionation which produced the rhyolitic derivatives and precipitation of their phenocryst assemblage. In the system Ab-An-Or-Qz, which is directly relevant to this discussion, an expansion of the quartz volume may result from an increase in either P_{H_2O} (Tuttle and Bowen, 1958; Luth, *et al.*, 1964) or P_{total} (Green and Ringwood, 1968; Ringwood, 1974).

The former is likely to be insignificant in water-deficient magmas while an increase in P_{total} is not really geologically feasible. Instead, the trend may conceivably reflect a decrease in activity of the ab and or components of the melt during crystallization brought about by the removal of Al_2O_3 in excess of stoichiometric porportions by fractionating alkali feldspar (see below).

Similarly, on the Ab-An-Or diagram (Fig. 7.6) displacement of the residual glasses towards the Ab-Or join relative to the host liquid may simply reflect their alumina-deficient condition insofar as this affects calculation of an in the C.I.P.W. norm. One of the phenocryst phases, namely alkali feldspar, contains excess Al_2O_3 over stoichiometric proportions. In fact most analysed sanidines (Table III.3c) contain 0.5-1.0% Al_2O_3 in excess of that required to balance Na_2O, K_2O, CaO and SiO_2 in a stoichiometric feldspar composition. It therefore cannot be adequately represented in terms of the components An,Ab and Or, so that the system is not strictly ternary and it is not completely valid to assess the whole rock residual groundmass trends in terms of this system.

A passing comment may be made with respect to the appearance of wo in the norm of residual glasses whose host rocks are in fact slightly corundum normative. A continuation of this trend, presumably brought about by removal of excessive amounts of Al_2O_3 in alkali feldspar, may ultimately result in the development of peralkaline derivative liquids. This observation is especially relevant in view of the occasional occurrence of small intrusive bodies of alkali rhyolite within the Shield (e.g. Lillian Rock,

north of Nimbin; see Appendix III). An important petrogenetic problem has been the genesis of oversaturated peralkaline rocks. Many have apparently formed by differentiation of peraluminous parent liquids (Carmichael and MacKenzie, 1963) and now occur in close association with peraluminous rocks in the field. Their genesis has commonly been attributed to the "plagioclase effect" (Bowen, 1945) which, in essence, involves removal of excess anorthite over that found in the C.I.P.W. norm which effectively depletes Al_2O_3 and enhances Na_2O in the residual liquid. Alternatively, Bailey and Schairer (1966) suggest that where peralkaline and peraluminous rocks are closely associated, the former are in fact parental with the latter resulting from assimilation of aluminous sialic material.

In view of the whole rock-residual glass data presented herein an additional mechanism may be suggested, with, it is emphasised, considerable caution. Peralkaline acid liquids may develop from a peraluminous rhyolitic parent through continued fractionation of quartz and alkali feldspar, the latter containing Al_2O_3 significantly in excess of stoichiometric proportions. Depletion of Al in the liquids through fractionation of this Al-excessive feldspar would progressively increase the Na_2O+K_2O/Al_2O_3 (mol.) ratio resulting firstly in the appearance of wo and ultimately of ac in the norm. It is worthy of note that the strong depletion in Ba exhibited by the peralkaline comendites of Mayor Island, New Zealand (Ewart *et al.*, 1968) are consistent with fractionation of significant quantities of alkali feldspars in which Ba may have substituted for K.

7.6 TECTONIC SETTING OF THE TWEED SHIELD

To conclude this discussion it is appropriate that the relationship

between the age, location and formation of the Tweed Shield Volcano and the Cainozoic tectonics of eastern Australia be briefly discussed. The Cainozoic volcanic belt of eastern Australia is situated wholly within the Indian lithospheric plate (le Pichon, 1968) which, on magnetic anomaly profile evidence, is alleged to have been migrating northwards at an average 56 mm per year since separation from the Antarctic plate about 55 m.y. ago (Weissel and Hayes, 1971).

Wellman and McDougall (1974b) have discussed the distribution of Cainozoic volcanism in eastern Australia and have related this to northward movement of the Indian Plate. They subdivide the Cainozoic volcanics into three types, the two most important being lava field and central volcano types, and contend that activity of the central volcano type, which includes the Tweed Shield, has migrated southwards at 66 ± 5 mm per year since the mid-Oligocene. This is interpreted as a consequence of the northward movement of the Indian plate over fixed magma sources (or "hot spots") in the upper mantle. According to this model the Tweed Shield Volcano formed between 23.0 and 20.0 m.y. ago during passage of the Indian plate over one of these melting sources. Factors controlling the actual location of the Tweed Shield are rather less clear. Central volcanic activity in eastern Australia has been sporadic, compared with the Hawaiian Islands which have been widely cited as a classic example of volcanism resulting from plate migration over a fixed melting source (Wilson, 1963; Morgan, 1971; McDougall, 1971; Dalrymple *et al.*, 1974). This sporadic character presumably reflects the substantial thickness of continental crust underlying eastern Australia hindering upward movement of magma through the crust.

A major weakness in the crust would be needed to localise volcanism sufficiently to form a major shield structure such as the Tweed Shield. It has previously been noted that the focal point of the Tweed Shield volcano, namely the Mount Warning intrusive complex, is located on a fault controlled boundary between strongly deformed and mildly metamorphosed Palaeozoic sediments and the near-underformed Mesozoic Chillingham Volcanics. Perhaps this fault is so deep seated that it allowed upward passage of magma during movement over the postulated melting source, especially since eastern Australia was probably in a tensional environment at the time (Wellman and McDougall, 1974). However, it is clear that the fault was not active during development of the Shield since there is no evidence of any displacement or tilting of the volcanic sequence.

The Ebor Volcano (McDougall and Wilkinson, 1968), the next major shield structure south of the Tweed Shield also has an intrusive complex as a focal point. It is notable that this is located on the major north-south trending Taylor's Arm Fault (Leitch, 1974).

Towards the end of the Mesozoic a ridge was active in the Tasman Sea off eastern Australia (Hayes and Ringis, 1973). Associated transform faults trend approximately east-west and therefore normal to the Australian east coast. However it is most unlikely that these have influenced the location of the Tweed Shield Volcano since the ridge has been inactive for the past 60 m.y. and in any case the ridge and associated transforms have not affected the pre-Cainozoic rocks now exposed on the eastern Australian mainland. Any genetic relation between the Tweed Shield and the Tasman

Sea spreading ridge is therefore discounted. It is more likely that the Tweed Shield Volcano originated when a melting source in the underlying mantle encountered a point of crustal weakness as the Indian Plate moved northward.

CHAPTER 8

SUMMARY AND PRINCIPAL CONCLUSIONS

The following summarizes the data and discussions presented in Chapters 1 to 7.

1. The stratigraphic nomenclature for the Lamington Volcanics in the southern part of the Tweed Shield Volcano is revised. An alkaline formation (the Kyogle Basalt) containing discontinuous rhyolitic agglomerate (the Homeleigh Agglomerate Member) and rhyolite flow (the Georgica Rhyolite Member) horizons is the basal unit of the volcanic succession. The Kyogle Basalt thins eastward where it is overlain by a subalkaline sequence comprising the Lismore Basalt, Nimbin Rhyolite and Blue Knob Basalt respectively. The Lismore Basalt is composed predominantly of tholeiitic andesite with minor icelandite and sporadic flows of mildly alkaline rocks; tholeiitic andesites predominate in the Blue Knob Basalt. The Nimbin Rhyolite consists of rhyolite flows, and a minor pyroclastic component (principally lapilli tuff).

2. Detailed mineralogical and chemical data enable recognition of two distinct tholeiitic series, respectively designated the low-Si and the high-Si series. In essence, the rocks of the low-Si series, almost exclusively tholeiitic andesites, are characterized by:

(a) the absence of Ca-poor groundmass pyroxenes;

(b) the absence of a reaction corona of Ca-poor pyroxene around olivine phenocrysts and the presence of groundmass olivine;

(c) mild iron enrichment on an AFM diagram;

(d) a very limited increase in the level of silica saturation with increasing degree of evolution.

On the other hand, rocks of the high-Si series (tholeiitic andesite → rhyodacite) are characterized by:

(a) the ubiquitous presence of pigeonite in the groundmass, commonly with phenocrysts of pigeonite and hypersthene;

(b) a reaction corona of Ca-poor pyroxene mantling olivine phenocrysts, at least in the more mafic representatives, and the absence of groundmass olivine;

(c) minimal iron enrichment and somewhat pronounced alkali enrichment on an AFM diagram;

(d) a marked increase in qz with increasing degree of evolution.

Rhyolites, comprising both vitric and microcrystalline variants, commonly contain phenocrysts of quartz, sanidine and minor oligoclase. Microphenocrysts of ferrohypersthene and ilmenite may also occur in these rocks.

3. Relatively high pressure pyroxenes and plagioclase occur in some rocks. In the low-Si series the pyroxenes (bronzite and subcalcic augite) which are enriched in Al^{VI} relative to groundmass augite, have crystallized at moderately high pressures (probably about 9 kb). Early formed ferroaugites in the high-Si series are not enriched in Al and are considered to be products of substantially lower pressure crystallization (ca 5 kb).

The moderately high pressure plagioclases of both volcanic series are enriched in Na relative to low pressure phenocrysts. They typically

consist of an unzoned relatively sodic core surrounded by a zone of sieving which is in turn mantled by a glassy clear margin of plagioclase comparable in composition to the groundmass plagioclase.

4. Groundmass pyroxenes from rocks of the low-Si series exhibit an increase in Ca with increasing Fe/Mg ratio. This trend is interpreted as a response to a decrease in the activity of Fe^{2+} caused by an increase in f_{O_2} through the series as inferred by the progressively changing nature of the opaque oxide assemblage i.e. from ilmenite to titanomagnetite (see No. 6 below). Low silica activities inhibited the crystallization of Ca-poor groundmass pyroxenes in members of the low-Si series.

5. In the high-Si series, phenocrysts of ferroaugite commonly preceded more magnesian pyroxene microphenocrysts and groundmass pyroxenes. This rather unusual trend is attributed to a combined effect of depletion of the host liquid in Fe by separation of ilmenite phenocrysts and an increase in f_{O_2} in the magma with ascent to near surface conditions, probably by addition of some water to the magma from the surrounding country rocks.

6. In the low-Si series there is a progressive change in the nature of the Fe-Ti oxide assemblage from ilmenite alone through ilmenite plus titanomagnetite to titanomagnetite alone with increase in the degree of evolution of the host rocks. R_2O_3-poor ilmenite is the predominant Fe-Ti oxide throughout the high-Si series and in the rhyolites. When present, the titanomagnetites from both series are rich in the ulvöspinel component (65-85 mol. %).

The Fe-Ti oxide data indicate that most of the tholeiitic magmas

possessed relatively low oxygen fugacities, estimated to be intermediate between those defined by the fayalite-magnetite-quartz and the wüstite-magnetite oxygen buffer assemblages.

7. The Fe and Or contents of plagioclases are discussed in relation to their environment of crystallization. Entry of Fe into plagioclase is strongly favoured by rapid rates of crystallization as is shown by significant enrichment of Fe in groundmass crystals and the margins of phenocrysts relative to the cores of phenocrysts. The Or contents of plagioclases are not controlled by external factors but are merely a function of host rock chemistries (normative feldspar components) as these control the location of the intersection of the solidus and solvus in the system Ab-An-Or.

Calculated liquidus temperatures based on the Kudo-Weill plagioclase geothermometer are lower for rocks of the high-Si series relative to comparable rocks of the low-Si series, probably due in part to the higher levels of silica saturation of members of the high-Si series.

8. Several lines of evidence, notably the absence of primary hydrous phases (even in the rhyolitic rocks), the abundance and sodic character of plagioclase phenocrysts and the predominance of ilmenite over magnetite in almost all of the rocks, collectively indicate that the tholeiitic magmas of both series and the rhyolites were relatively water-deficient during intratelluric crystallization and subsequent eruption.

9. Even the most mafic tholeiitic rocks are characterized by relatively high Na_2O (3-4%) and K_2O (rarely below 1%). With increase in the degree of evolution in both series, Na_2O remains relatively constant whereas K_2O

increases steadily. The rhyolites are enriched in K_2O and depleted in Na_2O relative to the more mafic rocks. The relatively high potash contents of the mafic rocks possibly result from the breakdown of small amounts of phlogopite in an inhomogeneous upper mantle source region.

10. It is proposed that the low-Si series resulted from fractionation of a mafic tholeiitic parent near the base of the crust (~9 kb) involving removal of plagioclase and aluminian clinopyroxene together with, or followed by olivine. This conclusion is supported by mineralogical and chemical data and by experimental studies at moderate pressures under anhydrous conditions on rocks of comparable composition.

The members of the low-Si series in which high pressure (pyroxene and plagioclase) megacrysts are preserved are chemically indistinguishable from other rocks of the series lacking these phases. The fractionation of aluminian clinopyroxene at elevated pressures prevented clinopyroxene becoming a near liquidus phase at low pressures, thereby inhibiting its appearance as a low pressure phenocryst phase in members of this series.

11. In contrast to the low-Si series, members of the high-Si series, which comprise a relatively minor component of the tholeiitic sequence (~5% by volume) probably developed at intermediate depths in the crust (i.e. at pressures in the vicinity of 5 kb) where the fractionating phases were olivine, ferroaugite, ilmenite and plagioclase, all of which occur as phenocrysts in most rocks of the series.

12. The two tholeiitic series conceivably may be genetically related via a common parent magma and the contrasting chemical trends within the two

series may have resulted from fractionation under significantly different pressure regimes.

13. The possible roles of fractionation of a mafic parent magma and partial anatexis of crustal material in the origin of the rhyolites are carefully assessed. The available field and chemical data are more consistent with an origin involving extreme fractionation than with a model based on crustal anatexis. Field data supporting this proposal include the relative volume of the rhyolites compared with the more mafic tholeiitic rocks and the intimate field association of the two groups of rocks in this part of the Shield. Supporting chemical data include the relatively continuous variation trends of many major and trace elements through the high-Si series to the rhyolites (e.g. MgO, $FeO+Fe_2O_3$, CaO, K_2O and trace elements, especially Rb and Sr) and the strong depletion of Ba and the resultant low Ba/Rb ratios (<0.5) in the rhyolites relative to the more mafic rocks (>5). The high eruptive temperatures (~1000°C) and water deficient nature deduced for the rhyolites also favour a fractionation origin since temperatures required for partial melting appear to be too high for a crustal environment.

14. A plate tectonic model is discussed wherein the Tweed Shield may have developed when a melting source in the upper mantle encountered a site of crustal weakness during northward migration of the Indian Plate in early Miocene times.